Microscale tools for rapid evaluation of two-liquid phase bio-oxidations of volatile alkanes

Johannes F Kolmar

A dissertation submitted in partial fulfilment

of the requirements for the degree of

Doctor of Engineering

of

University College London.

Department of Biochemical Engineering

University College London

31st January 2017

I, Johannes F Kolmar, confirm that the work presented in this thesis is my own. Where information has been derived from other sources, I confirm that this has been indicated in the thesis.

Abstract

The direct ω-oxyfunctionalisation of aliphatic alkanes in a regio- and chemoselective manner remains difficult to perform by industrial organic chemistry. Monooxygenases such as the AlkBGT enzyme complex from *Pseudomonas putida* efficiently catalyse these readily available substrates to fatty alcohols, aldehydes and acids under mild conditions. However, numerous challenges remain to achieve industrially competitive space-time-yields for bio-oxidations. The ability to rapidly screen bioconversion reactions for characterisation and optimisation is of major importance in bioprocess development and biocatalyst selection; studies at lab scale are time consuming and labour intensive with low experimental throughput.

This study developed and validated a robust high-throughput microwell platform for whole-cell two-liquid phase bio-oxidations of highly volatile alkanes. Using microwell plates machined from polytetrafluoroethylene and a sealing clamp, highly reproducible results were achieved with no significant variability such as edge effects determined. Further, the developed platform was extended by a fed-batch implementation revealing the large impact of feeding conditions on the resting cell bio-oxidation of volatile alkanes. The unpredictable nature and large differences between varying alkane substrates show the importance of being able to test fed-batch conditions early in development. Lastly, six co-solvents were screened to relieve organic phase toxicity and improve control over the product spectrum in the bio-oxidation of hydrocarbons. In combination with computational and statistical tools, it was shown that polar sur-

factants allow the extraction of the alcohol product, increasing the alcohol yield and reducing phase toxicity. Specifically, the solubility of co-solvents reaction substrate and product was revealed to be the determining factor for product selectivity.

Overall, the developed microwell plate greatly improves experimental throughput, accelerating the screening procedures specifically for biocatalytic processes in non-conventional media. Its simplicity, robustness and standardisation ensure high reliability of results. The accelerated data collection on biological as well as process options allows obtaining key process design data early on, de-risking and speeding up the translation of new processes from laboratory to pilot-plant scale.

Acknowledgements

For their invaluable advice and support and for giving me intellectual freedom throughout my work, I would like to thank my supervisors Dr Frank Baganz (UCL) and Dr Oliver Thum (Evonik Creavis); special thanks to Dr Jan Pfeffer for initiating the project at Evonik.

Thanks to the sponsors of this project, the Engineering and Physical Sciences Research Council and Evonik Industries, for their generous funding.

For their time and the insightful discussion at the end of my project, I thank my *viva* examiners, Dr Nuno Reis and Prof John Ward.

I am grateful to the UCL community, my fellow colleagues and friends, for making it such a great place, the moments shared and the many memorable trips. It was the best of times.

Most importantly, thanks to my parents and my sister, for their unconditional support and their patience.

Contents

List of Figures

List of Tables

Chapter 1

Introductory material

1.1   Industrial biotechnology

Industrial biotechnology approaches are typically applied for reactions that require optical resolution or other selectivity that cannot, or only with difficulties, be provided by traditional chemical synthesis. Primarily, efforts were focussed on high-value products for the pharmaceutical industry frequently using ketoreductases and hydrolases (Straathof, Panke, and Schmid 2002; Bornscheuer et al. 2012). However, leveraging the combination of protein, genetic, metabolic and reaction engineering has enabled the wider application of biocatalysts such as oxygenases and transaminases in organic synthesis (Pollard and Woodley 2007; Wohlgemuth 2010; Schrewe et al. 2013). Furthermore, increasing attention is paid to finding environmentally benign solutions in the chemical industry (Constable et al. 2007). The mild conditions used in biocatalytic processes are expected to reduce the environmental impact of an industry that has increasing difficulties to innovate novel, more environmentally friendly processes (Wenda et al. 2011). Over 20 Presidential Green Chemistry Challenges (US Environmental Protection Agency) won by biocatalytic processes since 2000 exemplify this development. With most of these innovations in sectors other than pharmaceuticals, it seems clear that fine chemicals and intermediates are brought more into focus of biocatalysis.

A key strength of biocatalysis compared to chemical synthesis is the high chemo-,

regio-, and stereo-selectivities that can be achieved. Together with the ability to work in mild conditions, non-toxic media and the potential for one-pot reactions with a reduction in protection and deprotection steps, the use of biocatalysts results in reduced environmental impact and provides a potent alternative to chemical synthesis (Ghisalba, Meyer, and Wohlgemuth 2010; Wenda et al. 2011). More importantly for industrial processes, economic aspects need to be considered. Based on the above characteristics, economic efficiencies can be envisioned from minimised waste due to high atom efficiency, increased energy efficiency and a reduction in process steps due to potential for one-pot synthesis.

It is important to note, however, that the sustainability and productivity cannot be assumed for biocatalytic processes and a detailed, quantitative assessment on a case-by-case basis in terms of both, the economic as well as environmental factors is critical (Tufvesson et al. 2011; Wenda et al. 2011; Kuhn et al. 2012; Jegannathan and Nielsen 2012).

1.2 Direct alkane oxidation

The majority of current industrial pathways for the utilisation of saturated linear hydrocarbons rely on cracking or dehydrogenation processes under high pressures and temperatures and optionally in presence of catalysts such as acids or metals (Hill 1989; Jong et al. 2010; Bordeaux, Galarneau, and Drone 2012). These processes typically result in a large product range including shorter chain alkenes, alkynes and aromatics (Arakawa et al. 2001). These primary building blocks can be separated and upgraded and, through condensation or oligomerisation reactions, indirectly yield (oxy)-functionalised products of varying chain lengths (Musser 2011; Pradham et al. 2012). These processes are highly endothermic; in combination with partial oxidation of products this leads to a large amount of CO_2 production.

Alternatively, the direct oxidation of hydrocarbons aims at achieving activation of a specific C–H bond and molecular oxygen whilst controlling chemo-, regio-, and

stereo-selectivities without intermediate products.

1.2.1 Routes to direct alkane oxidation

For industrial synthetic chemistry, the direct chemo-, regio and stereoselective oxidation of non-activated carbon atoms using molecular dioxygen as oxidant is still a great challenge (Urlacher, Lutz-Wahl, and Schmid 2004; Roduner et al. 2012; Munz and Strassner 2015). Under conditions of homogeneous catalysis, with no steric constraints, the oxidation selectivity of carbon atoms in n-alkanes increases with decreasing bond dissociation energies. Thus, selectivity towards secondary carbon atoms is thermodynamically favoured over primary carbons with $C-H$ bonds around $15\,kJ\,mol^{-1}$ higher in energy than at the methylene positions (Newhouse and Baran 2011; Bordeaux, Galarneau, and Drone 2012). In addition, the activation of the very inert $C-H$ bonds requires harsh conditions that often leads to over-oxidation (Zhang et al. 2012). This makes terminal oxidation of n-alkanes a particular challenge.

1.2.2 Biocatalysis

The biocatalytic route, which this work focusses on, can achieve the direct oxyfunctionalisation of reduced organic molecules with very high selectivity mainly due to the molecular recognition of enzymes that leverages substrate orientation, shape and size (Beilen et al. 2005; Fasan et al. 2008; Hollmann et al. 2011). Thus, the application of oxygenases is of particular interest for their (Li et al. 2002; Julsing et al. 2008; Lewis, Coelho, and Arnold 2011):

- ability to perform reactions that do not have chemical counterparts or that are difficult to perform with required selectivity

- use of oxygen as cheap and environmentally friendly oxidant in contrast to toxic chemical equivalents

- operation under generally mild conditions

1.2.3 Chemocatalysis

There have been attempts at the direct hydroxylation of alkanes, for example, by inorganic heterogeneous catalysts embedded into scaffolds to increase regioselectivity (Battioni et al. 1988; Thomas et al. 1999; Labinger 2004; Gómez-Hortigüela et al. 2010; Kamata et al. 2010; Thomas 2012). However, industrial application has been hindered by issues such as mass transfer limitations resulting in slow reaction rates (Thomas et al. 1999; Thomas and Raja 2006), overoxidation and selfdegradation of the catalyst and generally poor product selectivity especially for the functionalisation of n-alkanes (Kamata et al. 2010). Consequently there are few commercial direct oxidation reactions; an example is the conversion of n-butane to maleic anhydride (Contractor et al. 1987; Hutchenson et al. 2010).

1.2.4 Substrates

N-alkanes are linear, saturated hydrocarbons that originate from natural gas or crude oil with the general formula C_nH_{2n+2}. They find wide application as cheap chemical raw materials and building blocks as well as fuels.

The inertness of these compounds is a major issue for regio- and chemoselective oxyfunctionalisation. As illustrated by Bordeaux, Galarneau, and Drone (2012), n-hexane does not react with boiling nitric acid, concentrated sulfuric acid, potassium permanganate or chromic acid. This is due to the energy of an unactivated $C-H$ bond of almost $400\,\text{kJ mol}^{-1}$. Selective oxidation is further complicated by $C-H$ bonds at the terminal carbon being $15\,\text{kJ mol}^{-1}$ higher than at the adjacent position. Hence, terminal oxidation suffers from low selectivity according to the relative bond strengths. Recently, alternative substrates such as fatty acids methyl esters from renewable plant oils have been used for biocatalytic oxidations (Schrewe et al. 2014). Besides linear substrates, there is a large range of further substrates that have been shown to be activated enzymatically such as cyclic/aromatic/branched alkanes, (cyclic/aromatic) alkenes, terpenes and more complex organic molecules (Beilen and Funhoff 2007).

1.2.5 Products and markets

Products from direct alkane oxidations are fatty alcohols, aldehydes and fatty acids. These find wide application in the chemical industry as well as the pharmaceuticals and cosmetics sectors, mainly as intermediates and building blocks. Applications may include fragrances and flavours (esp. aldehydes and acids) and fuels and intermediates for polymers (esp. alcohols). Biocatalytically produced diols and dicarboxylic as well as ω-hydroxy fatty acids have received particular interest as potential products for their use as monomers in the plastics industry (Huf et al. 2011; Lu et al. 2010; Song et al. 2013; Schaffer and Haas 2014).

A range of commercial bioprocesses for the activation of C – H bonds have been established (Liese, Seelbach, and Wandrey 2006). For examples, Lonza AG uses *Achromobacter xylosoxidans* LK1 in a whole-cell bioconversion to hydroxylate nicotinic acid at $12\,m^3$ scale. A more recent example commercialised by DSM is the epoxidation of styrene by the styrene monoxygenase from *Pseudomonas* sp. VLB120 in a two-liquid phase system (Panke et al. 2002).

Further, coupling terminal hydroxylation with transamination *in vivo* using a whole-cell biocatalyst allows the industrial production of the bifunctional Nylon precursor ω-aminododecanoic acid methyl ester from renewable resources (Ladkau et al. 2016; Evonik Industries AG 2013).

1.3 Enzymatic oxidation of alkanes

Despite their relative inertness as a chemical compound, numerous microorganisms able to oxidise a wide range of hydrocarbons have been identified early on (Leadbetter and Foster 1960; McKenna and Kallio 1965). Usually, the initial oxidation to a primary alcohol is followed by oxidation to the fatty acid, which enters the β-oxidation cycle and allows its use as carbon and energy source (Figure 1.1). Investigations into the pathways of aerobic alkane oxidation revealed molecular oxygen as the oxidant for the

hydroxylation of terminal methyl groups to a primary alcohol groups by prokaryotic and eukaryotic enzymes (Baptist, Gholson, and Coon 1963; Jones and Howe 1968).
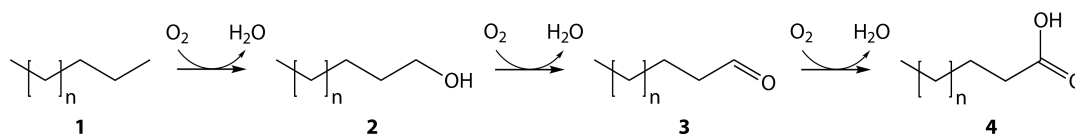
Figure 1.1: Alkane oxidation pathway; **1** – Alkane, **2** – 1-alcohol, **3** – aldehyde, **4** – fatty acid.

In past decades, research has been focused on few enzymes involved in hydrocarbon oxidation and their genetics (McKenna and Coon 1970; Grund et al. 1975; White and Coon 1980; Kok et al. 1989b) as well as process and industrial considerations (Schwartz and McCoy 1973; Nakahara, Erickson, and Gutierrez 1977).

More recently, with the advent of more powerful molecular biology techniques, it became apparent that there is a great diversity of alkane oxygenases in both, prokaryotic and eukaryotic organisms (Table 1.1) (Nelson et al. 1993; Smits et al. 1999; Beilen et al. 2003; Kubota et al. 2005; Prince, Gramain, and McGenity 2010).

Oxygenases are highly diverse in terms of their active site and co-factors, catalytic mechanisms, phylogenetic relationship and substrate specificity. Recent studies have revealed a large variety of homologous *alkb* and *cyp* genes from a range of organisms and environments (Nie et al. 2014). Oxygenases incorporate one (monooxygenases) or both (dioxygenases) oxygen atoms of molecular dioxygen into the substrate, in case of monooxygenases the remaining oxygen atom is protonated and reduced to water. Typically, they depend on a redox co-factor such as NAD(P)H, which functions as an electron donator, and thus are coupled to redox metabolism in whole cells, the most common form in which these oxidoreductases are applied for biocatalysis. Oxygenases generally require an organic or metallic co-factor to activate molecular oxygen upon donation of electrons. The formed reactive oxygen intermediate allows specific oxygenation of the organic substrate in the active size of the enzyme without causing uncontrolled oxidative damage to other biomolecules (Pazmino et al. 2010; Lewis, Coelho, and Arnold 2011).

Table 1.1: Overview of n-alkane oxidising enzyme classes, their characteristics and substrate range.

Enzyme class	Characteristics & co-factors	Substrate range	References
Haem-iron:			
Class I (CYP153)	Ferredoxin, ferredoxin reductase	C4–C16	Beilen et al. (2003)
Class II (CYP52)	Reductase	C10–C16	Rojo (2010b)
Di-iron:			
AlkB	Trimeric hydroxylase, rubredoxin, rubredoxin reductase	C4–C18	Beilen and Funhoff (2007) and Liu et al. (2014)
sMMO	$\alpha_2\beta_2\gamma_2$ hydroxylase, reductase, regulatory subunit	C1–C8	Beilen and Funhoff (2007)
sBMO	$\alpha_2\beta_2\gamma_2$ hydroxylase, reductase, regulatory subunit	C2–C9	Cooley et al. (2009)
Di-copper:			
pMMO	$\alpha_3\beta_3\gamma_3$ hydroxylase	C1–C5	Culpepper and Rosenzweig (2012)
Copper:			
Dioxygenase	Homodimeric hydroxylase	C10–C30	Maeng et al. (1996)
Flavin:			
LadA	Homodimeric hydroxylase	C15–C36	Wentzel et al. (2007)
AlmA		C24–C36	Wang and Shao (2014)

Recent years have seen important findings related to monooxygenases, their reaction mechanism, structure and identification of novel variants, leading to intensified biotechnological exploitation. In the following sections, the three major families of monooxygenases are introduced, namely the cytochrome P450s, the membrane-bound AlkBGT family and the methane monooxygenases. The focus is on their reaction mechanism and structure as it relates to alkane oxidation.

1.3.1 Cyctochrome P450

P450s have received considerable scientific and commercial interest for their crucial involvement in drug metabolism and their synthetic application potential (Grogan 2011; Paddon and Keasling 2014; Urlacher and Schulz 2014). With a sequence identity of often less than 20 %, it is a highly varied family (Gricman, Vogel, and Pleiss 2013).

Consequently, they have been found to be functionally versatile and have a high diversity in reaction chemistry and substrates, such as the hydroxylation of alkanes, the hydroxylation of rings and n-deisopropylation of propranolol during its metabolism as well as the reductive denitration of the explosive RDX (Munro et al. 2013). Nevertheless, this ubiquitous, highly divergent family of enzymes can be described by conserved structural and catalytic features around a haem prosthetic group (Figure 1.2) (Gricman, Vogel, and Pleiss 2013).

Further, they generally rely on a reductase to supply electrons from co-factors. P450s can be broadly categorised by their reductase type and activation of molecular oxygen in ten categories. The largest, Class I and II, account for over 90 % of P450s.
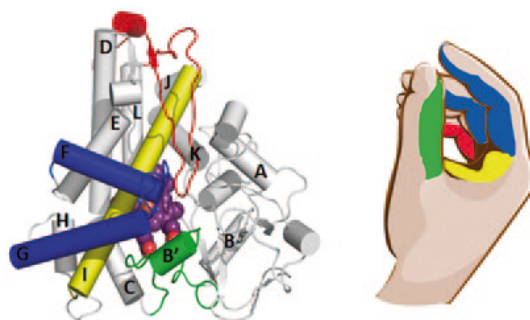
Figure 1.2: Cartoon representation of typical P450 fold, the haem co-factor atoms are coloured spheres, key structural helices for substrate binding are coloured and represented by a hand; adapted from McLean, Leys, and Munro (2015).

In class I, the P450 enzyme complex usually consists of three components, the hydroxylase (CYP), a FAD-reductase and ferrodoxin that shuttles electrons from co-factors (NAD(P)H) to the hydroxylase; this type predominantly includes prokaryotic and mitochondrial, membrane bound eukaryotic P450s. This is in contrast to class II in which P450s receive electrons via discrete soluble FAD- and FMN-containing reductases (Figure 1.3); these are mostly found in eukaryotes. However, the much-studied bacterial P450BM-3 is fused to a reductase domain containing two flavin prosthetic groups (FAD and FMN) (Class 8) (Munro, Girvan, and McLean 2007; Fasan et al. 2008; Whitehouse, Bell, and Wong 2012). This avoids low electron transfer rates due to suboptimal interaction between the P450 and the reductase. High levels of

uncoupling can lead to the undesired formation of reactive oxygen species and inactivation of the P450 and reduction in efficiency due to wasting reducing equivalents.

R-OH, H$_2$O   Reductase red   NAD(P)H + H$^+$
Monooxygenase
RH, O$_2$ Reductase ox   NAD(P)$^+$
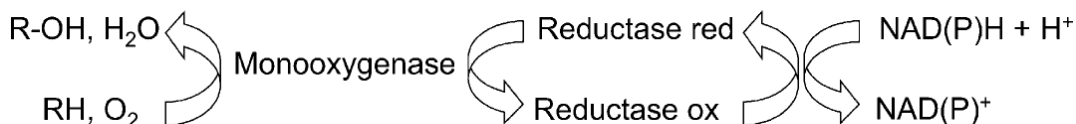
Figure 1.3: Typical P450 reaction scheme; adapted from Ayala and Torres (2004).

Extensive work has been done elucidating the reaction mechanism of P450s (Sono et al. 1996; Ortiz de Montellano 2010). All intermediate states of the reaction mechanism were experimentally observed and the general catalytic cycle is now widely accepted (Figure 1.4) (Ortiz de Montellano 2010; Whitehouse, Bell, and Wong 2012). The reaction mechanism of P450 monooxygenases can be conceptually separated into two processes. On the one hand, molecular oxygen is split by binding to the haem complex and subsequent heterolytic cleavage of the O – O bond. On the other hand, the hydrocarbon substrate is hydroxylated by the formed reactive haem species through a radical rebound mechanism.

The process begins in the resting state of the enzyme with the substrate binding and replacing a water molecule from the active site. Binding of the substrate allows the first electron transfer and reduction of the ferric haem iron to the ferrous state. The ferrous iron can then bind dioxygen and, after a further electron transfer and two protonation steps to the ferric-peroxyanion and ferric-hydroperoxo intermediates (Compound 0), the release of a water molecule results in the formation of the highly reactive porphyrin cation radical ferryl-oxo (Compound I). The abstraction of a proton from the substrate forms a protonated ferryl intermediate (Compound II) which hydroxylates the substrate radical through a radical rebound mechanism (Rittle and Green 2010). Subsequently the substrate is released.

Extensive protein engineering efforts have focused on improving stability or selectivity and substrate profile of P450s. Generally, substrate specificity is the result of three factors (Ortiz de Montellano 2010):
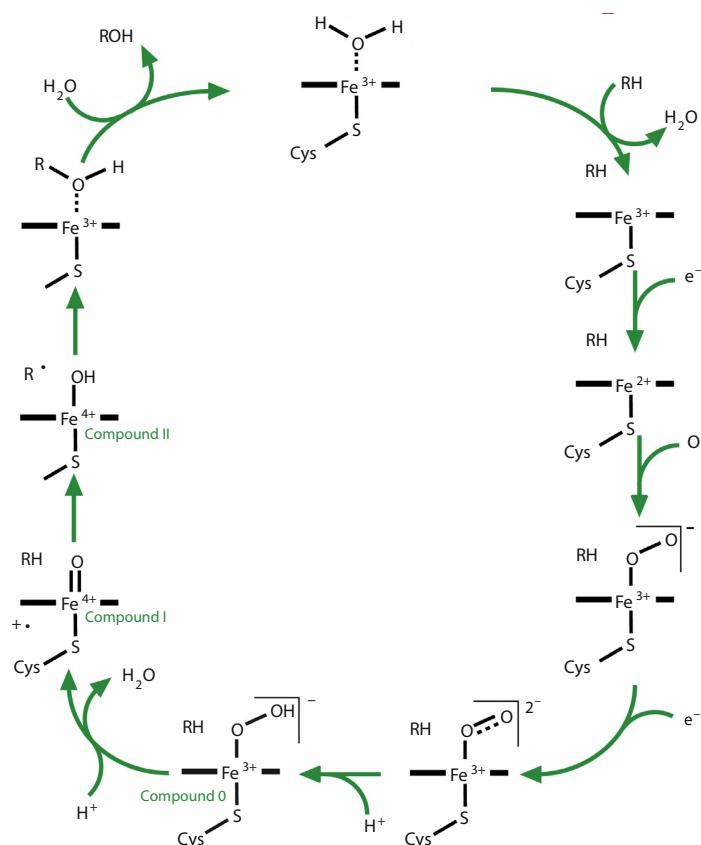
Figure 1.4: Generalised P450 catalytic cycle, the resting state haem at the top and the reactive species (Compound I), refer to text for detailed description; adapted from Girvan and Munro (2016).

- affinity of the substrate for the active site (function of substrate lipophilicity and its compatibility with active site architecture)

- intrinsic reactivity of individual C – H bonds in substrate, this is largely determined by C – H bond strength

- constraints of active site on oxidation reaction (substrate orientation/mobility relative to the haem-bound reactive oxygen)

For the monooxygenase P450 BM3 there is now a range of engineered variants accompanied by crystal structures that provide knowledge of the structure – function relationship of P450s (Landwehr et al. 2007; Jung, Lauchli, and Arnold 2011; Whitehouse, Bell, and Wong 2012). This has allowed semi-rational approaches to P450 enzyme engineering (Xu et al. 2005; Fasan et al. 2008; Chen et al. 2012).

1.3.2   Membrane-bound alkane hydroxylase

In contrast to P450s, the transmembrane alkane hydroxylases (EC: 1.14.15.3) do not contain a haem group, instead centre around a diiron active site. Similarly to P450s, this group of enzymes are monooxygenases, removing a single oxygen atom from molecular oxygen to hydroxylate its substrate. The most characterised alkane hydroxylase is AlkB from *Pseudomonas putida* GPo1 harboured on the OCT-plasmid (Beilen, Wubbolts, and Witholt 1994). Despite, an array of homologs having been identified (Smits et al. 1999; Wang et al. 2010; Bertrand et al. 2013), the genetic analysis of environmental samples by Jurelevicius et al. (2013) suggests that there is an as yet uncharacterised diversity of *alkB* genes.
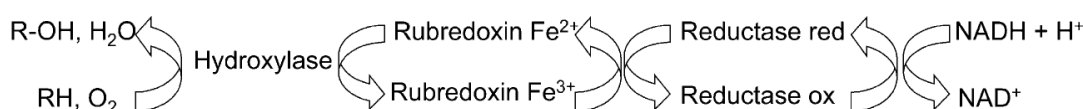
Figure 1.5: Typical AlkB reaction scheme; adapted from Ayala and Torres (2004).

The AlkBGT alkane hydroxylase complex from *Pseudomonas putida* GPo1 is composed of the membrane bound monooxygenase AlkB (Kok et al. 1989b) and the soluble electron transfer proteins AlkT (rubredoxin reductase) (Eggink et al. 1990) and AlkG/AlkF (rubredoxins) (Kok et al. 1989a; Beilen et al. 2002) that channel electrons from NADH to AlkB in order to reduce the remaining oxygen to water (Figure 1.5) (Beilen et al. 2001).

Further identified components of the system from *Pseudomonas putida* GPo1 include the AlkJ alcohol dehydrogenase (Kirmair and Skerra 2014), AlkH aldehyde dehydrogenase (Kok et al. 1989a), AlkK acyl-CoA synthetase (Beilen et al. 1992), AlkL outer membrane transport channel for hydrophobic substrates (Julsing et al. 2012; Grant et al. 2014) and AlkS regulatory protein of AlkB system expression (Canosa et al. 2000) (Figure 1.6). AlkN is a putative methyl-accepting chemotaxis protein (MCP) (Beilen et al. 1992; Wang and Shao 2013). Ultimately, this pathway allows metabolism of alkanes via the β-oxidation cycle (Beilen et al. 2001).
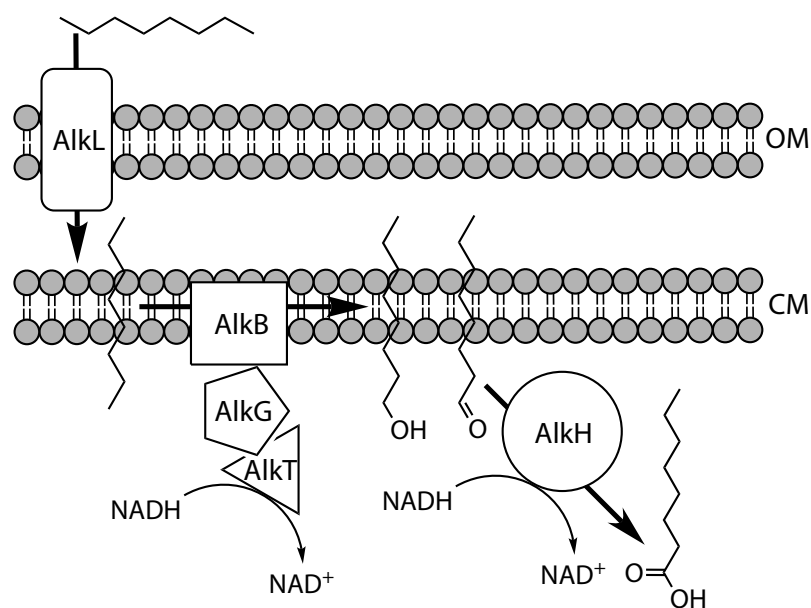
Figure 1.6: AlkBGT enzyme system; alkane hydroxylase AlkB, rubredoxin AlkG, rubredoxin reductase AlkT, aldehyde dehydrogenase AlkH, outer membrane transport channel AlkL, outer membrane OM, cytoplasmic membrane CM.

It has proven difficult to isolate and purify the integral membrane protein AlkB (Austin et al. 2015). Consequently, the structural and kinetic characterisation of this monooxygenase has been slow and relied on whole cells, or partially purified extracts.

Beilen, Penninga, and Witholt (1992) first proposed a topology model for AlkB based on fusion studies with alkaline phosphatase and β-galactosidase. This led to the prediction for AlkB of a hexagonal structure consisting of six transmembrane alpha-helices forming a hydrophobic pocket (Figure 1.7). The N-terminus, two-hydrophilic loops and C-terminus are in the cytoplasm, only three short loops are exposed to the periplasm. However, little is known about the spatial arrangement and relative alignments of the transmembrane helices due to the lack of a three-dimensional structure of AlkB or related enzymes. Alonso and Roujeinikova (2012) reported the two-dimensional arrangement of AlkB in agreement with the previously proposed model (Figure 1.8). The study proposes a trimeric structure for AlkB with the transmembrane helices in a mostly perpendicular orientation relative to the membrane.

Further, several important amino acid positions have been identified to be re-
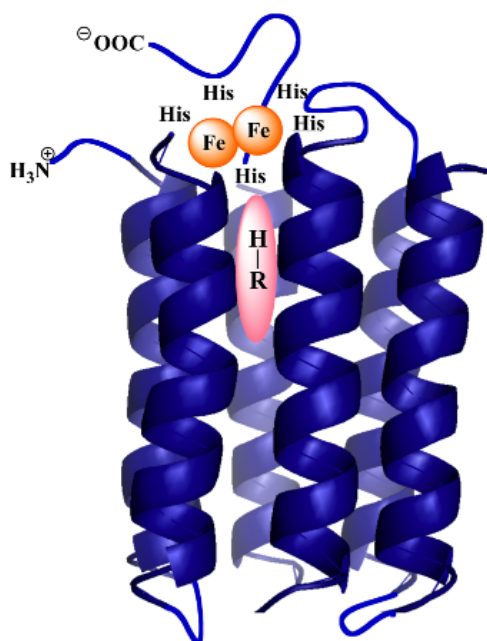
Figure 1.7: Cartoon representation of proposed AlkB structural model with six transmembrane helices forming substrate pocket, catalytic iron atoms are coloured spheres with substrate present; adapted from Cooper et al. (2012).

sponsible for binding the active site iron atoms as well as involved in the substrate binding and specificity (Beilen, Kingma, and Witholt 1994; Beilen et al. 2005; Rojo 2005). This further clarified the hydrophobic pocket as the substrate pocket and the nature of its substrate selectivity. Eight conserved histidine residues were identified that vitally coordinate the two catalytic iron molecules locating the active site towards the cytoplasm (Shanklin and Whittle 2003). Additional work supports the established structural model and critical residues (Alonso et al. 2014). To date, it has not been possible to further elucidate the three-dimensional structure of AlkB.

As a consequence of the little structural data and difficulty of purifying the enzyme, the reaction mechanism of AlkB is less well understood. Unlike with P450s, the reaction mechanism is mostly studied using diagnostic substrates such as norcarane, but is not directly observable through methods such as cryospectroscopy (Denisov, Grinkova, and Sligar 2012).

Experimental data supports a radical-rebound mechanism where a long-lived substrate radical is formed from hydrogen abstraction by an iron-oxo intermediate
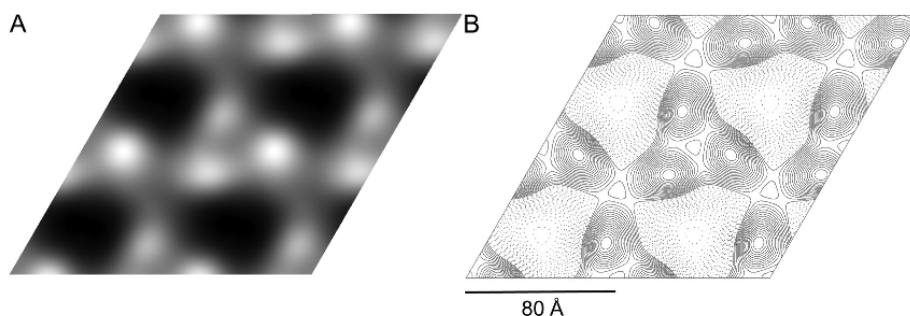
Figure 1.8: Reconstruction of 2D lipid-reconstituted AlkB crystal; A – projection map, protein shown in white over dark background, B – reconstruction map, trimer formation with elliptical monomers of 40 Å by 30 Å; adapted from Alonso and Roujeinikova (2012).

(Austin et al. 2008; Cooper et al. 2012; Naing et al. 2013). This is similar to the P450 mechanism where the Compound I intermediate is responsible for C – H hydroxylation. However, no intermediates of the AlkB reaction cycle have been elucidated.

Consequently, the rational modification of AlkB for biotechnological application has largely been hindered by the lack of detailed information about amino acids residues at the catalytic site or the substrate pocket. One study used directed evolution to improve butane oxidation by AlkB with very high selectivity for the primary alcohol (Koch et al. 2009).

1.3.3 Methane monooxygenases

A further class of alkane activating oxgenases are the methane monooxygenases (MMO). There are two distinct MMOs that catalyse the oxidation of methane to methanol: membrane bound particulate MMO (pMMO - EC 1.14.18.3) and soluble MMO (sMMO - EC 1.14.13.25). Whereas sMMOs are thought to have a diiron centre, pMMOs have a dicopper unit to split molecular oxygen for activation of short chain alkane C – H bonds.

Soluble methane monooxygenases

The sMMO quaternary structure has been found to consist of a dimeric $\alpha_2\beta_2\gamma_2$ architecture. The active site, diiron coordinated by four glutamate and two histidine residues, is situated within a helical bundle of the alpha subunits (Tinberg and Lip-

pard 2011). Similarly to AlkB and P450, sMMOs consist of a FAD/[2Fe-2S]-reductase (MMOR) and an additional regulatory protein (MMOB or Protein B) (Lee et al. 2013). The MMOB component is likely to competitively inhibit binding of the reductase to the hydroxylase in resting state and thereby controlling the flow of electrons from NAD(P)H to the hydrolase (Wang et al. 2014). To initiate the catalytic cycle, the reductase displaces the MMOB from the hydroxylase and reduces the diiron catalytic site. Next the regulatory protein rebinds displacing the MMOR, and thereby initiates activation of molecular oxygen and substrate binding and oxidation (Wang and Lippard 2014). Only at the end of the catalytic cycle once the hydroxylase returns to its resting state can the reductase bind again for the next catalytic cycle.
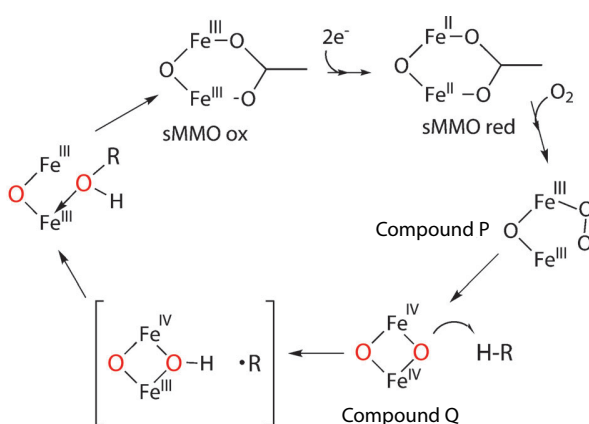
Figure 1.9: Generalised soluble methane monooxygenase catalytic cycle, the resting state active site at the top and the reactive species (Compound Q), refer to text for detailed description; adapted from Austin and Groves (2011).

The sMMO catalytic cycle has been investigated to some detail and a consensus pathway has focused on the catalytically active Compound Q (Figure 1.9) (Baik et al. 2003; Tinberg and Lippard 2011). The proposed mechanism is similar to P450 except that molecular oxygen binds to the reduced active site to form a diferric-peroxo species (Compound P) followed by homolytically cleavage to generate the diferryl Compound Q. A radical rebound has been proposed as the mechanism for hydrocarbon hydroxylation by Compound Q.

Particulate methane monooxygenases

In contrast to soluble MMOs, pMMOs have a trimeric $\alpha_3\beta_3\gamma_3$ architecture and a histidine coordinated dicopper active site. There is good evidence that the active site is located in the soluble beta subunit facing the periplasmic side of the membrane (Balasubramanian et al. 2010; Culpepper and Rosenzweig 2012; Culpepper et al. 2012; Culpepper et al. 2014). In addition, there is a further copper site in the beta subunit and a mononuclear site coordinated between the alpha and gamma subunits; these metal centres are not conserved. An associated reductase is not known (Culpepper and Rosenzweig 2012). The overall catalytic cycle remain unknown, however, recent work has proposed a bis(μ-oxo) dicopper(III) complex responsible for C−H bond cleavage (Da Silva et al. 2016).

1.4 Whole-cell bioprocess considerations

Despite recent developments in cell-free biocatalytic redox reactions (Kara et al. 2013) there are few successful examples of isolated monooxygenases for hydrocarbon oxidation with *in situ* co-factor regeneration (Hollmann et al. 2005; Staudt et al. 2012; Müller et al. 2013). The main issue remains co-factor regeneration (Funhoff and Beilen 2007; Holtmann et al. 2014). The complexity of the AlkB enzyme system, in particular as an integral membrane protein, complicates its use in cell-free processes. Thus, for economic reasons whole-cell processes are often the preferred option for industrial biocatalytic redox reactions (Tufvesson et al. 2011). The following sections focus on considerations around alkane oxidation bioprocesses.

1.4.1 Two-liquid phase concept

Two-liquid phase (2LP) processes are routinely used in bioprocesses to supply substrates that are sparingly water soluble. In case of alkane bio-oxidations, the whole-cell biocatalyst is suspended in the aqueous phase, whilst an immiscible non-polar organic phase frequently consists of the alkane substrate (Favre-Bulle et al. 1993; Wubbolts,

Favre-Bulle, and Witholt 1996; Bühler and Schmid 2004). These aqueous-organic two-liquid phase systems aim at compartmentalising the biocatalyst in the aqueous phase on the one side and the non-polar substrate and products in the organic phase on the other side (Wubbolts et al. 1994). This separation can reduce potential inhibition or toxicity of substrate or products towards the biocatalyst, ultimately increasing the biocatalyst stability and avoiding reaction product metabolisation. In addition, the reaction kinetics and equilibrium can be influenced in favour of product synthesis (Bühler et al. 2003; Schrewe et al. 2014). The selective accumulation of product in the organic phase can also facilitate product recovery during downstream processing or allow continuous removal of product (Daugulis 1988; Kollmer and Rohr 1998; Mathys, Kut, and Witholt 1998; Mathys et al. 1998; Dafoe and Daugulis 2013). In case of alkane oxidation the dilution in an inert auxiliary solvent can also facilitate the safe operation by reducing flammability of the organic phase (Schmid et al. 1999).

To similar ends, a range of variations of this concept have been exploited for biocatalysis where the auxiliary phase consists of a polymer solution (aqueous two-phase system) (Kühn 1980; Tonova and Lazarova 2008), non-ionic surfactants (cloud point system) (Wang et al. 2008b; Glembin, Kerner, and Smirnova 2013) or ionic liquids (Pfruender, Jones, and Weuster-Botz 2006; Oppermann, Stein, and Kragl 2010). These systems generally have a more polar auxiliary phase to allow *in situ* extraction of more polar products (Figure 1.10a). Depending on the ratios of the ternary mixture of water, hydrocarbon substrate and amphiphilic auxiliary phase, these complex systems can form a variety of different microemulsions (Figure 1.10b) (Tonova and Lazarova 2008; Correa et al. 2012; Sintra, Ventura, and Coutinho 2014). The complexity of these systems is increased further by the large influence of temperature on the phase morphology (Myers 1999).

Despite emulsion formation being advantageous for mass-transfer due to solubilisation, the formation of stable emulsions in 2LP bioconversions can complicate
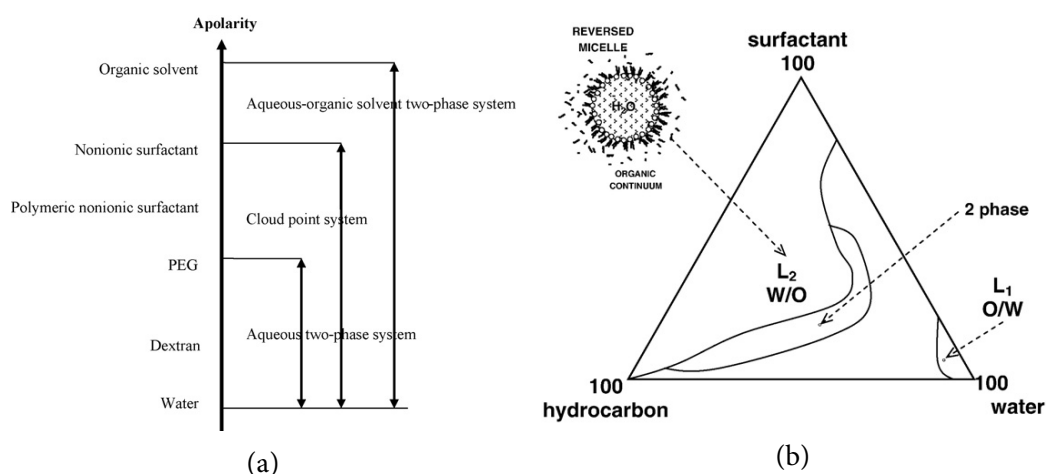
Figure 1.10: Schematic representation of (a) polarity spectrum of various two-liquid phase systems (adapted from Wang and Dai (2010)) and (b) phase behaviour in a general ternary mixture hydrocarbon/surfactant/water (adapted from Tonova and Lazarova (2008)).

downstream processing (Kollmer 1997; Brandenbusch et al. 2010). The increased difficulty of phase separation and product extraction can negatively impact the overall process economics (Mathys et al. 1998). There are a wide range of factors influencing emulsion formation and stability including synthetic or biological amphiphilic substances (Schmid, Kollmer, and Witholt 1998; Perfumo et al. 2010; Ławniczak, Marecik, and Chrzanowski 2013). Recently, the impact of the whole-cell biocatalyst and its physiology on emulsion formation and stability has been shown (Collins et al. 2015). The complexity of two-phase systems is reinforced by the mass transfer considerations and their impact on the reaction kinetics (Kollmer et al. 1999; Schmid, Sonnleitner, and Witholt 1998; Schrewe et al. 2014). Table 1.2 summarises some advantages and disadvantages of these systems as they relate to biocatalytic processes.

With this complexity and diverse interactions in mind it becomes clear that an integrated approach to process, reaction and biological engineering for 2LP biooxidations would be most effective (Lundemo and Woodley 2015).

1.4.2 Hydrophobic substrate uptake

There are two mechanisms by which the hydrophobic substrate can be accessed by a whole-cell biocatalyst from the organic phase (Figure 1.11) (Déziel, Comeau, and

Table 1.2: Potential advantages and disadvantages of two-liquid phase bioprocesses; adapted from Kollmer and Rohr (1997) and Lye and Woodley (2001).

Advantages	Effect on process	Disadvantages	Effect on process
Reduction of inhibitory or toxic substances in the aqueous phase	Higher productivity	Inhibition or toxicity of solvent	Loss in viability, lower productivity
Solubilisation of poorly water soluble substances	Higher productivity / Simplification of substrate addition	Emulsification	Complication of downstream processing
Higher substrate and product concentrations possible	Higher productivity	Mixing/Mass transfer limitations between phases	Lower productivity
Simplified isolation of biocatalyst and product	Simplification of downstream processing	Foaming	Reduced operational stability
		Explosion hazard	Safety measures necessary

Villemur 1999; Harms, Smith, and Wick 2010; Parales and Ditty 2010; Hua and Wang 2014). The hydrophobic substrate can pass into the aqueous phase within its solubility limits before being taken up and converted to an oxidised product by the biocatalyst. To maintain the thermodynamic equilibrium further substrate molecules solubilise in the aqueous phase. In case the maximum activity of the catalyst is not reached at the maximum solubility of the substrate, the production rate will be limited by the substrate mass transfer rate (B in Figure 1.11). Conversely, the reaction products will accumulate in the organic phase relative to their solubility (A in Figure 1.11). Another way of substrate uptake is by direct contact of the microorganism with the organic phase at the phase boundary (C in Figure 1.11). It is likely that in *E. coli* the former is the predominant uptake path (Grant et al. 2012). Although, specialised hydrophobic microbial consortia have been reported that predominantly associate with the organic

phase (Muñoz et al. 2013).
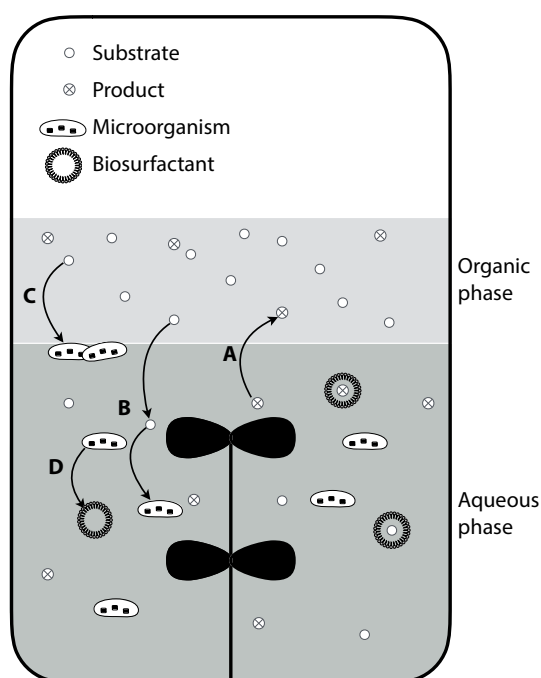
Figure 1.11: Transport processes in two-liquid phase processes: A – solution of hydrophobic products in organic phase, B – uptake of dissolved substrate in aqueous phase, C – interfacial uptake of substrate, D – interaction with micelles by microbes; adapted from Déziel, Comeau, and Villemur (1999).

Thus, both mechanisms seem to play a role although it is difficult to test experimentally as an increase in the phase boundary area will increase not only the area available for cell contact, but also the mass transfer rate. In any case, the droplet size is an important measurement, as interfacial area increases with smaller droplets (Schmid 1997; Kollmer et al. 1999; Cull et al. 2002).

Lastly, the presence of surfactants can result in the formation of hydrocarbon micelles and increased mass transfer (D in Figure 1.11). Especially in *Pseudomonas* spp. biosurfactants are produced in response to hydrocarbon exposure (Schmid, Kollmer, and Witholt 1998; Ławniczak, Marecik, and Chrzanowski 2013). In other bacterial cultures, the presence of other surface active biological compounds often results in emulsification of two-liquid phase (Collins et al. 2015). The use of synthetic surfactants is well documented for hydrocarbon degradation, as well (Keane, Lau, and Ghoshal

2007; Li and Chen 2009).

A further aspect that needs to be considered in transport and uptake of hydrophobic compounds is the lipopolysaccharide (LPS) layer of gram-negative bacteria that presents an effective barrier for these compounds (Nikaido 2003). The polar nature of the polysaccharide component reduces the diffusion of small hydrophobic by 100 to 150 times compared to a usual phospholipid bilayer (Chen 2007).

Thus, whilst the AlkB monooxygenase is situated in the inner membrane allowing access to hydrocarbon substrates solubilised in its lipophilic core, substrate mass transfer across the outer membrane barrier can pose a rate limiting step. This makes permeability of LPS an important issue in the development of biocatalysts and bioprocesses (Chen 2007). In fact, changes to the outer membrane by mutation has been shown to impact cellular adhesion, susceptibility to and oxidation reaction rates of hydrophobic molecules (Aono and Kobayashi 1997; Ni and Chen 2004; Ni and Chen 2005).

Recently, transmembrane channels have been identified that facilitate the diffusion of hydrophobic substrates across the outer membrane (Hearn et al. 2009; Berg 2010; Lepore et al. 2011). Increasingly, there have been efforts to include membrane transporters into the cellular engineering toolkit for increased flux control in whole-cell biocatalysis (Kell et al. 2015). This is in addition to solvent tolerance engineering in microbial catalysts where specifically transporters have emerged as a powerful tool (Mukhopadhyay 2015). Several channel proteins, such as the AlkL channel from the OCT plasmid of *Pseudomonas putida* GPo1, have been used to reduce substrate limitations during the whole-cell catalysis of hydrophobic compounds (Julsing et al. 2012; Cornelissen et al. 2013; Call et al. 2016).

1.4.3 Toxicity of organic solvents

Non-polar solvents such as alkanes are toxic mainly due to their accumulation in and disruption of cell membranes (Sikkema, Bont, and Poolman 1995; Heipieper and

Martínez 2010). This preferential partitioning in membranes causes an increase in its fluidity leading to non-specific permeabilisation and destabilisation, ultimately causing cell lysis.

The partition coefficient log*P* of an organic solvent between 1-octanol and water has been shown to be proportional to the toxicity of the solvent (Equation 1.1). As a rule of thumb, solvents with a log*P* larger than 4 are generally regarded to be biocompatible (Laane et al. 1987).

$$logP_{oct/wat} = log \left(\frac{[solute]_{octanol}}{[solute]_{water}} \right)$$ (1.1)

Table 1.3 shows that log*P* values for substrates and products of an alkane oxidation increase with increasing carbon chain length. The reaction products generally show lower log*P* values in the proposed toxic range. Their relative polarity adds to the toxicity.

Table 1.3: Exemplary partition coefficient (log*P*) values for C6, C8 and C12 alkanes and oxidation products; data from Lide (2005).

Carbon chain length	Functionality	Partition coefficient (log*P*)
C6	Alkane	4.0
C6	1-Alcohol	2.0
C6	Aldehyde	1.8
C6	Acid	1.9
C8	Alkane	5.2
C8	1-Alcohol	3.1
C8	Aldehyde	3.2
C8	Acid	3.1
C12	Alkane	6.1
C12	1-Alcohol	5.0
C12	Aldehyde	5.6
C12	Acid	4.5

The log*P* parameter is particularly useful as it can be predicted based on the molecular structure of the solvent independent of experimental measurements. Nevertheless, the impact of other factors such as the cell membrane and cell wall structure of

a particular microorganism make empirical measurements necessary to confirm the biocompatibility. In addition, compounds with additional functional groups, such as aldehydes or epoxides, are usually more toxic than their log$P$ value indicates due to their additional, specific chemical toxicity (Vermuë et al. 1993). For organic acids, toxicity depends on pH and thus the concentration of the protonated form, with exposure triggering changes in outer and inner membrane physiology (Royce et al. 2013).

Consequently, Filho et al. (2003), postulate that log$P$ is a poor generalisation of solvent compatibility for biocatalytic reactions. They show that especially the chemical functionality has to be considered when selecting solvents for a two-phase system.

Cellular response to organic solvents

Not only does solvent toxicity depend on physicochemical parameters but also on intrinsic tolerance mechanisms of bacterial species and strains. In general, gram-negative bacteria have several mechanisms that lead to their solvent tolerance towards hydrocarbons. They include the metabolism of toxic to non-toxic compounds, changes in membrane composition and fluidity, efflux of toxic compound and formation of vesicles to bind toxic compounds (Ramos et al. 2002; Segura et al. 2012). Changes in the saturated fatty acid as well as *trans*-isomer content of cellular membrane as a response to solvent exposure increases their rigidity and stability. Other observed effects are the alteration of lipopolysaccharide composition (Rühl et al. 2012). A range of efflux proteins have been identified that actively remove toxic compounds from the cytoplasm such as multidrug resistance efflux systems (Nikaido and Takatsuka 2009; Dunlop et al. 2011). Further, chaperons have been identified to be upregulated to ensure correct protein folding in the presence of solvents. Generally, there are increasing efforts to exploit natural adaptation mechanisms for engineering biocatalysts towards improved tolerance (Nicolaou, Gaida, and Papoutsakis 2010; Dunlop 2011; Lo et al. 2013).

Host considerations

Pseudomonas spp. are examples of particularly solvent resistant bacteria (Poblete-Castro et al. 2012; Krell et al. 2012; Udaondo et al. 2012). These gram-negative bacteria have evolved to adapt to a range of environmental challenges gaining not only resistance to a diverse range of solvents but also to metabolise these compounds as carbon and energy sources using monooxygenases such as AlkB (Ramos et al. 2009). *Escherichia coli* on the other hand is generally regarded as less tolerant to harsh environments and increasing tolerance towards solvents remains a challenge for production of bulk chemicals. It is recognised that merely increasing tolerance does not necessarily result in greater productivities (Dunlop 2011).

The complex interaction of stress responses with engineering efforts to increase yields needs to be studied on a systems levels to balance both and maximise overall productivity (Nicolaou, Gaida, and Papoutsakis 2010). Thus, research has focused on holistically understanding biocatalytic processes for their optimisation (Kuhn et al. 2010). This includes quantitatively studying the microbial physiology based on a systems biology approach and integrating this with systematic strain and process engineering. This is explicitly important for whole-cell redox reactions due to their requirement for co-factor regeneration and resulting integration with cellular metabolism (Blank et al. 2008a; Blank et al. 2010). Characterisation studies for two-phase systems have revealed a clear correlation between biocatalytic activity and metabolic activity in response to organic solvents (Bühler et al. 2008; Blank et al. 2008b; Olaofe et al. 2013; Kuhn et al. 2013). Vallon et al. (2013) outline the potential of *Pseudomonas putida* as a production host due to its ability to boost cellular metabolism to provide enough reductive potential to maintain energy demanding tolerance mechanisms such as active efflux systems as well as productivity.

Thus especially for a two-phase system it is not only important to optimise the enzymatic catalysis but also microbial physiology and metabolism of the whole cell

biocatalyst either by engineering or by choice of host (Volmer, Schmid, and Bühler 2015). This includes screening for different host strains, carbon and energy sources and feeding strategies to optimise cellular energy demands, resistance to solvents and ultimately biocatalytic productivity (Cornelissen et al. 2011; Ebert et al. 2011; Kuhn et al. 2013). Several systematic studies have recently identified targets and strategies for improving performance of *E. coli* strains in the presence of high concentrations of alcohols (Woodruff, Boyle, and Gill 2013; Abdelaal et al. 2014; Peabody and Kao 2016) and fatty acids (Lennen et al. 2011; Royce et al. 2015; Tan et al. 2016).

1.5 Microscale tools for two-liquid phase systems

Numerous challenges remain to achieve industrially competitive space time yields and product titers for bio-oxidations (Schrewe et al. 2013). To improve on this, the ability to rapidly screen bioconversion reactions for characterisation and optimisation is of major importance in biocatalyst selection and process development (Baboo et al. 2012; Neubauer et al. 2013). Further, the search for more efficient bioprocesses and their industrial adoption is increasingly leading to the integration of bioprocess development with biocatalyst development (Cuellar, Heijnen, and Wielen 2013; Neubauer et al. 2013; Woodley, Breuer, and Mink 2013). Studies at lab scale are time consuming and labour intensive with low experimental throughput. In recent years a range of sophisticated scale-down systems (<10 ml) have emerged with new monitoring and control strategies to accelerate conventional bioprocess development (Long et al. 2014; Lattermann and Büchs 2015; Wewetzer et al. 2015). These systems range from microwell plates (Duetz 2007; Fernandes 2010) to miniaturised bioreactors (Betts and Baganz 2006).

Several key engineering issues have been extensively characterised at small scale such as mixing, oxygen transfer, power input and hydrodynamic stress in microwell plates (Duetz and Witholt 2004; Hermann, Lehmann, and Büchs 2002; Micheletti et al. 2006; Zhang et al. 2008; Funke et al. 2009), shake flasks (Peter et al. 2006; Peter,

Suzuki, and Büchs 2006; Büchs et al. 2007; Suresh, Srivastava, and Mishra 2009; Tan, Eberhard, and Büchs 2011; Klöckner and Büchs 2012), miniature bioreactors (Lamping et al. 2003; Weuster-Botz et al. 2005; Betts, Doig, and Baganz 2006) and bubble column reactors (Doig et al. 2005; Doig et al. 2008). In particular microwell plate (MWP) with square wells and pyramidal bottoms have been shown to provide good mixing and oxygen transfer (Duetz and Witholt 2004; Islam et al. 2007) The advantages of these technologies for biocatalytic process development has been shown for a range of applications including the scale-up to pilot plant scale (Ferreira-Torres, Micheletti, and Lye 2005; Islam et al. 2008; Marques et al. 2010; Grant et al. 2012; Baboo et al. 2012).

Thus microscale technologies for the high-throughput screening and characterisation of processes and biocatalysts are of crucial importance for the rapid evaluation and optimisation of bioprocesses. However, research is almost exclusively focused on aqueous single-phase systems rather than more complex non-conventional media. There have been only few examples of studies involving a microscale aqueous-organic two-phase system (Marques et al. 2009; Giese et al. 2014; Schlepütz and Büchs 2014). Very little work on alkane oxidation has been carried out in MWPs (Grant et al. 2012). A range of studies used other microscale approaches such as Eppendorf tubes with a working volume of 0.5 ml (Scheps et al. 2011) or sealed glass screw cap vials (Nodate, Kubota, and Misawa 2006; Bordeaux et al. 2011; Gudiminchi et al. 2012; Olaofe et al. 2013) (total volume ranging from 12 ml to 40 ml with 1 ml to 5 ml liquid phase). In addition, there have been no attempt to systematically characterise the mixing and mass transfer of aqueous-organic two-phase systems in shaken scale-down systems.

Further, no studies report the successful application of highly volatile organic substrates in two-liquid phase systems. Although, a commercialised small-scale platform exists for the parallel screening at extreme conditions in terms of pressure and temperature (Allwardt et al. 2008). Several factors may be responsible for the difficulties encountered when scaling-down two-phase systems. Marques et al. (2007)

note the interaction of an undefined polymer plate material with dioctyl phthalate. Further studies recognise the difficulties of volatile organic phases at microscale requiring tightly capped vessels to control evaporation (Marques et al. 2009; Baboo et al. 2012). Heinig et al. (2010) report instability and absorption/adsorption issues of commonly used plate materials such as polystyrene, polyethylene and particularly polypropylene when used with organic solvents and isoprenoids. Further they found that even glass-coated plates selectively adsorb lipophilic products resulting in poor recoverability and reproducibility in subsequent analysis. Similarly, many of the optical online measuring techniques used in scale-down setups are incompatible with organic solvents diminishing the usefulness and applicability of these systems (Ramesh et al. 2015). This is in addition to frequently reported location bias in microwell plates due to evaporation or temperature gradients in commercial MWP systems (Grosch et al. 2016).

The frequent use of non-standardised tools make method transfer difficult and reduce the ability to run reactions in parallel whilst reducing manual handling. This complicates routine use and is prone to introducing variability ultimately hindering adoption of high-throughput methods for biocatalysis in non-conventional media. The significant negative economic impact of prevalent low reproducibility has been recently documented and discussed (Freedman, Cockburn, and Simcoe 2015). Generally, the reproducibility and robustness of applied methods is central to this discussion (Goodman, Fanelli, and Ioannidis 2016). In bioprocess development automation of experimental tasks has been an important step towards ensuring reproducibility of results. Recently, interesting expansions on managing reliability of results in this field have been made. A particular focus is on reducing ambiguity and complexity when communicating and executing research to enable computer aided design and optimisation and avoid human error (Galdzicki et al. 2014; Beal, Adler, and Yaman 2015; Sadowski, Grant, and Fell 2016).

1.6   Aims and objectives

Studies at lab scale are time consuming and labour intensive with low experimental throughput. The ability to rapidly screen bioconversion reactions for characterisation and optimisation is of major importance for accelerating bioprocess development. This study aimed to overcome issues of microscale tools for the characterisation of oxidative bioconversions in non-conventional media and to implement a customised high-throughput platform. Primarily, the use of highly volatile n-alkane substrates as a second, organic phase was investigated. Equally, methods were investigated to increase the information output and utility at this scale to be able to quantify not only product concentrations but also metabolic parameters and interactions between parameters. Resultant specific aims of the project are listed below:

- establish a microwell platform customised for the systematic characterisation of the bio-oxidation of volatile alkanes in non-conventional media (Chapter three)

- demonstrate the reliability and mixing characteristics of the developed platform (Chapter three)

- investigate the extension of the platform by a fed-batch implementation (Chapter four)

- evaluate process options to overcome previously identified bottlenecks such as phase toxicity leveraging the developed platform (Chapter five)

Chapter 2

Materials and methods

Unless otherwise mentioned, the work in all chapters draws on the following materials and methods.

2.1   Strains and plasmids

For all bioconversions *Escherichia coli* GEC137 pGEc47ΔJ (Figure 2.1) was used (Beilen et al. 1992; Eggink et al. 1987). pGEc47ΔJ contains all alkane oxidation genes of the OCT plasmid of *Pseudomonas putida* GPo1 (formerly known as *Pseudomonas oleovorans*), except the deleted alcohol dehydrogenase gene *alkJ*, cloned into the broad host range vector pLAFR1 (Friedman et al. 1982; Vanbleu, Marchal, and Vanderleyden 2004).

2.2   Media composition

2.2.1   Growth medium

The aqueous phase used for fermentations was as described by Wubbolts, Favre-Bulle, and Witholt (1996): KH_2PO_4, $4\,\mathrm{g\,l^{-1}}$; K_2HPO_4 ($3\,H_2O$), $15.9\,\mathrm{g\,l^{-1}}$; NH_4Cl, $0.2\,\mathrm{g\,l^{-1}}$; $(NH_4)_2SO_4$, $1.2\,\mathrm{g\,l^{-1}}$; Na_2HPO_4 ($12\,H_2O$), $7\,\mathrm{g\,l^{-1}}$; L-Proline, $0.6\,\mathrm{g\,l^{-1}}$; L-Leucine, $0.6\,\mathrm{g\,l^{-1}}$; yeast extract, $5\,\mathrm{g\,l^{-1}}$ (all Sigma-Aldrich, UK); thiamine, $5\,\mathrm{mg\,l^{-1}}$ (Alfa Aesar, UK); sterilised by autoclaving. The pH was adjusted to 7.2 before autoclaving.
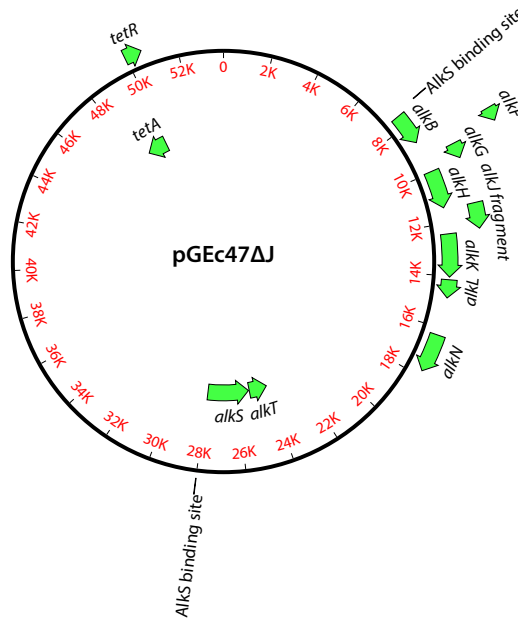
Figure 2.1: Plasmid map of pGEc47ΔJ.

The following were heat sterilised separately and added subsequently: $MgSO_4$ (7 H_2O), $1\,g\,l^{-1}$; D-glucose, $10\,g\,l^{-1}$ (all Sigma-Aldrich, UK); $CaCl_2$ (2 H_2O) $0.04\,g\,l^{-1}$; (Alfa Aesar, UK); and $1\,ml\,l^{-1}$ of the following trace elements. Further, filter sterilised tetracycline, $15\,mg\,l^{-1}$ (all Sigma-Aldrich, UK) was added. The pH was routinely measured at 7.1 after additions.

The trace element solution contained per litre of $5\,mol\,l^{-1}$ HCl: $FeSO_4$ (7 H_2O), 40 g; $MnSO_4$ (H_2O), 10 g; $CoCl_2$ (6 H_2O), 4.75 g; $ZnSO_4$ (7 H_2O), 2 g; H_3BO_3, 0.5 g; MoO_4Na_2 (2 H_2O), 2 g; (all Sigma-Aldrich, UK); $CuCl_2$ (2 H_2O), 1 g (Riedel-de Haën, Germany).

Tetracycline stock solutions were made at $15\,g\,l^{-1}$ from tetracycline hydrochloride (Sigma-Aldrich, UK) in $0.5\,ml\,ml^{-1}$ ethanol. Aliquots of the stock solution were stored at $-20\,°C$.

2.2.2 Bioconversion buffer

For bioconversion reactions with resting cells a $150\,mmol\,l^{-1}$ potassium phosphate buffer (adjusted to pH 7.2) with thiamine, $5\,mg\,l^{-1}$ was supplemented with separately heat sterilised: $MgSO_4$ ($7\,H_2O$), $1\,g\,l^{-1}$; D-glucose (all Sigma-Aldrich, UK), according to experimental design; $CaCl_2$ ($2\,H_2O$), $0.04\,g\,l^{-1}$ (Alfa Aesar, UK); and $1\,ml\,l^{-1}$ of the above trace elements (subsection 2.2.1). Further, filter sterilised tetracycline (all Sigma-Aldrich, UK), $10\,mg\,l^{-1}$ was added. The pH was routinely measured at 7.1 after addition.

2.2.3 Further hydrocarbon substrates

All n-alkane substrates were purchased from commercial sources (Sigma-Aldrich, UK) at the highest available purity (>99 %).

2.3 Two-liquid phase bioconversion in shaken microwell plates

2.3.1 Microwell plates

Bioconversions were carried out in either polypropylene (PP) or polytetrafluoroethylene (PTFE) 24 deep square well (DSW) microwell plates (MWP). PTFE MWPs were machined from a single block of virgin PTFE according to the specifications in Figure 2.2 (Radley's, UK). The volume of a well was determined to be 11 ml. The plates were either sealed or a sandwich cover (System Duetz; Enzyscreen, Netherlands) allowing mass transfer to the outside, was used. Sealing was achieved by compressing a aluminium foil mounted on a silicone rubber sheet on the plate between two aluminium plates. Before usage, all plates were subsequently washed overnight in $1\,mol\,l^{-1}$ NaOH and $1\,mol\,l^{-1}$ HCl to remove any residual extractables (Duetz et al. 2000).
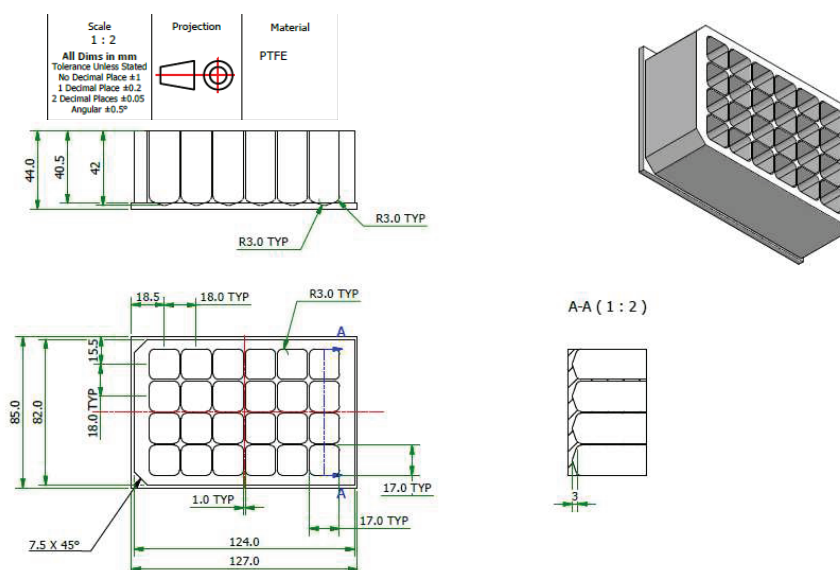
Figure 2.2: Schematic of microwell plates machined from PTFE.

2.3.2 Growing cells bioconversion

Bioconversions with growing cells in MWPs were carried out at 250 rpm and 37 °C. The aqueous phase was inoculated with 100 ml l^{-1} overnight culture and 100 ml l^{-1} to 200 ml l^{-1} organic substrate phase according to the experimental design. Overnight cultures were grown in 5 ml LB medium with 15 mg l^{-1} tetracycline in Falcon tubes at 250 rpm with 25 mm throw and 37 °C for 14 h to 16 h. Bioconversions with substrates other than octane were induced with dicyclopropyl ketone (DCPK) (Merck Millipore, Germany) added in the substrate at a concentration of 2.5 ml l^{-1} (Staijen, Marcionelli, and Witholt 1999).

2.3.3 Resting cells bioconversion

For bioconversions with buffered resting cells, bacteria were cultured in medium according to subsection 2.2.1 in 2 l unbaffled shake-flasks. 200 ml medium were inoculated with 10 ml overnight culture. After 3 h (OD$_{600}$ = 4 − 5) at 37 °C and 200 rpm, the temperature was dropped to 25 °C, followed by induction with DCPK (2.5 ml l^{-1}) after another 30 min. After a further 18 h cells were aliquoted and harvested by centrifugation at 5000 rpm for 10 min at 4 °C and pellets frozen at −80 °C.

Aliquoted pellets were thawed on ice for 10 min to 15 min as required and resuspended in buffer according to subsection 2.2.2. The bioconversion was then performed similar to growing cells at 30 °C and 250 rpm with 25 mm throw. Unless otherwise mentioned, 350 µl total reaction volume was used with 200 ml l^{-1} organic substrate. Figure 2.3 provides a schematic description of the steps involved with reaction preparation in MPWs.

3a. Add resuspended cell suspension to microwell (270 µl)

3b. Add alkane substrate to microwell (70 µl)

2. Resuspend cells in buffer on ice

1. Prepare aqueous reaction buffer from stock solutions to final concentration

4. Seal plate and incubate plate in shaker
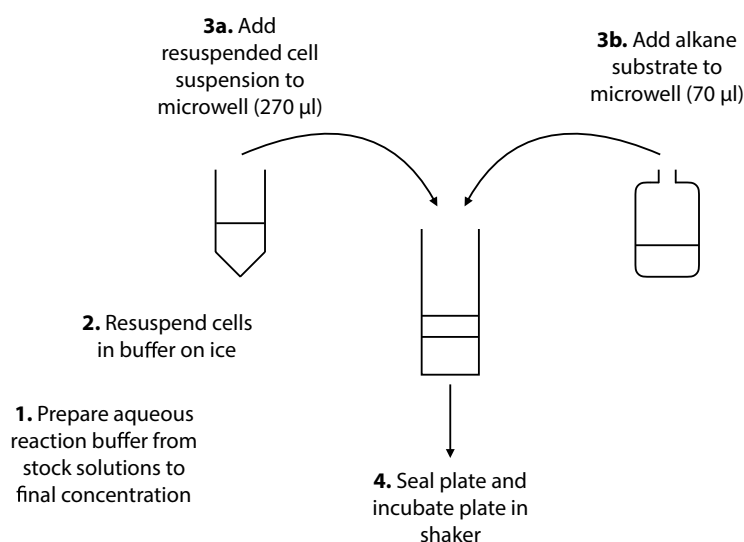
Figure 2.3: Scheme of microwell plate reaction preparation.

High-speed camera

For *in situ* recording of non-conventional media when shaken in well mimics a high-speed camera was used. A Photron FASTCAM MC2 camera with a macro lens (AF-S Zoom-Nikkor 28-70mm f/2.8D IF-ED) was mounted inside a temperature controlled shaker with halogen lighting supplied from the outside. An acrylic cuvette (1 cm side length) was used as a transparent well mimic that allows recording of liquid motion inside the cuvette. For the recordings, the same volume ratios and liquid phases were used as in reaction mixtures, but without the whole-cell biocatalyst. After addition of aqueous buffer and organic substrate phase to the cuvette, the platform was shaken for 15 min at 30 °C and various shaking frequencies (with 25 mm throw) to reach steady state before recording. Cuvettes were sealed with parafilm to avoid excessive evapor-

ation of organic phase over the course of the experiment. Bursts of 512 by 512 frames at 2000 frames per second and a shutter speed of $8000\,\text{s}^{-1}$ were recorded using Photron FASTCAM Viewer data system. The individual frames are cropped to show the cuvette and presented without further modification.

2.4 Analytic procedures

2.4.1 Gas chromatography

1-alcohol, aldehyde and acid bioconversion products were quantified using flame ionisation gas chromatography (GC-FID). Bioconversions were first stopped by acidifying with a 50 µl addition of $10\,\text{mol}\,\text{l}^{-1}$ H_3PO_4, subsequently 300 µl of an internal standard in cyclohexane was added. Depending on the alkane substrate chain length, the 1-alcohol with n + 2 chain length relative to the reaction substrate was used as an internal standard. The organic phase was separated by centrifugation (5 min at 5000 rpm) after extraction by shaking on a thermomixer (3 min at 800 rpm).

Organic phase samples were analysed by GC-FID either on a Perkin Elmer Autosystem XL with TotalChrom 6 data system (PerkinElmer, USA) or on a Thermo Scientific Trace 1300 with Chromeleon 7.2 data system (ThermoScientific, USA). The instruments were equipped with a Restek Rxi-5Sil MS column (30 m × 0.25 mm × 0.5 µm; Restek, USA). Helium was used as a carrier gas at constant pressure (27.6 kPa) with splitless injections or constant flow ($1.8\,\text{ml}\,\text{min}^{-1}$) with split injections (split ratio of 20). The volume of injections was 1 µl.

Table 2.1: Gas chromatography temperature programs.

Method	Injector T °C	Initial oven T °C	Ramp speed °C min^{-1}	Final oven T °C
C6	270	90 for (1.5 min)	25	280
C8	290	90 for (0.5 min)	25	290 for (1 min)
C12	290	120 for (1 min)	25	290 for (1.5 min)

Table 2.1 shows the temperature settings for the various analytes. Pentane and

hexane reaction were analysed with method C6, heptane and octane reaction with method C8, and dodecane reactions with method C12. Detector temperature was maintained at 300 °C.

Using peak area measurements, quantification of analytes was achieved with external standards spanning the range of sample concentrations. All reported concentrations are in relation to the aqueous reaction volume. Exemplary standard curves and extraction efficiencies can be found in section B.1.

2.4.2 High pressure liquid chromatography

Glucose and acetate concentrations in aqueous samples were determined using HPLC. Centrifuged (13 000 rpm, 10 min) and acidified (50 µl of $10 \, mol \, l^{-1}$ H_3PO_4) aqueous samples were injected (25 µl) on a Dionex Summit or Thermo Scientific Ultimate 3000 system equipped with an Aminex HPX-87H column (300 mm × 7.8 mm; Bio-Rad, USA) at 60 °C. HPLC analysis was carried out with a mobile phase of $20 \, mmol \, l^{-1}$ H_2SO_4 in $100 \, ml \, l^{-1}$ acetonitrile at an isocratic flow of $0.4 \, ml \, min^{-1}$.

Glucose was detected with a refractive index detector (RI-101, Shodex or RefractoMax 520, Thermo Scientific) set at 55 °C, acetate was detected on a ultraviolet detector (UV 170U, Dionex) at 210 nm.

All analytes were quantified using external standards using peak height measurements on a Chromeleon 7.2 data system. Exemplary standard curves and reproducibility of injections can be found in section B.2.

2.4.3 pH measurement

For pH measurements a combination microelectrode in a needle housing was used (MI-411) (Microelectrodes Inc., USA). When connected to a Mettler-Toledo pH meter (MP220, Mettler-Toledo, USA) this was used to measure pH of small volume MWP samples after clarification at 13 000 rpm for 10 min.

2.4.4   Sampling

Sampling from MWP was routinely done using a sacrificial approach. Thus, when performing time course experiments or endpoint experiments, rather than taking small samples from one well over the duration of the experiment, complete well contents were sampled for each time point. Thus, when taking multiple samples, these represent independent experimental and analytical replicates. In chapter 3 sampling from sealed MWP was frequently done by piercing the cover with a needle (Terumo, Neolus NN-2070S, short bevel 18.5°) and removing samples from a well with a syringe to avoid opening the cover. After removing from a well, the sample was transferred to an Eppendorf tube and prepared as described above.

In figures or tables the number of independent samples (n) are reported together with the standard deviation (SD) where replicates were run.

2.5   Reproducibility

To maintain reproducibility, volumetric pipetting of organic solvents or viscous solutions was performed using positive displacement pipettes (Repetman, Gilson, UK), wherever possible.

2.6   Statistical analysis

Statistical analyses and visualisation of data were performed using the OriginPro 2016 software package (OriginLab Corp., USA). These include descriptive statistics, regression analysis and ANOVA calculations.

Chapter 3

Development of a microwell platform for biphasic whole-cell biocatalysis

3.1 Introduction

Aqueous-organic two-liquid phase systems have long been employed in bioprocesses to supply organic substrates as well as extract inhibitory or toxic products back into the auxiliary organic phase (Witholt et al. 1990; Woodley et al. 2008; Dafoe and Daugulis 2013). However, despite recent advances, numerous challenges remain to achieve industrially competitive space time yields and product titers for bio-oxidations (Schrewe et al. 2013). To improve on this, the ability to rapidly screen bioconversion reactions for characterisation and optimisation is of major importance in biocatalyst selection and process development (Baboo et al. 2012; Neubauer et al. 2013). Studies at conventional lab scale are time consuming and labour intensive with low experimental throughput. In recent years a range of sophisticated scale-down systems (<10 ml) have emerged with new monitoring and control strategies to accelerate conventional bioprocess development (Lattermann and Büchs 2015). However, research is almost exclusively focused on aqueous single-phase systems rather than more complex non-conventional media. The feasibility of parallel microwell systems to characterise and scale-up two-liquid phase whole-cell bioconversions has previously been shown for longer chain alkane substrates (Grant et al. 2012) and sitosterol (Marques et al. 2010).

A range of studies used other microscale approaches such as Eppendorf tubes with a working volume of 0.5 ml (Scheps et al. 2011) or sealed glass screw cap vials (Nodate, Kubota, and Misawa 2006; Bordeaux et al. 2011; Gudiminchi et al. 2012; Olaofe et al. 2013) (total volume ranging from 12 ml to 40 ml with 1 ml to 5 ml liquid phase). This frequent use of non-standardised tools makes method transfer difficult and reduces the ability to run reactions in parallel whilst reducing manual handling. This complicates routine use and is prone to introducing variability ultimately hindering adoption of high-throughput methods for biocatalysis in non-conventional media.

Further, no studies report the successful application of highly volatile organic substrates in two-liquid phase microscale screening systems. Several factors may be responsible for the difficulties encountered when scaling-down two-phase systems. Studies recognise the difficulties of volatile organic phases at microscale requiring tightly capped vessels to control evaporation (Marques et al. 2009; Baboo et al. 2012). In addition, either the extraction of compounds from commonly used laboratory plastics or the loss of volatiles can be a source of variability. Marques et al. (2007) reported unidentified compounds in reactions from interactions of plate material with organic solvents; whereas Heinig et al. (2010) reported the adsorption of analytes onto the plate material and extraction of plasticisers from polypropylene resulting in poor recoverability and reproducibility. Further they found that even glass-coated plates selectively adsorb lipophilic products resulting in poor recoverability and reproducibility in subsequent analysis. Similarly, many of the optical online measuring techniques used in scale-down setups are incompatible with organic solvents diminishing the usefulness and applicability of these systems (Ramesh et al. 2015). This is in addition to frequently reported location bias in microwell plates (MWPs) due to evaporation or temperature gradients in commercial MWP systems (Grosch et al. 2016).

Despite the significant negative economic impact associated with low reproducibility (Freedman, Cockburn, and Simcoe 2015), there are only few studies that re-

port the practicability and reproducibility of standardised scale-down microwell systems for complex applications in industrial biotechnology research involving non-conventional media.

This chapter investigates the suitability of polymer microwell plates for high-throughput experiments on bio-oxidations of highly volatile alkanes and proposes a simple, robust and reliable microwell platform specifically customised for use with those. Particular attention was paid to material compatibility, evaporation and reliability, exemplarily using the whole-cell ω-oxyfunctionalisation of aliphatic alkanes by AlkBGT in a two-liquid phase system.

3.2 Materials and methods

3.2.1 Media composition

All bioconversion media or buffers contained Triton X-100 (Sigma-Aldrich, UK) at $1\,\mathrm{ml\,l^{-1}}$.

3.2.2 Analytic procedures

Oxygen measurements

Headspace oxygen levels in sealed microwell plate (MWP) wells were determined using a NTH-PSt1 needle mounted optical oxygen sensor connected to a TX3 light emitting diode and photodetector via a polymer optical fibre (all PreSens, Germany). Oxygen levels were recorded using the OxyView TX-6.02 software (PreSens, Germany). The sensor was calibrated at 0 % and 100 % air saturation in a stream of nitrogen and compressed air respectively. The sensor calibration was routinely verified with a test gas (oxygen in nitrogen) to within ±1 % of the certified value and has a reported response time of t_{90}<1 s.

Oxygen depletion method

To mimic the oxygen consumption by microbial cells and bioconversion and test leak-tightness of sealed plates, the reaction of sodium sulphite to sodium sulphate catalysed by $Co(NO_3)_2$ was used (Hermann et al. 2001). In these reactions no organic phase was present.

1.7 ml of a freshly prepared $30 \, g \, l^{-1}$ Na_2SO_3 solution were added to each well. $25 \, \mu l$ of a $1 \, g \, l^{-1}$ $Co(NO_3)_2$ catalyst solution in $0.5 \, mol \, l^{-1}$ HNO_3 was transferred to the Na_2SO_3 solution in each well shortly before sealing the plate the start of the experiment. Based on the stoichiometric equation, the theoretical oxygen requirement of the reaction is $202 \, \mu mol$ (Equation 3.1). Thus, the oxygen consumption capacity of the solution in each well was $\approx 20 \, \%$ more than present in the well headspace (see Appendix C). This was done to ensure completely oxygen free wells at the start of the experiment allowing for any additional dissolved oxygen and oxidation of Na_2SO_3 before the plate was sealed. Oxygen influx in the headspace was then measured using the optical oxygen sensor.

Liquid chromatography mass spectrometry

Bioconversion product concentrations in section 3.3.4 were determined using a liquid chromatography mass spectrometry (LC-MS) method.

Reactions were stopped by addition of $7 \, ml$ $0.80 \, ml \, ml^{-1}$ acetonitrile with $1 \, ml \, l^{-1}$ formic acid to each well. The liquid was transfer into a tube, vortexed and centrifuged ($13\,000 \, rpm$, $5 \, min$). The supernatant was diluted in $0.80 \, ml \, ml^{-1}$ acetonitrile with $1 \, ml \, l^{-1}$ formic acid as required.

Liquid chromatography separation was carried out on a Agilent 1260 HPLC equipped with a Kinetex C18 column ($100 \, mm \times 2.1 \, mm$ column dimensions, $2.6 \, \mu m$ particle size, $100 \, Å$ pore size) (Phenomenex, Aschaffenburg) and KrudKatcher Ultra HPLC pre-column filter ($0.5 \, \mu m$ filter depth, $4 \, \mu m$ internal diameter) (Phenomenex,

Aschaffenburg). The injection volume was 0.7 μl, the column temperature was set at 50 °C with a mobile phase flow rate at 0.6 ml min^{-1}. The mobile phase consisted of Eluent A (1 ml l^{-1} aqueous formic acid) and Eluent B (0.80 ml ml^{-1} acetonitrile with 1 ml l^{-1} formic acid). Gradient elution according to Table 3.1 was used.

Table 3.1: Gradient elution for liquid chromatography–mass spectrometry method.

Time	Eluent A	Eluent B
min	%	%
0.0	77	23
0.3	77	23
0.4	40	60
2.5	40	60
2.6	2	98
5.5	2	98
5.6	77	23
9.0	77	23

For mass spectrometry an Agilent 6410 triple quadrupole system was used with electrospray ionisation in positive ion mode. Gas temperature was set at 280 °C, gas flow rate at 11 l min^{-1}, nebuliser pressure at 50 psi and capillary voltage at 4000 V. Quantification of analytes was achieved with external standards spanning the range of sample concentrations, with the instrument either in selected-ion-monitoring (SIM) or multiple-reaction-monitoring (MRM) mode for detection. All reported concentrations are in relation to the aqueous reaction volume.

3.2.3 Design of Experiments

Computer aided statistical design and analysis of experiments was carried out with Design-Expert 8 (Stat-Ease, USA). A response surface methodology was used to gain detailed understanding of glucose and cell concentration and well fill volume on 1-dodecanol and dodecanoic acid yields. The fill volume of a well denotes the total volume of the liquid, including aqueous and organic phases. Minimum and maximum levels for both factors were chosen based on initially collected data and previous understanding of the system. The number and value of the remaining levels were de-

termined by an IV-Optimal algorithm to minimise the average variance of predicted responses throughout the design space (Table 3.2). The factors were varied in a total of 48 experiments over seven levels each; experiments were evenly split in two blocks.

Table 3.2: Description of factors and levels for characterisation RSM study.

		Levels		
Factor	Effect	Low	High	Total number
Cell density ($g_{DCW}\,l^{-1}$)	Intensity of bioconversion/ Oxygen consumption	4	10	7
Glucose ($g\,l^{-1}$)	Carbon source for NADH regeneration	2	14	7
Fill volume (µl)	Ratio of gaseous to liquid phase	250	600	7

Next, multiple linear regression was used to model the relationship between the factor and response data. Data was transformed as required following the software's recommendations. To that end, least square regression analysis was performed to fit cubic response surface models for each response, minimising the sum of squares of residuals. Analysis of variance (ANOVA) was performed to validate the models in terms of fit and predictive power and test the significance of the model as well as each factor in the model. For this the *F*-value was determined by dividing the mean squares of the regression by the residual mean square and the associated *p*-value was calculated. All presented models are significant ($p < 0.0001$). Further diagnostics revealed no outliers in the data and response surface plots were subsequently used for model interpretation.

3.3 Results and discussion

3.3.1 Variability in microwell plates

Material compatibility

Initially, it was noted that standard thick-walled polypropylene (PP) plates were prone to discolouration after long-term use. Subsequent investigation showed that especially short-chain substrates such as pentane result in considerable softening and swelling of

PP plates leading to deformation of the plate. With increasing chain length substrates such as dodecane seem to have much reduced effects on PP. Alternative materials of construction were considered in order to avoid any permeation or sorption interactions of substrate or products with the plate material. Ultimately, virgin polytetrafluoroethylene (PTFE) was investigated as a relatively easy to fabricate and reusable alternative. Other materials such as glass were not considered due to the difficulty of fabricating complex well geometries as well as its susceptibility to mechanical damage. 24 deep square well (24-DSW) plates were machined from PTFE, a material that provides chemical inertness over a wide range of conditions whilst offering the option to be milled into the desired shape (subsection 2.3.1).
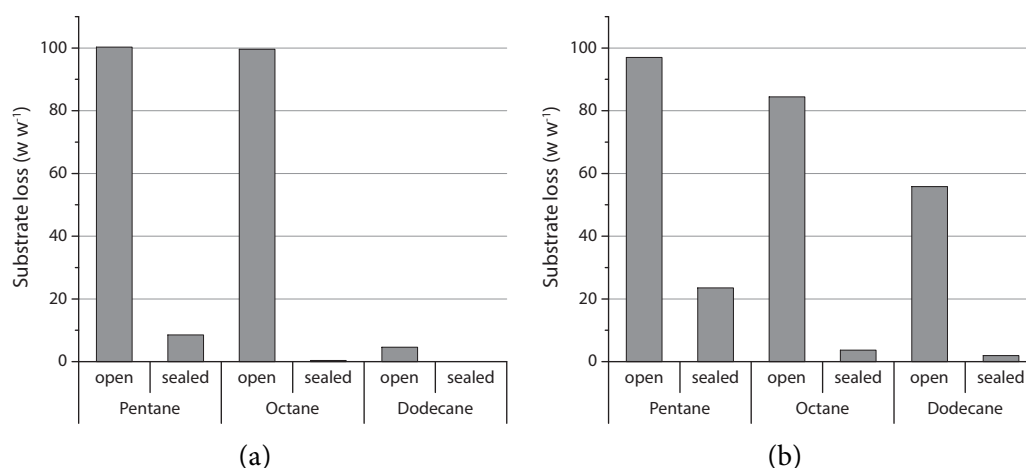
Figure 3.1: Substrate loss of n-alkanes from sealed or open PTFE (a) and PP (b) plates filled with 500 μl alkane per well after 24 h at 37 °C and 250 rpm, C5 filled in cold room at 4 °C.

Figure 3.1 shows the loss of alkane substrates from MWPs manufactured from PTFE or PP. As can be seen from Figure 3.1b despite sealing a PP plate, slight substrate loss was measurable even for higher boiling substrates over 24 h, whereas in the PTFE plate no loss occurred with octane and dodecane (Figure 3.1a). Only in case of pentane a loss of 8.5 % occurred in the PTFE plate. Conversely, in an open plate complete loss of lower boiling n-alkanes was expected and recorded from PTFE plates, whereas 18 % of octane was retained by weight in visibly dry PP plates. Thus, it is suggested that the reduced evaporation of octane from the open PP plate is due to a proportion of the

alkane being absorbed and trapped in the polymer, retarding or preventing complete evaporation. Interestingly, in case of dodecane, there was twelve times more loss from the open PP plate than the PTFE plate. Here, the permeation across the PP could increase the effective surface area across which the alkane can evaporate resulting in higher evaporation rates than in the PTFE plate.

Moreover, the rubber seal of the Duetz open cover system is unsuitable for organic solvents. It was found that a portion of short chain substrate that evaporates from a plate is absorbed into the cover material. In case of octane, it was found that the weight of the lid including the rubber seal increased in weight by 4 % to 5 %. This was attributed to an absorption of octane by the rubber seal. At the same time the seal material starts swelling, potentially restricting the holes for aeration and reducing reproducibility. In fact, in case of dodecane in PP plates visual inspection after the 24 h period revealed non-uniform evaporation across the plate. This effect is highly dependent on alkane chain length. With pentane or dodecane, no visible swelling or weight increase of the open lid material was noted. Similarly to the lid material, sealed PP plates showed visible swelling and wall deformation when exposed to pentane and octane.

The superior properties of PTFE plates are likely due to the chemical inertness of PTFE as well as its generally very low surface adhesion or adsorptive forces. The latter result in PTFE not only being hydrophobic but also lipophobic. In contrast, polypropylene is hydrophobic but lipophilic. This leads to further benefits of PTFE were complete removal of samples from a well is possible due to the entire sample accumulating at the lowest point of the pyramidal bottom. In contrast, in a PP plate the organic phase coats the inside of a well making it difficult for sample removal without *in situ* sample extraction.

Despite the hydrophobicity of PP and PTFE, Doig et al. (2005) showed that surfactants in common aqueous fermentation media still enable wetting of surfaces of

these materials to a similar extent. This is particularly important for oxygen mass transfer (Büchs et al. 2007). Heinig et al. (2010) reported the detection of plasticisers in samples extracted from PP plates with cyclohexane. The PP or PTFE plates were not tested for extractables or leachables that may contaminate the bioconversion. However, the virgin PTFE used is highly unlikely to contaminate the samples due to the inertness of the material.

The observed effects make PTFE a better choice when using alkane substrates for bio-oxidations in microwell plates. Compared to PP, using PTFE avoids interactions of organic substrates with the polymer MWP, thus potentially avoiding:

- well-to-well carryover of organic substrates by permeation,

- reduction in substrate concentration by permeation or absorption, and

- leaching of compounds from polymer.

Organic phase evaporation

A further complication encountered with short-chain alkane substrates and products is their high vapour pressure. This results in excessive evaporation when used in an open system using a plate cover (Figure 3.1). Despite this, Schlepütz and Büchs (2014) successfully optimised this Duetz cover to allow the bio-oxidation of ethanol to acetic acid whilst minimising evaporation of the organic liquids to 5 %. However, with the evaporation of octane as high as $50\,\mu l\,h^{-1}$ in 24 PP MWPs sealed with the conventional cover (Grant et al. 2012), a different measure that avoids escape of very volatile substrates and products is required for this screening tool. Some commercially available designs aimed at parallel process development in the chemical industry use reflux condensing at small scale to control evaporation (Zinsser, Germany and HEL Group, UK). However, these solutions operate exclusively with round glass flask and at their smallest volumes ($\approx$10 ml), provide no external mixing. As previously found for shaken MWPs, a square well geometry with pyramidal bottom provides satisfactory mixing

and oxygen transfer for aqueous media due to the baffling effect of the perpendicular walls and the high surface area to volume ratio (Duetz and Witholt 2004; Islam et al. 2007). Thus, the relatively large volumes of the commercially available systems and their likely inferior mixing render them unsuitable for the heterogeneous mixtures of two-phase whole-cell biocatalysis.

Instead, a simple plate seal was investigated, that allows leak-tight closure of plates to prevent evaporation of organic substrates. This keeps the geometry of the previously developed system for longer chain alkane substrates (Grant 2012). Since, the new system is planned to cope with even lower boiling substrates such as pentane (boiling point: 36 °C) a simple plate closure was investigated that allows sealing the plate entirely. The tested seal consists of three layers; an aluminium sealing film is mounted on a butyl rubber sheet backed by a sheet of silicone foam. The layers were assembled into a stainless steel holder and pressed onto the plate by fixing the holder and MWP between two aluminium plates (Figure 3.2).
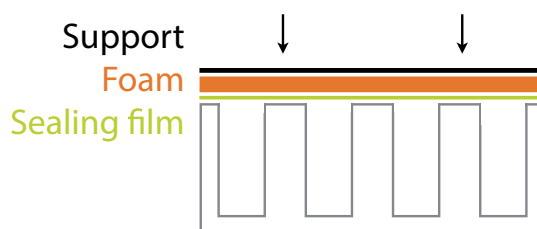
Figure 3.2: Schematic cross-section of microwell plate with sealing layers, pressure is applied uniformly as indicated by arrows.

Initially, the tightness and uniformity of the seal was tested using a needle mounted oxygen probe together with an oxygen quenching Na_2SO_3 solution (section 3.2.2). The oxidation to sodium sulphate catalysed by $Co(NO_3)_2$ (Equation 3.1) was used to mimic the oxygen consumption of microbial cells and bioconversion (Hermann et al. 2001). The solution added to each well had an oxygen quenching capacity $\approx$20 % over the theoretical well content. The limited capacity meant that after the initial oxygen is removed from the atmosphere, any influx over the 48 h period would be measured.

$$2\,Na_2SO_3 + O_2 \xrightarrow{Co(NO_3)_2} 2\,Na_2SO_4 \qquad (3.1)$$
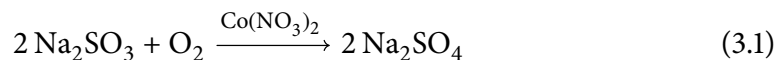
Figure 3.3 shows that an adequately uniform distribution of oxygen ingress can be achieved over 48 h into a sealed plate. The figure shows exemplary results from a single plate and with very little oxygen ingress overall it demonstrates the ability of the clamp to seal the plate.
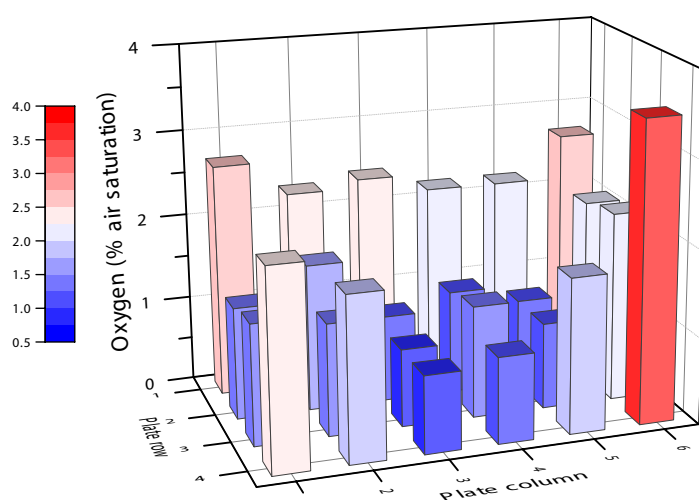
Figure 3.3: Oxygen ingress in individual wells of a 24 deep square well PTFE plate, filled with 1.7 ml of Na_2SO_3 to provide oxygen free conditions initially, of a PTFE plate sealed with clamp; endpoint measurements after 48 h at 37 °C, 250 rpm using a PreSens needle mounted sensor.

However, a bio-oxidation reaction carried out with growing cells revealed an oxygen limitation when compared to an open plate (Figure 3.4a). When comparing the major product, dodecanoic acid, of a dodecane bio-oxidation from an open and a sealed plate, four times lower overall product yields were recorded after a 30 h period in the sealed plate despite very good similarity over the initial 4 h. This deviation coincides with a rapidly decreasing oxygen concentration (10 % at 6 h) in sealed wells. Based on this information, it was hypothesised that sealing plates would result in oxygen limitation when using growing cells for high-yield bioconversions such as the dodecane oxidation.

In both, open and sealed plates, the initial glucose (10 g l^{-1}) is rapidly used up after

the first 9 h and aerobic overflow metabolism results in high acetate concentrations after 12 h (Figure 3.4b). However, only the cells in the non oxygen limited condition subsequently metabolise the acetate completely. In case of reactions in sealed plates, no oxygen is available for the cells to further metabolise the acetate. Concurrently, the pH in reactions in the sealed plates drops and does not recover to the same level as in the open plates.
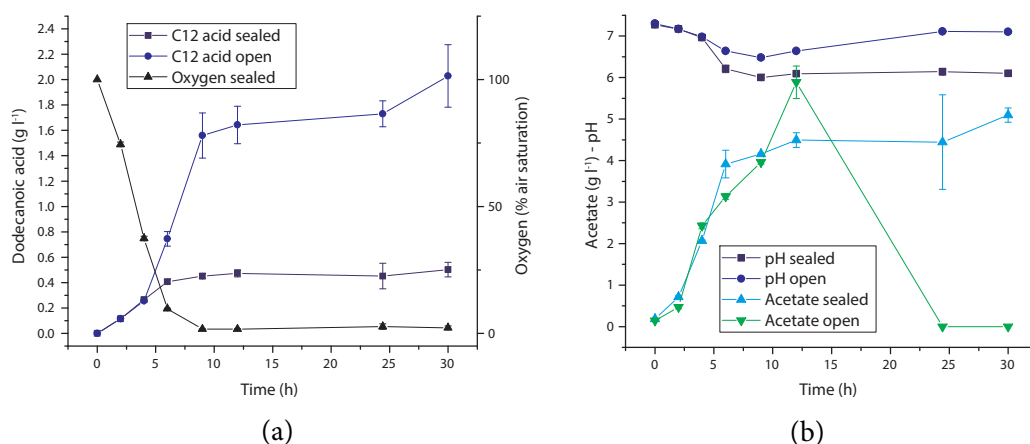
Figure 3.4: Bioconversion of dodecane with growing *E. coli* cells in sealed and open PTFE MWPs (see subsection 2.3.1) with 1 ml growth media, 0.1 ml inoculum, 0.1 ml dodecane at 37 °C and 250 rpm; Bioconversion acid product and remaining oxygen in wells (a) and metabolic profile (b); $n = 3$, ±SD.

In order to ensure non-limiting conditions in sealed plates several options were subsequently investigated. Initially, the ratio of available gaseous headspace volume to liquid phase volume was increased by lowering fill volumes in order to increase available oxygen. Secondly, a shift to metabolically active, stationary cells suspended in buffer was projected to reduce oxygen demand.

3.3.2 Characterisation of microwell platform for bio-oxidations

A design of experiment (DoE) approach using response surface methodology (RSM) was adopted to systematically characterise the impact of sealing on the bioconversion and identify optimised, non-limiting conditions. For these experiments, metabolically active, stationary cells suspended in a phosphate buffer were used. In contrast to growing cells, active resting cells can more efficiently exploit oxygen, carbon

and energy sources for bioconversion, instead of competing with biomass production (Julsing et al. 2011). Nevertheless, resting cells also show reduced stability and self-regeneration. Further, these experiments were carried out using dodecane as substrate, due to the oxygen sensor being incompatible with shorter chain alkane substrates. This allowed measurements not only of product concentrations but also of the remaining oxygen concentration in each well.

An Optimal design was chosen to increase the coverage of the design space and utilise the capacity of two MWPs. Three factors were varied in 48 runs over seven levels each with all samples taken after 24 h incubation at 30 °C and 250 rpm (Table 3.2). It was hypothesised that sealing plates would result in oxygen limitation for high-yield bioconversions such as the dodecane oxidation. Changing cell concentration allows control over the intensity of the bioconversion hence avoid limiting conditions especially in terms of oxygen availability. Further, by reducing the total fill volume, the ratio of available oxygen to culture increases thus avoiding limiting conditions. The control of glucose concentration allows optimisation of co-factor regeneration and avoids catabolite repression depending on cell density. The major product of the reaction, dodecanoic acid was used as the main response in these experiments. The dodecane substrate was supplied at 20 % of the fill volume.

(a)   (b)
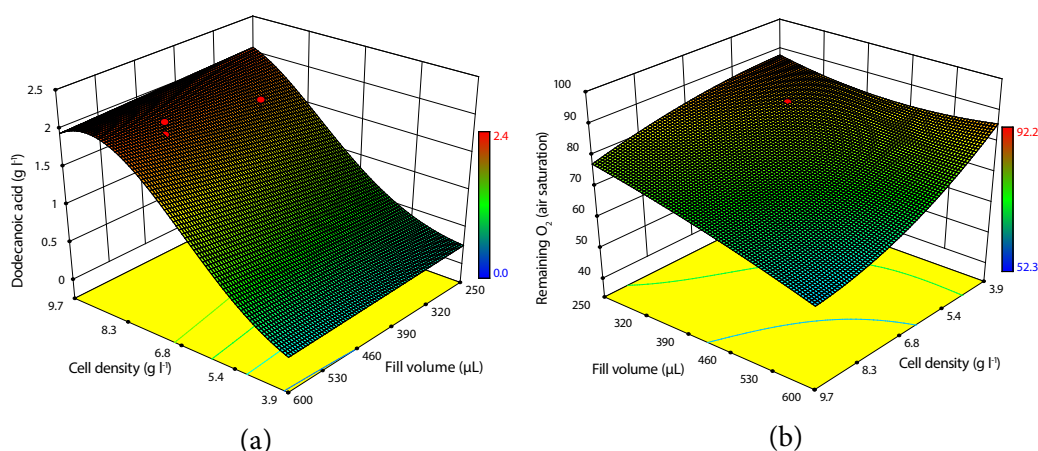
Figure 3.5: Response surface plots showing the of fill volume (µl) and resting cell density ($g_{DCW} l^{-1}$) on dodecanoic acid yields (a) and oxygen remaining in a well (b), at $5 g l^{-1}$ glucose after 24 h at 30 °C, 250 rpm.

Distinct optima in dodecanoic acid yields were found for the combination of factors. Generally, cell density has the largest impact on final dodecanoic acid concentration with highest yields at around $9\,\mathrm{g_{DCW}\,l^{-1}}$ (Figure 3.5a). Fill volume has only moderate impact on yields over the range investigated here. Further, with only a small influence on yield, it is unlikely that changes in this parameter dramatically alter the flow regime and mixing in the shaken microwell.

When considering the residual oxygen concentration, it seems clear that with high cell concentrations and high fill volumes oxygen can become limiting, especially with future improvements of the biocatalyst and increased yields (Figure 3.5b). Importantly, remaining oxygen increases considerably with decreasing fill volumes and low cell concentrations. Thus, it seems beneficial to reduce fill volumes to a workable level whilst keeping biomass concentrations in a certain range in order to avoid limiting conditions.

Operating window

Based on the RSM study, the conditions were optimised towards increasing the total product yield and increasing the remaining oxygen level in each well. A clear optimum can be seen in Figure 3.6 at $5.4\,\mathrm{g\,l^{-1}}$ initial glucose, $8.7\,\mathrm{g_{DCW}/l}$ cell density and $328\,\mathrm{\mu l}$ fill volume resulting in $1.2\,\mathrm{mmol\,g_{DCW}^{-1}}$ total product yield, $76\,\%$ remaining oxygen. Based on this information, a window of operation was defined with a minimum $1.1\,\mathrm{mmol\,g_{DCW}^{-1}}$ yield and $70\,\%$ remaining oxygen for the three parameters. The yellow areas in Figure 3.7 show the combinations of cell density with glucose (Figure 3.7a) and cell density with fill volume (Figure 3.7b) that meet the defined minimum.

Thus, conditions for operation of the microwell system were defined by reducing total fill volume to $350\,\mathrm{\mu l}$, maintaining glucose at $5.5\,\mathrm{g\,l^{-1}}$ and cell concentration at $8.7\,\mathrm{g\,l^{-1}}$. These conditions provide significant product levels, whilst ensuring non limiting conditions in terms of oxygen and optimum amounts of glucose. Under these conditions, the bioconversion yield has a theoretical oxygen demand of $13.0\,\mathrm{\mu mol}$ (see
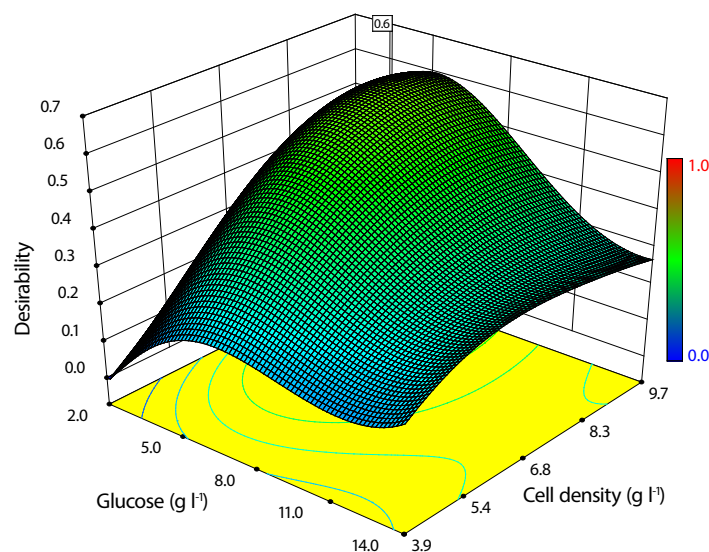
Figure 3.6: Response surface for glucose and cell concentration optimised for maximum remaining oxygen and total product yield at 328 µl fill volume after 24 h at 30 °C, 250 rpm; Desirability = 1 represents the maximised values of total product yield and remaining oxygen level based on the RSM study.

Appendix C for calculations). This represents 14.0 % of the theoretically available oxygen in the headspace. Similarly, 1.8 µmol glucose is theoretically required to provide NADH for the bioconversion representing 16.7 % of total provided glucose (see Appendix C). This calculation does not include any further requirements for cell maintenance.

However, there is a chance of limitations when using this platform for further strain improvement work such as enzyme engineering, that often sees major yield improvements and consequently higher consumption of oxygen and carbon sources. A further possible limitation is the reduced mass transfer rate of oxygen into the liquid phase as the oxygen in the headspace is consumed by the reaction and cell metabolism. This is due to a drop in the oxygen partial pressure and the total pressure of the headspace in a sealed well. However, the low percentage of oxygen that is consumed reduces this effect. Potentially, these limitations can be further reduced by measures such as flooding the plate with oxygen enriched air before sealing or reducing the cell concentration in the buffer.
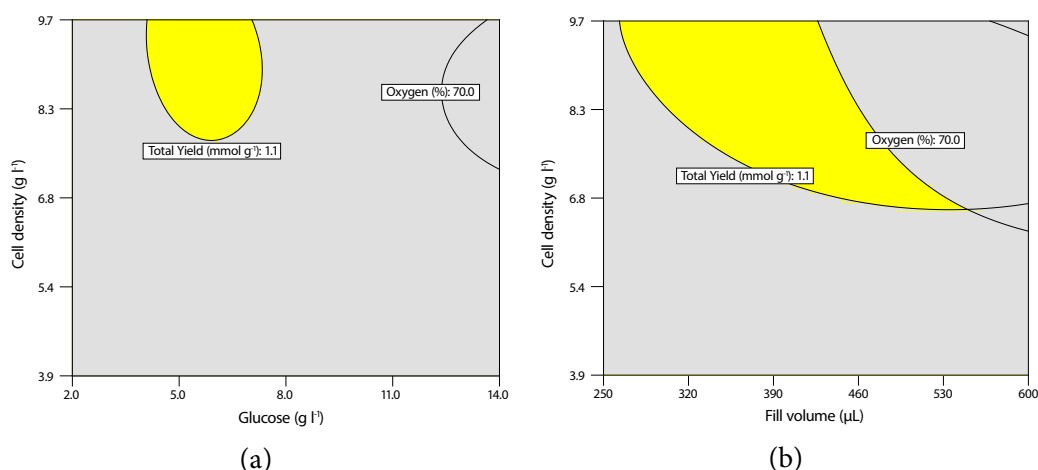
Figure 3.7: Operating window for (a) glucose and cell weight at 328 µl fill volume and (b) fill volume and cell weight at 5.4 g l^{-1} glucose; based on RSM study.

Figure 3.8a and 3.8c show time course data over 24 h for bioconversions of octane and dodecane, respectively at the optimised conditions in sealed plates. Furthermore, Figure 3.8b and 3.8d allow the comparison of bioconversion results to open plates for the same substrates. In case of octane, the comparison of sealed to open plates shows reduced product concentration after 24 h despite initial similarity. Especially the fact that the octanoic acid (bp: 237 °C) concentration is similar over the entire 24 h period whereas the more volatile aldehyde (bp: 171 °C) and alcohol (bp: 196 °C) products are much reduced after 3 h makes loss by evaporation of these products the most likely reason for the lower concentrations. Not only does evaporation directly influence product concentrations, but also indirectly by improving process conditions due to reduced amounts of toxic products in the reaction. Thus the open plates produces results for volatile short chain alkane products that are not representative of the actual reaction conditions and yields when evaporation is controlled. The results for the much less volatile dodecane substrate, on the other hand, show good similarity between the two different set-ups (Figure 3.8).

Figure 3.9 shows the time course data over 24 h for the successful hexane bioconversion. The very high volatility of this substrate and the respective products results in no measurable bioconversion products when using an open PTFE plate due to ex-
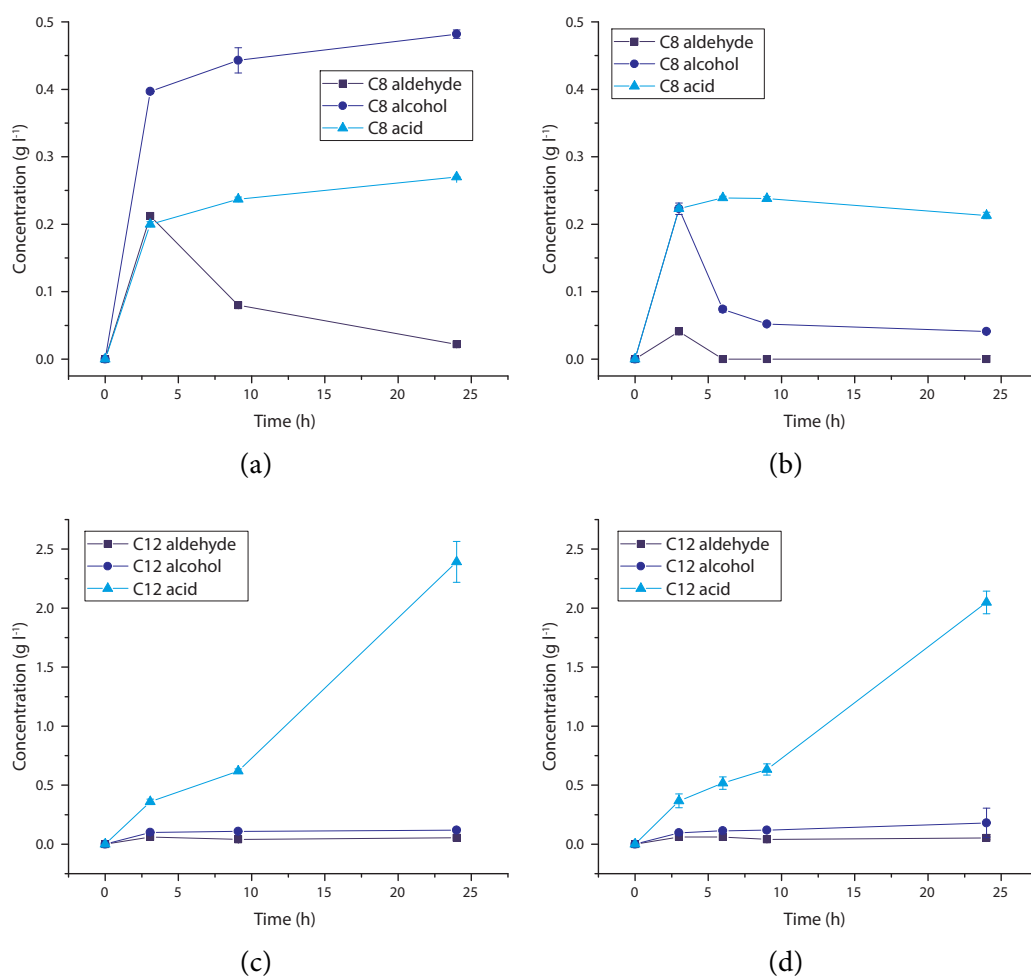
Figure 3.8: Bioconversion products of octane in (a) sealed and (b) open PTFE plates and of dodecane in (c) sealed and (d) open PTFE plates at optimised conditions over 24 h at 30 °C and 250 rpm; $n = 3$, ±SD.

cessive evaporation.

Thus, the comparison of open to sealed plates in case of the dodecane shows no limitation by the seal, making its use non-obligatory. However, in case of the more volatile octane and hexane bioconversions, a seal is required to contain the volatile components.

Lastly, the optimised conditions were used for a comparison of sealed plates made from PP or PTFE. Table 3.3 compares the alcohol and acid product concentrations of hexane and octane bioconversions after 24 h. The results from the PP plates show consistently lower product concentrations compared to the PTFE plates. Al-
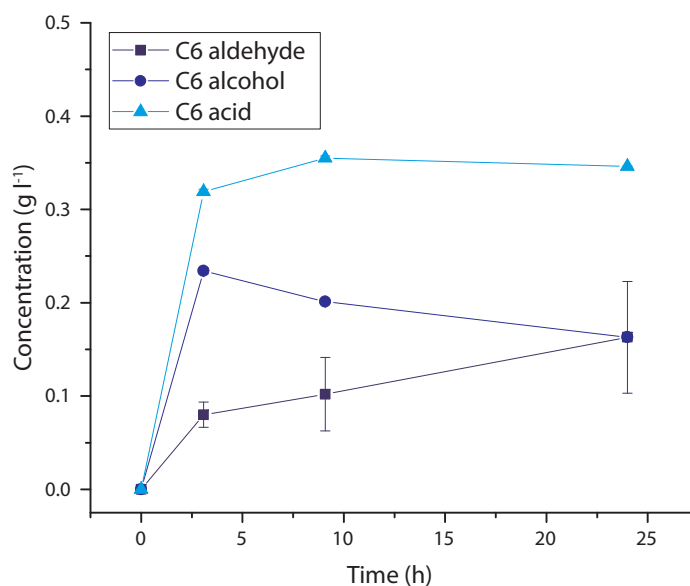
Figure 3.9: Bioconversion products of hexane in sealed PTFE plates at optimised conditions over 24 h at 30 °C and 250 rpm; $n = 3$, ±SD.

Table 3.3: Comparison of bioconversion products for PTFE and PP plates for C6 and C8 substrates at optimised conditions after 24 h at 30 °C, 250 rpm; $n = 2$.

Substrate	Product	Plate material	Concentration ± SD ($g\,l_{tot}^{-1}$)
Hexane	1-Hexanol	PP	0.08 ± 0.003
		PTFE	0.16 ± 0.003
	Hexanoic acid	PP	0.26 ± 0.025
		PTFE	0.35 ± 0.000
Octane	1-Octanol	PP	0.11 ± 0.001
		PTFE	0.48 ± 0.006
	Octanoic acid	PP	0.26 ± 0.024
		PTFE	0.27 ± 0.000

though, it is unclear what effect is responsible for this specifically, a combination of the permeability or absorptive properties of the PP material (section 3.3.1) as well as the change in reaction conditions due to the reduction in toxic organic concentrations is likely to be the cause. To avoid taking any adsorption effects into account, sampling was carried out by performing sample extraction directly in the plate.

3.3.3 Phase behaviour

In order to identify phase behaviour and mixing of two-liquid phase reaction mixtures, cell-free two-liquid phase media were shaken with a 25 mm throw in transpar-

ent microwell mimics and recorded using a high speed camera. Figure 3.10 shows the agitated two-liquid phase media for bio-oxidation of octane and dodecane.

(a)	(b)	(c)	(d)
(e)	(f)	(g)	(h)
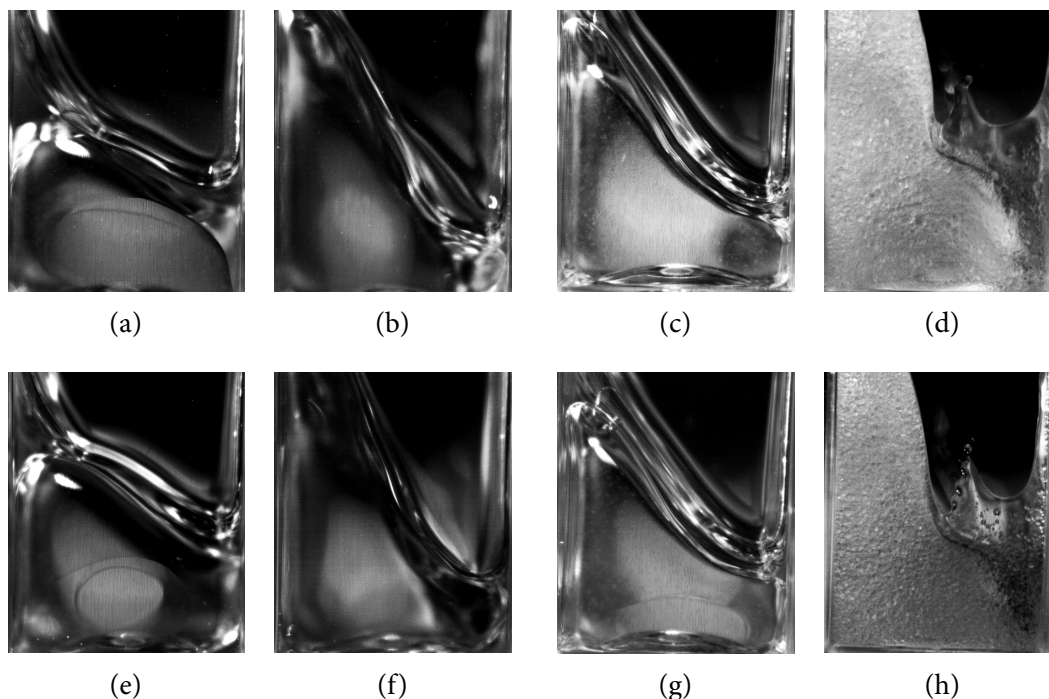
Figure 3.10: Mixing visualisation of two-phase bioconversion media in well mimic: with octane at (a) 250 rpm, (b) 350 rpm, with octane with 0.1 % Triton X-100 at (c) 250 rpm, (d) 350 rpm, with dodecane at (e) 250 rpm, (f) 350 rpm, with dodecane with 0.1 % Triton X-100 at (g) 250 rpm, (h) 350 rpm; all at 30 °C.

The figure shows droplet formation upon addition of the surfactant Triton X-100, similar to results from Grant et al. (2012) with dodecane (Figure 3.10d and 3.10h). The density of the created emulsion appears to depend on shaking speed with fewer droplets formed at 250 rpm (Figure 3.10c and 3.10g). The attempt to quantify parameters such as droplet size to more accurately describe the interfacial area for mass transfer and as a potential scale-up parameter (see Cull et al. (2002)) failed due to high density emulsion formation or the insufficient resolution of the recording. It is important to note that at the microscale, the interfacial area to volume ratio is already higher compared to large scale systems even without emulsion formation. Overall, the results confirm previous findings that Triton X-100 addition promotes droplet formation and with that emulsion formation can be achieved in shaken square microwells.

3.3.4 Assessment of system reliability

In order to assess the robustness of the developed microwell system, replicate reactions under the optimised conditions were run, grouped and compared to each other using the one-way ANOVA method. For this analysis raw gas chromatograph peak area values (pA min) of alcohol and acid products for each well were used as exemplary results for a typical run. All data points were used and no modifications were made to the data. All group data was verified to be normally distributed and of equal variance.

Table 3.4: Statistical parameters from one-way ANOVAs comparing bioconversion product quantities of two separate PTFE plates with replicate bio-oxidation of either octane or dodecane and coefficient of variation (CoV) of the 24 replicate reactions in single plate; after 24 h at optimised conditions, 30 °C, 250 rpm.

Variable	*F*-statistic	*p*-Value	CoV (%)
1-Octanol	2.15	0.15	16.8
Octanoic acid	4.09	0.05	17.2
1-Dodecanol	6.14	0.02	9.7
Dodecanoic acid	0.56	0.46	5.2

Two comparisons were made: Table 3.4 shows the results for two times 24 replicate octane and dodecane oxidations between two plates and the coefficient of variation (CoV) of the 24 replicate reactions in a single plate. Table 3.5 compares replicates from the 16 edge wells facing outside to the eight inside wells of a single plate.

Table 3.5: Statistical parameters from one-way ANOVA comparing bioconversion product quantities in edge wells with inside wells of a PTFE plate replicate bio-oxidation of either octane or dodecane; after 24 h at optimised conditions, 30 °C, 250 rpm.

Variable	*F*-statistic	*p*-Value
1-Octanol	0.60	0.45
Octanoic acid	0.59	0.45
1-Dodecanol	0.48	0.50
Dodecanoic acid	0.11	0.74

The one-way ANOVA analyses show that the deviations between replicates were not significant ($\alpha = 0.01$). The CoV shows very low variation of results in case of the dodecane bioconversion (5.2 % with dodecanoic acid), in reactions with octane

the variation is higher likely due to the more volatile reactions compounds and lower concentrations. However, the deviations between replicates are still not significant (α = 0.01). It needs to be considered that the ANOVA analysis not only captures the variability due to the characteristics of the microwell setup, but also the inherent variability of the biological reaction and the variability introduced during sample handling and the GC analysis. Overall, the entire process and methodology shows good reproducibility.

Visualisation of the data as box plots for octane (Figure 3.11) and dodecane (Figure 3.12) shows that, apart from a few outliers, the data points are tightly grouped around the median and are normally distributed. This reduces the likelihood of any systematic errors are occurring undetected, such as pronounced edge effects. Overall, the combination of improved material compatibility and a uniform seal result in very low variability in results.

(a) (b)
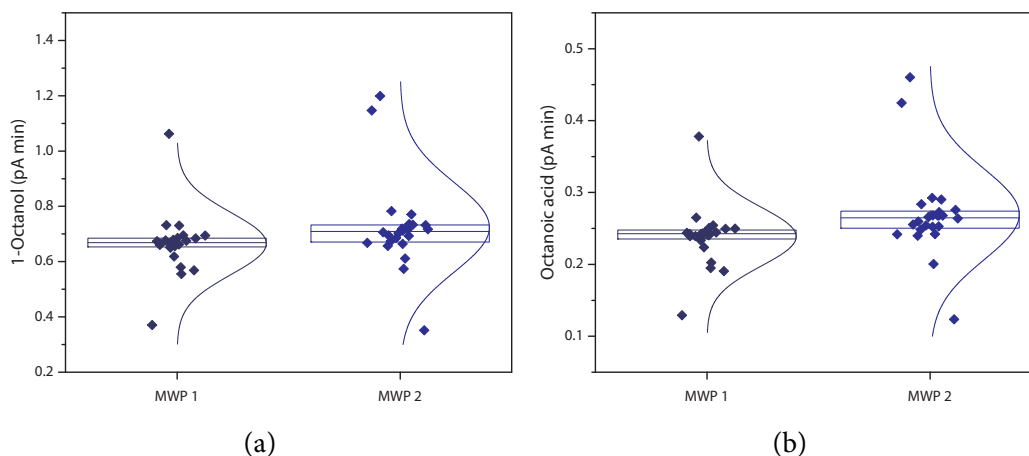
Figure 3.11: Distribution of (a) 1-octanol and (b) octanoic acid raw GC area counts in replicate octane bio-oxidations after 24 h incubation at 30 °C and 250 rpm; For each microwell plate, the median, first and third quartile and normal distribution are shown.

Method transfer[i]

In order to further test the reliability and robustness of the developed system, the method was transferred to an industrial laboratory. The focus was on ensuring easy
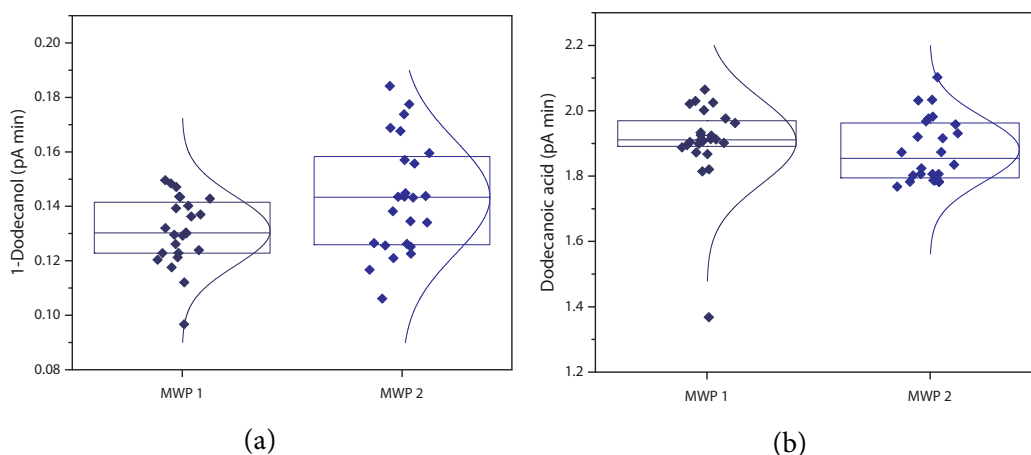
Figure 3.12: Distribution of (a) 1-dodecanol and (b) dodecanoic acid raw GC area counts in replicate dodecane bio-oxidations after 24 h incubation at 30 °C and 250 rpm; For each microwell plate, the median, first and third quartile and normal distribution are shown.

transferability of the microwell methodology and hardware without compromising reproducibility due to changes in operational variables such as the experimenter, analytical methods and consumables. To this end, replicate bioconversion reactions of dodecane were run using AlkBGT-based whole-cell biocatalysts under conditions determined in section 3.3.2 except for using 15 g l^{-1} glucose, varying cell concentrations and host strains. A liquid chromatography mass spectrometry method was used for reaction product detection and quantification (section 3.2.2).

Table 3.6: Dodecane bioconversion products after method transfer using the *E. coli* GEC137 pGEc47ΔJ biocatalyst; Product concentrations and coefficient of variation (CoV) of replicate reactions after 6 h and 25 h at optimised conditions with 200 ml l^{-1} substrate except for 10.5 g l^{-1} dry cell weight and 15 g l^{-1} glucose, 30 °C, 250 rpm; $n = 6$, ±SD; nd – not determined; * – $n = 2$.

Product	Concentration at		CoV at	
	t = 6 h	t = 25 h	t = 6 h	t = 25 h
	g l^{-1}	g l^{-1}	%	%
1-Dodecanol	nd	0.4 ±0.009*	nd	2.4
Dodecanoic acid	1.2 ±0.023	2.2 ±0.069	2.0	3.2
12-Hydroxydodecanoic acid	0.1 ±0.003	0.2 ±0.009	2.5	4.2

Table 3.6 shows the average product formation and CoV of replicate reactions using the whole-cell biocatalyst described in section 2.1 at 10.5 g l^{-1} dry cell weight. A second batch of reactions was run using a proprietary AlkB-based *E. coli* biocatalyst

at $13.1\,\mathrm{g\,l^{-1}}$ dry cell weight with results shown in Table 3.7. The strain and details of the biocatalytically active enzyme of this *E. coli* biocatalyst are confidential.

Table 3.7: Dodecane bioconversion products after method transfer using a proprietary AlkBGT-based *E. coli* biocatalyst; Product concentrations and coefficient of variation (CoV) of replicate reactions after 6 h and 24 h at optimised conditions with $200\,\mathrm{ml\,l^{-1}}$ substrate except for $13.1\,\mathrm{g\,l^{-1}}$ dry cell weight and $15\,\mathrm{g\,l^{-1}}$ glucose, 30 °C, 250 rpm; $n = 3$, ±SD; L – below lowest calibration standard $(0.1\,\mathrm{mg\,l^{-1}})$.

Product	Concentration at		CoV at	
	t = 6 h	t = 25 h	t = 6 h	t = 25 h
	$\mathrm{g\,l^{-1}}$	$\mathrm{g\,l^{-1}}$	%	%
1-Dodecanol	L	0.6 ±0.074	–	12.1
Dodecanoic acid	2.0 ±0.046	2.9 ±0.144	2.3	5.0
12-Hydroxydodecanoic acid	0.1 ±0.016	0.2 ±0.013	19.9	7.2

The coefficient of variation of the collected data shows very good reproducibility between individual wells with CoVs frequently under 5 %. Only with lower concentrations of dodecane and 12-hydroxydodecanoic acid higher CoVs were recorded (up to 19.9 % with 12-hydroxydodecanoic acid). The experimental differences in glucose and cell concentration make it difficult to compare reproducibility of absolute product concentrations between experiments. Despite this, the recorded dodecanoic acid results are very similar to previous results and 1-dodecanol results are well within an order of magnitude, supporting the reliability claims of the system.

This method transfer test provides further evidence of the robustness and good reliability of the developed system. Moreover, it confirms the validity of the sacrificial sampling approach.

Interestingly, the alternative analytical method allowed determining the amount of bifunctional reaction products. In addition to the 1-dodecanol and dodecanoic acid product, significant amounts of 12-hydroxydodecanoic acid, and trace amounts (low $\mathrm{mg\,l^{-1}}$) of 1,12-dodecanediol, dodecanedioic acid and 12-oxododecanoic acid were found (data not shown), confirming the ability of the AlkBGT enzyme system to produce bifunctional products.

3.4 Conclusion

Although MWPs have been successfully applied to two-liquid phase systems before, the use of highly volatile short-chain alkanes was shown to be problematic with current tools. To improve material compatibility with the organic phase, MWPs machined from PTFE were investigated for these bioconversions. In contrast to PP, the new material does not show any interaction with the liquid phases allowing reliable time resolved monitoring of bioconversion products. In combination with a sealing clamp, no significant variability such as edge effects could be determined ($\alpha = 0.01$) whilst containing even highly volatile substrates and products.

A systematic statistical approach was adopted to show that a large space of the experimental conditions results in non-limiting conditions with over 70 % oxygen left after a 24 h bioconversion in sealed plates. By reducing fill volume and keeping cell density within a certain range it is possible to operate in optimised, non-limiting conditions with respect to oxygen and glucose supply.

Replicate reactions showed very high reproducibility between wells and plates with no significant edge effects found. Similarly, during method transfer no drop in reproducibility was seen, reiterating the robustness and reliability of the system.

This simple and robust MWP protocol greatly improves the experimental throughput and accelerates the screening procedures for two-liquid phase biocatalytic systems in early process development and catalyst selection. It allows the rapid investigation of numerous parameters such as host strains, biocatalysts, media, substrates and process conditions as well as the interactions between these. The simplicity and robustness of this tool result in a user friendly system for characterising bioconversions in non-conventional media.

Chapter 4

Development of a controlled glucose delivery system for bio-oxidations in microwells

4.1 Introduction

During initial high-throughput screenings for strain selection or biocatalyst improvement, conventional batch conditions with high initial nutrient concentrations are commonly used. This is especially true for microscale systems such as microwell plates and shake flasks. The high initial carbon source concentrations can have a range of adverse effects on bioprocess productivity such as carbon catabolite repression, high growth rates leading to oxygen limitations and formation of other inhibitory metabolites (Rojo 2010a; Valgepea et al. 2010). Scaled down stirred tank reactors often have more sophisticated process control options, allowing feeding strategies. However, the pulsed feeding can cause temporary spikes in substrate concentration immediately after an addition and potentially result in temporary batch effects.

Further into development, feeding strategies, with carbon source limitation to control growth rate, are frequently preferred. This strategy usually allows higher cell densities and product yields (Jeude et al. 2006). The discrepancy between initial screening and later optimisation conditions can lead to mis-selection of strains with poor performance in production conditions (Wilming et al. 2014). Even though for

a resting cell process growth control is not relevant, formation of inhibitory metabolites due to rapid carbon catabolism can still impact the bio-oxidation of alkanes and reaction efficiency (Olaofe et al. 2013). Moreover, similar to oxygen limiting the Alk-BGT reaction in order to avoid the over-oxidation (Grant 2012), it is hypothesised that through a carbon limited fed-batch culture over-oxidation to the acid product may be reduced. It was previously shown that limited access to the alkane substrate contributes significantly to the over-oxidation to the acid product (Schrewe et al. 2014). By reducing the reaction rate through carbon limitation it may be possible to realign the balance between alkane substrate access and reaction rate to reduce the over-oxidation of the 1-alcohol product.

Table 4.1: Overview of different scale-down fed-batch implementations.

Method	Details & Commercial products	References
Controlled release	Release of crystallised nutrients from silicone matrix; e.g. FeedBead® for shake flasks – Feed Plate® in MWP format	Jeude et al. (2006) and Scheidle et al. (2010)
Microfluidic systems	MWP with reservoirs, active/passive microfluidic addition of liquid nutrient feed; e.g. BioLector® Pro ('available in 2016')	Funke et al. (2010a) and Wilming et al. (2014)
Enzymatic hydrolysis	Release of glucose from gelled starch deposit or soluble polysaccharide by an amylase; e.g. EnPresso® and FIT media	Panula-Perälä et al. (2008) and Hemmerich (2011)

Several different approaches mimicking fed-batch implementations in small-scale shaken culture have been detailed in the literature, Table 4.1 shows them divided into three groups. Whereas the controlled release and microfluidic techniques potentially allow the addition of a wide range of nutrients, the addition by enzymatic hydrolysis is limited to polysaccharide hydrolysis products. Similarly to the controlled release, the enzymatic hydrolysis technique initially relied on a solid phase in form of a gelled starch deposit. Solubilised polysaccharide is then exposed to enzymatic hydrolysis and glucose released in the liquid phase. The release rate of these systems can be controlled by varying the enzyme concentration. Subsequent improvements

to this technique have allowed using fully soluble polysaccharides (Krause et al. 2010; Glazyrina et al. 2012). Only the microfluidic systems, with the use of micro-pumps, allow active, pulsed feeding of nutrients and also pH control, resulting in a controllable and adaptable near-continuous release rate (Funke et al. 2010b). In contrast, the passive, pre-set feed rate of the other two options may be influenced by the glucose concentration and pH of the liquid phase, resulting in varying feed rates throughout the duration of the reaction. More importantly, the controlled release and microfluidic systems regularly use PDMS in their design, a material that is largely incompatible with alkanes (Lee, Park, and Whitesides 2003).

Consequently, this chapter aims at implementing a controlled glucose release approach in the previously developed microwell system (see chapter 3). In order to leverage the good material compatibility and robustness of the developed system, an enzymatic release technique was investigated.

4.2 Materials and methods

All materials and methods are as described in chapter 2 except for the following items.

4.2.1 Buffer composition

The bioconversion reaction buffer for glucose fed-batch reactions contained $10\,\mathrm{g\,l^{-1}}$ maltodextrin with 4-7 dextrose equivalent (Cat-#: 419672, Sigma-Aldrich, UK) or soluble starch (Cat-#: 33615, Sigma-Aldrich, UK). A $40\,\mathrm{g\,l^{-1}}$ stock solution was prepared for each. The maltodextrin was solubilised and sterile filtered with a $0.22\,\mathrm{\mu m}$ bottle-top vacuum filter. The starch was solubilised by slowly adding to RO water ($80\,\mathrm{°C}$) and stirred for 30 min immediately followed by sterilisation by autoclaving. The solutions were used fresh. For dodecane bioconversion, the buffer was supplemented with $1\,\mathrm{ml\,l^{-1}}$ Triton X-100.

4.2.2 Enzymatic hydrolysis

For enzymatic hydrolysis, a lyophilised fungal amyloglucosidase (Cat-#: 10115, Sigma-Aldrich, UK) was used. The amyloglucosidase was resuspended in 75 mmol l^{-1} phosphate buffer (subsection 2.2.2) at 1000 U l^{-1}, aliquoted, stored at $-20\,°C$ and used within four months. The text conventionally uses 'enzyme' or 'enzyme concentration' when referring to the amyloglucosidase or its concentration in a reaction.

4.2.3 Design of Experiments

Computer aided statistical design and analysis of experiments was carried out with Design-Expert 8 (Stat-Ease, USA). Initially, a response surface methodology was used to gain detailed understanding of the influence of amyloglucosidase and initial glucose concentration on 1-dodecanol and dodecanoic acid yields. The amyloglucosidase concentration was varied in order to investigate the effect of a range of glucose release rates on reaction yields. The initial glucose concentration was varied to mimic an initial batch phase to provide a simulated fed-batch regime. Minimum and maximum levels for both factors were chosen based on initially collected data and previous information. The number and value of the remaining levels were determined by an IV-Optimal algorithm to minimise the average variance of predicted responses throughout the design space (Table 4.2). The factors were varied in a total of 24 experiments.

Table 4.2: Description of factors and levels for DoE fed-batch characterisation.

| | | Levels | | |
Factor	Effect	Low	High	Total number
Enzyme concentration (U ml^{-1})	Glucose release rate	0.01	0.50	11
Initial glucose (g l^{-1})	Batch phase glucose	0	1	10

Multiple linear regression was used to model the relationship between the factor and response data. Data was transformed as required following the software's recommendations. To that end, least square regression analysis was performed to fit cubic

response surface models for each response, minimising the sum of squares of residuals. Analysis of variance (ANOVA) was performed to validate the models in terms of fit and predictive power and test the significance of the model as well as each factor in the model. For this the *F*-value was determined by dividing the mean squares of the regression by the residual mean square and the associated *p*-value was calculated. All presented models are significant ($p < 0.0001$).Further diagnostics revealed no outliers in the data and response surface plots were subsequently used for model interpretation.

4.3 Results and discussion

4.3.1 Enzymatic hydrolysis substrates for glucose release in microwells

Initially, several carbon sources were considered as a substrate for enzymatic hydrolysis. The aim was to find an oligo- or polysaccharide that was both soluble at high enough concentrations to provide enough glucose whilst avoiding gelling, as well as being not immediately accessible by the microbial catalyst as a carbon source. The focus was on maltodextrins and starch. Specifically, a long-chain maltodextrin (dextrose equivalent 4-7) was chosen assuming it would not be directly accessible as a carbon source by the microbial biocatalyst, as well as a soluble starch.
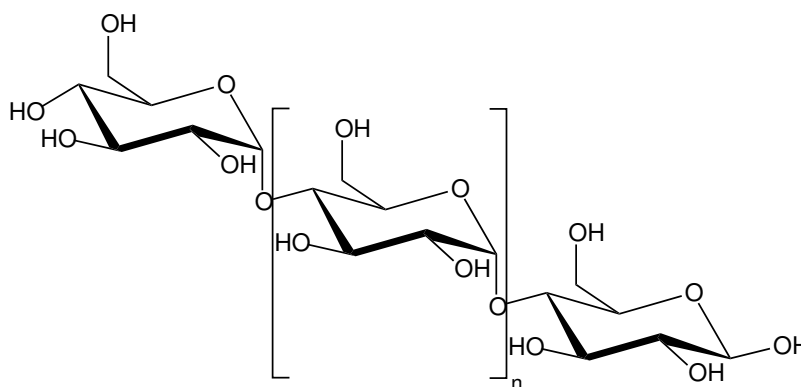
Figure 4.1: Glucose linked with α-1,4-glycosidic bonds.

A commercially available amyloglucosidase was used to catalyse the irreversible hydrolysis of terminal α-1,4-glycosidic bonds at non-reducing ends of the used carbon

source and release glucose (Figure 4.1) (Norouzian et al. 2006). Thus, the combination of maltodextrin or starch and amyloglucosidase yields a single carbohydrate monomer in the form of glucose.
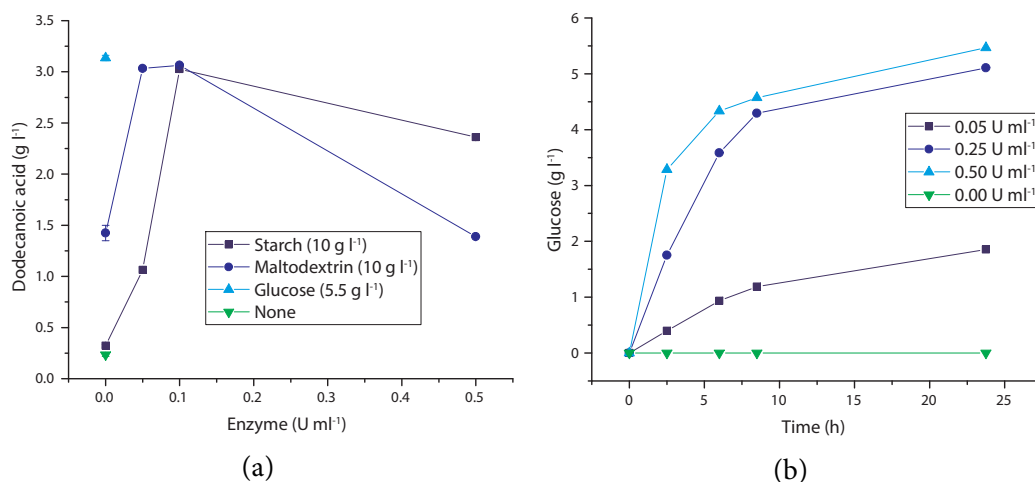
Figure 4.2: (a) – Dodecanoic acid yields after 24 h bioconversion with different carbohydrate sources and a range of amyloglucosidase concentrations ($n = 2$, ±SD); (b) – Glucose release over 24 h from starch ($10 \, \mathrm{g \, l^{-1}}$) in reaction buffer under varying amyloglucosidase concentrations.

Figure 4.2a investigates the ability of the whole-cell biocatalyst to digest and metabolise the different polymeric carbon sources. To that end, dodecane bio-oxidation reactions were run over 24 h with different carbon sources and amyloglucosidase concentrations with major dodecanoic acid product reported. In addition a control reaction was run using the glucose concentration ($5.5 \, \mathrm{g \, l^{-1}}$) determined in chapter 3.

It is clear that with maltodextrin significant dodecanoic acid yields are achieved even without or at low enzyme concentration. In fact, with no enzyme present to release glucose, an over three times higher product yield was achieved with maltodextrin than with starch or no carbohydrate source present. At $0.05 \, \mathrm{U \, ml^{-1}}$ enzyme concentration and maltodextrin, the yield was approximately that of the glucose-only control reaction. Without enzyme, $0.1 \, \mathrm{g \, l^{-1}}$ of glucose was detected in the bioconversion buffer with $10 \, \mathrm{g \, l^{-1}}$ maltodextrin and no cells present. Although this glucose contamination may contribute to the background activity, it is unlikely to be solely responsible. This

indicates that the maltodextrin carbon source can be, at least partially, accessed as a carbon source by the microbial catalyst. In fact, some maltodextrins, maltoheptaose and smaller, can be accessed by *E. coli* (Boos and Shuman 1998). Hence, no good glucose release control is possible by varying enzyme concentration when using this maltodextrin substrate.

In contrast to maltodextrin, the tested starch resulted in very little dodecanoic acid production without enzyme present, similar to the control with no carbohydrate source present (Figure 4.2a). Further, control of the release rate based on enzyme concentration was possible with near linear behaviour over the first 6 h and no glucose was detected when no enzyme was present (Figure 4.2b). Previously the batch bioconversions of volatile short-chain substrates such as octane or hexane were found to be most productive over the first 6 h to 9 h (section 3.3.2), thus, the limited linear range of glucose release over this time was thought to be adequate. Table 4.3 shows estimated release rates for the first 6 h based on the best fit lines indicated in Figure 4.2b.

Table 4.3: Estimated release rate from starch ($10\,\mathrm{g\,l^{-1}}$) at various amyloglucosidase concentrations.

Enzyme concentration $\mathrm{U\,ml^{-1}}$	Release rate $\mathrm{g_{glucose}\,h^{-1}}$
0.05	0.16
0.25	0.61
0.50	0.81

Since the release rates in Figure 4.2b were determined in the reaction buffer without cells present, the reduction in release rate is not due to a change in pH or similar reaction related inhibition. Further, the fact that the glucose release rate slows after 6 h despite the same starting polysaccharide concentration indicates an enzyme inactivation unrelated to the substrate concentration may be the cause. With the glucose concentration being different at the various enzyme concentrations, it is also unlikely that product inhibition is the cause for the slowing of release after 6 h. More likely this plateau is due to limited enzyme stability and subsequent activity loss. Optimum

conditions for amyloglucosidases are generally in acidic pH ($\approx$pH 4.5) and elevated temperatures ($\approx$60 °C) (Norouzian et al. 2006). Thus, the reaction conditions around neutral pH and 30 °C may be detrimental to maintaining activity of the enzyme in the reaction buffer over prolonged time periods. This is in addition to other proteolytic mechanisms such as released proteases from lysed cells in the reaction buffer. Moreover, at higher enzyme concentrations the overall release of glucose may be further limited by the initial polysaccharide substrate concentration since the final glucose concentration with 0.50 U ml^{-1} is only marginally higher than with 0.25 U ml^{-1} and at the highest enzyme concentration the glucose concentration plateau is reaches quickest. Due to the ability to control glucose release in the presence of cells, the starch substrate was chosen for further characterisation of the system.

4.3.2 Characterisation of fed-batch strategies for bio-oxidations

A DoE Response Surface Methodology (RSM) was used to characterise the behaviour of the fed-batch implementation across a range of conditions using the starch polysaccharide substrate. Similarly to chapter 3, dodecane was used as a diagnostic substrate for system characterisation, with 1-dodecanol and dodecanoic acid yields as responses.

The amyloglucosidase concentration was varied resulting in different glucose feed rates and different initial glucose concentrations were used to simulate a fed-batch mode. The two factors were varied over the design space as determined by a IV-Optimal algorithm in a total of 24 experiments (Table 4.2).

The combination of factors resulted in three scenarios: An entirely glucose fed system with different glucose release rates but no initial glucose present; a batch system with up to 1 g l^{-1} initial glucose present; and a combination of the two where different release rates are combined with different initial glucose concentrations.

Figure 4.3a shows the dodecanoic acid production over the varying conditions of the DoE design. The point with no glucose and 0.01 U ml^{-1} enzyme (lowest release rate) shows the least productivity, as expected. A maximum production can be seen
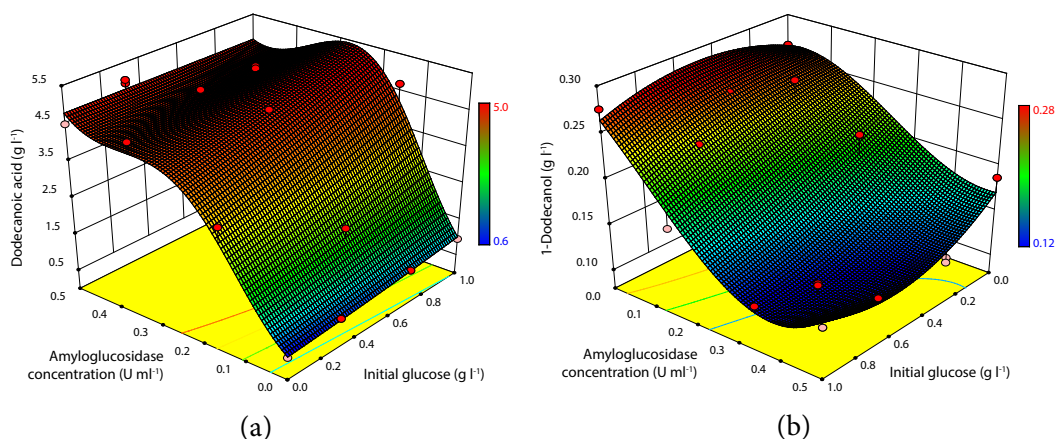
Figure 4.3: Response surface plots showing the influence of amyloglucosidase concentration (U ml-1) concentration (U ml^{-1}) and initial glucose (g l^{-1}) on dodecanoic acid (a) and 1-dodecanol yields (b), after 24 h at 30 °C, 250 rpm.

at around 0.3 U ml^{-1} of enzyme. With further increases in enzyme concentration, no increase in product yield can be seen. It is likely that the resulting high feed rates result in a near-batch behaviour and the release and product yield is increasingly limited by the plateau emerging after 6 h to 8.5 h as shown in Figure 4.2b. Moreover, at low glucose release rates there is a tendency that increasing initial glucose concentrations increase the acid yield, suggesting that glucose is limiting in this dimension, as well.

In contrast, the 1-dodecanol concentration opposes the behaviour of the dodecanoic acid and overall lower yields were recorded (Figure 4.3b). At high initial glucose and enzyme concentrations the alcohol yield is at its minimum and with decreasing enzyme concentration, the alcohol yield increases. Thus, at conditions were glucose is likely limiting the dodecanol production is relatively high.

Overall, a substantial over-oxidation of the 1-dodecanol product to dodecanoic acid, similarly to previous findings (chapter 3), can be seen. At 0.01 U ml^{-1} enzyme, an average alcohol to acid ratio of 0.37 ± 0.086 (SD) was recorded, whereas at 0.50 U ml^{-1} a ratio of 0.03 ± 0.007 (SD) was recorded. Thus, carbon source limiting conditions using a feeding strategy can have a positive effect on the alcohol to acid product ratio. However, with an increase of this ratio the average total molar product concentration drops 4.6-fold, mostly due to the reduction in dodecanoic acid yield. At any partic-

ular release rate, a change in initial glucose concentration had limited effects on the product concentrations. Therefore, glucose limiting the reaction is not a promising strategy by itself to influence the product ratio of the dodecane oxidation.

4.3.3 Glucose feeding for volatile alkane bio-oxidation

In order to investigate the impact of a carbon fed-batch strategy on the volatile alkane substrates, octane and hexane bioconversions were tested based on the response surface characterisation (see section 4.3.2) at $0.3 \, \text{U ml}^{-1}$ of enzyme and $1 \, \text{g l}^{-1}$ of initial glucose over 24 h. This is compared to a fed-batch reaction with no starting glucose and a control batch reaction with $5.5 \, \text{g l}^{-1}$ glucose. The overall amount of glucose available in both systems was aimed to be similar considering that with $0.3 \, \text{U ml}^{-1}$ enzyme about $4.5 \, \text{g l}^{-1}$ glucose are released in the system after 8.5 h. With the initial concentration of $1 \, \text{g l}^{-1}$ a total of approximately $5.5 \, \text{g l}^{-1}$ glucose is released similar to the initial amount in the batch reaction within the initial 8.5 h of the reaction.
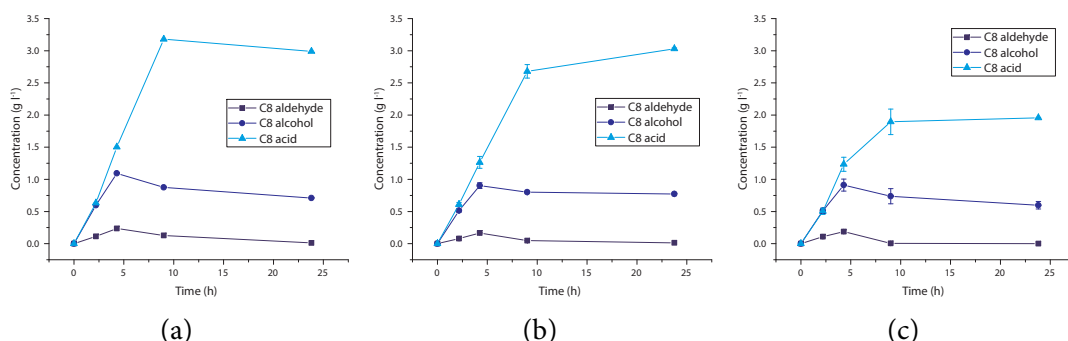
Figure 4.4: Bioconversion products of octane under fed-batch conditions with $1 \, \text{g l}^{-1}$ initial glucose (a), without initial glucose (b) and batch conditions with $5.5 \, \text{g l}^{-1}$ glucose (c), over 24 h at 30 °C and 250 rpm; $n = 2$, ±SD.

In case of octane, there is very little difference in product yields for the fed-batch conditions with (Figure 4.4a) and without initial glucose (Figure 4.4b). Compared to the batch reaction higher product concentrations were achieved, especially of the octanoic acid (+54 %) (Figure 4.4c). Overall, similar reaction rates are achieved over the initial 4.3 h (Table 4.4). However, in case of the fed-batch reaction with initial glucose the rates were elevated with the rate of 1-octanol and octanoic acid 20 % higher

on average over the other conditions.

For hexane, there are large differences between the fed-batch conditions with (Figure 4.5a) and without initial glucose (Figure 4.5b). In the fed-batch bioconversion with initial glucose, there is a high initial yield and production rate with accumulation of the aldehyde product; after 24 h similar product concentrations are recorded in both cases. The batch reaction shows an even higher initial production rate for the hexanal and accumulation of over $5\,\mathrm{g\,l^{-1}}$, more than 5-fold higher than the fed-batch reaction without initial glucose, albeit with large variability (Figure 4.5c).

(a) (b) (c)
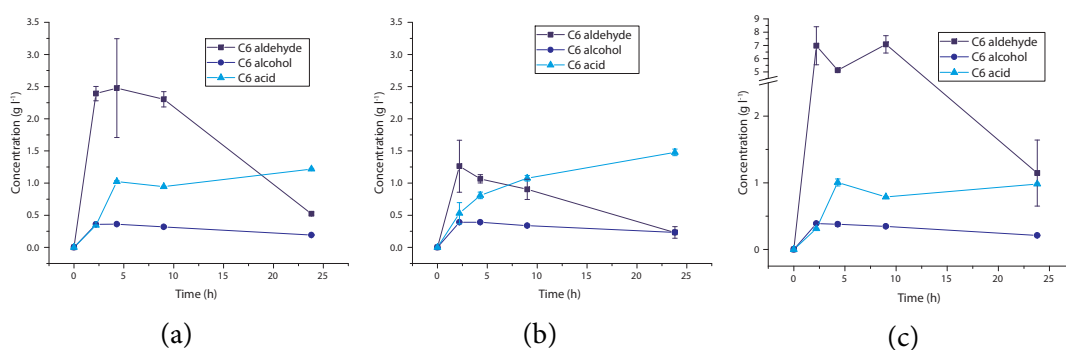
Figure 4.5: Bioconversion products of hexane under fed-batch conditions with $1\,\mathrm{g\,l^{-1}}$ initial glucose (a), without initial glucose (b) and batch conditions with $5.5\,\mathrm{g\,l^{-1}}$ glucose (c), over 24 h at 30 °C and 250 rpm; $n = 2$, ±SD.

Further, the hexanal production rate is almost 5-fold increased in the batch reaction compared to the fed-batch without initial glucose (Table 4.4). This indicates that the hexane oxidation is initially strongly energy limited when glucose is fed only without any initial supply compared to a reaction with initial glucose concentration of $5.5\,\mathrm{g\,l^{-1}}$. This effect has not been reported in the literature before, where often only endpoint product concentrations of the major alcohol or acid products are given.

This poses the question what causes the high hexanal production and if other substrates can potentially be oxidised by AlkBGT with similarly high turnover, but instead other factors such as mass transfer limitations reduce turnover or rapid metabolism of products and production of undetected by-products prohibits capturing this behaviour. With hexane being highly membrane soluble it is possible that it has lesser

Table 4.4: List of production rates over initial 4.3 h for hexane and octane reaction products, at 30 °C, 250 rpm; (* fed-batch with initial glucose of $1\,g\,l^{-1}$).

Substrate	Carbon strategy	Aldehyde $\mu g\,h^{-1}$	Alcohol $\mu g\,h^{-1}$	Acid $\mu g\,h^{-1}$
	Fed-batch	87.9	32.2	66.6
Hexane	Fed-batch*	204.0	29.8	84.3
	Batch	422.1	31.1	82.8
	Fed-batch	13.7	74.3	104.1
Octane	Fed-batch*	19.5	90.0	123.8
	Batch	15.4	75.1	101.7

mass transfer limitations than other substrates and is rapidly oxidised to 1-hexanol by AlkB, followed by oxidation to the aldehyde by the same enzyme. The new rate limiting step appears to be the aldehyde oxidation.

In all cases, the high initial hexanal concentrations do not result in similarly high hexanoic acid concentrations, whilst the aldehyde concentration falls over the course of the reaction. It is unclear what pathways are involved in this hexanal degradation and the fluxes across them. It is possible that the hexanal dimerises, however, during GC analysis no by-products were found. Moreover, so far it was assumed from the literature and previous data that 1-alcohol, aldehyde and acid are the major reaction products. The routine use of a mass spectrometric method would allow identification of unknown compounds. Further, to detect larger, less volatile molecules such as dimers, a liquid chromatography base method may be more suitable than gas chromatography.

4.4 Conclusion

This chapter demonstrated a proof-of-principle fed-batch implementation using enzymatic hydrolysis of a suitable oligosaccharide by an amyloglucosidase. This allowed preserving the design of the developed microwell plate system for two-liquid phase systems with full compatibility with volatile organic solvents. Whilst this approach foregoes the possibility to feed a variety of nutrients, and instead focuses on glucose,

the enzymatic release from a polysaccharide provides a flexible implementation for this system. This method allows the routine simulation of feeding glucose for biocatalytic oxidation reactions, with control of the release rate possible during a whole-cell biocatalytic reaction.

Initially, starch was identified as a suitable hydrolysis substrate allowing control over the amount of glucose released. The characterisation using the dodecane substrate showed a maximum product yield around $0.3\,U\,ml^{-1}$ of amyloglucosidase. For dodecane, the total product concentration and product distribution did not change considerably when varying initial glucose concentration at any particular glucose feed rate.

In contrast, large differences for the more volatile alkane substrates were found. The octane substrate showed a substantial increase in overall yields and thus productivity on the carbon source when using fed-batch strategies. Particularly, the octanoic acid yields were increased by over $50\,\%$.

In case of the hexane substrate it was shown that the fed-batch strategy can have a large effect on the aldehyde product concentration with a 5.5-fold decrease in the aldehyde product concentration at $2.2\,h$ relative to the batch reaction. Interestingly, the AlkBGT enzyme system appears to be capable of very high oxidation rates exemplified by the achieved hexanal concentrations under batch and fed-batch conditions of up to $7\,g\,l^{-1}$. This poses the question what causes the high oxidation rates of hexane and if it is possible to achieve similar rates for other substrates through biocatalyst or reaction engineering. Further, to follow and understand the unclear fate of the initially produced hexanal likely requires changes in analytical techniques to be able to capture and identify a wider range of potential products.

Although, in case of the hexane bio-oxidation the feeding strategy had an effect on the product ratios, it is unclear what the high aldehyde concentrations can be attributed to. In case of dodecane, the over-oxidation of the alcohol product could not

be reduced without considerably reducing the overall reaction yield at the same time, as shown in case of the dodecane oxidation. Overall, the results suggest that there are distinct optima for each substrate in terms of carbon source supply and it is difficult to generalise the results for other substrates.

The results not only show the successful implementation of a glucose feeding strategy in the developed microwell system, but also the impact of fed-batch conditions even on a resting cell biocatalytic reaction. The unpredictable nature and large differences between varying substrates show the importance of being able to test fed-batch conditions early in development.

Chapter 5

Characterising the impact of ternary solvent mixtures on alkane bio-oxidations

5.1 Introduction

Bioprocess conditions have a large impact on two-liquid phase bioconversions. Despite improvements in biocatalytic oxidation of alkanes and existing commercial processes, large efficiency gains are necessary for broader industrial application. Blank et al. (2008a) estimate a maximum specific activity of 367 mmol g_{DCW}^{-1} min^{-1} based on *in silico* modelling of co-factor regeneration for monooxygenase based bio-oxidation of hydrocarbons in resting *E. coli* cells under conditions with optimal NADH yield on glucose. This would result in $\approx$25 g l^{-1} h^{-1} of 1-octanol in case of the octane bioconversion. Despite this, the cellular energy balance is markedly influenced by the presence of organic compounds, due to an increase of NADH demand to maintain cellular integrity even at subtoxic levels, and results in a reduced biocatalytic efficiency (Kuhn et al. 2013).

The application of two-liquid phase media has long been established to supply hydrophobic organic substrates (Nakahara, Erickson, and Gutierrez 1977; Brink and Tramper 1985; Wubbolts et al. 1994; Déziel, Comeau, and Villemur 1999; Kim, Pollard, and Woodley 2007; Darracq et al. 2012) and/or remove organic reaction products *in*

situ (Daugulis 1988; Woodley et al. 2008; Wang and Dai 2010; Dafoe and Daugulis 2013) to reduce their inhibitory and toxic effects on the biocatalyst. For the whole-cell alkane bio-oxidation, the excess alkane substrate is commonly used as an second phase for product extraction. However, substrate dilution in an inert, non-toxic and non-aqueous solvent or addition of surfactants has been shown to improve yields (Grant, Woodley, and Baganz 2011), biocompatibility, downstream processing (Mathys, Kut, and Witholt 1998) and ultimately process economics (Schmid, Sonnleitner, and Witholt 1998). Thus, the selection and optimisation of non-conventional media is of major importance for process development and performance to fully leverage the biocatalytic capability of a whole-cell biocatalyst (Bruce and Daugulis 1991). This chapter refers to the third reaction medium component to a 'co-solvent', that predominantly solubilises the organic alkane phase and not the aqueous phase, which constitute the other two medium components.

The selection of inert co-solvents as carrier phases is difficult due to the large amount of parameters that are involved such as: biocompatibility, substrate bioavailability, product yield, environmental impact, partition coefficient and extraction selectivity. The last issue is especially applicable for controlling the specificity of the AlkB mediated oxidation and its product spectrum of primary alcohol, aldehyde and acid, where over-oxidation often leads to accumulation of the acid product.

Despite this, there is no clear guide for solvent selection. Computer-aided property estimation (CAPE) was proposed to generate a short list of candidates for testing (Lima-Ramos, Neto, and Woodley 2013; Murray et al. 2016). Nevertheless, consideration of experimental data on a case-by-case basis is necessary, ideally under process conditions.

There have been attempts to identify co-solvents rationally and design unconventional media for biological reactions based on physical parameters of substrate and co-solvents. Brink and Tramper (1985) relate the Hildebrand solubility parameter (δ)

and molecular size measurements (molecular weight and molar volume) of various organic solvents to biocatalytic activity of whole-cells in the biphasic epoxidation of gaseous alkenes. They found high activity retention with solvents of low to mid polarity and high molecular size such as dibutyl phthalate. Further, the solubility parameter can be used to estimate the capacity of the organic solvent for the substrate or products. However, the Hildebrand parameter is only applicable to largely non-polar, non-hydrogen bonding solvents.

Similarly, the alternative hydrophilic-lipophilic balance (HLB) system is only applicable to classify nonionic surfactants according to their water or oil solubility and is consistent only within homologous series of such surfactants (Schott 1995).

Laane et al. (1987) simplified the approach of Brink and Tramper (1985) by using the 1-octanol in water partition coefficient (log$P$) as a superior descriptor of solvent polarity and biocompatibility (Equation 5.1). The authors proposed the general rule that solvents with a log$P > 4$ are suitable for biocatalytic applications.

$$logP_{oct/wat} = log \left(\frac{[solute]_{octanol}}{[solute]_{water}} \right) \tag{5.1}$$

This is generally attributed to the destabilising effect of solvents with log$P < 4$ on essential water bound to the biocatalyst and membrane integrity (Vermuë et al. 1993). Further, Laane et al. (1987) suggest that by matching the polarity (log$P$) of the biocatalyst-continuous interphase to that of the substrate and/or dematching the polarity of the continuous organic phase with that of the substrate, the substrate concentration in the interphase can be maximised resulting in the optimum activity of an enzyme in a micelle. Similarly, the polarity of the continuous phase can be matched to the product polarity to extract the product away from the biocatalyst to avoid product inhibition or toxicity and shift the reaction equilibrium into the desired direction. Lastly, optimisation of the polarity of substrate and interphase can be im-

portant when substate inhibition occurs.

Schneider (1991) suggests to widen the scope of parameters that are used for correlation and prediction of biocatalytic activity in organic solvents. Instead of the one-dimensional log*P* or Hildebrand parameter, use of the three-dimensional Hansen solubility parameters (Hansen 2012) is proposed. The Hansen solubility space is comprised of three independent parameters that describe the diversity of solute-solvent interactions namely, dispersive forces (δ_d), polar interactions (δ_p) and hydrogen bonding (δ_h). The vector sum of all three parameters gives the previously mentioned Hildebrand parameter (δ) (Equation 5.2).

$$\delta = (\delta_d^2 + \delta_p^2 + \delta_h^2)^{0.5} \tag{5.2}$$

The solubility of a compound is displayed as a sphere in three-dimensional space with a geometric centre point (δ_d, δ_p, δ_h). In general, the solubility of two compounds decreases with increasing distance from each other.

Since then, there have been efforts to gain more mechanistic (thermodynamic) insight into biocatalytic reaction systems in multiphase non-conventional media to improve systematic predictability of these reactions (Halling 1994). The review proposes that the influences of simple physicochemical effects of solvents (such as changes in solvation or partitioning of water, organic substrates, products or ions between phases) should be allowed for before seeking explanation for residual effects from direct, difficult to predict interactions of solvents with the biocatalyst. In addition, physicochemical effects on mass transfer that occurs between liquid phases in the heterogeneous mixtures of biocatalysis in non-conventional media need to be considered.
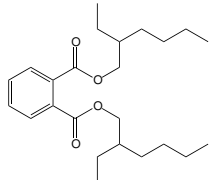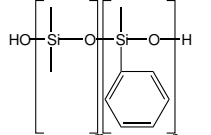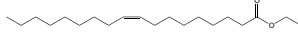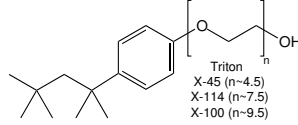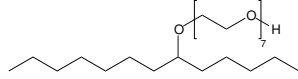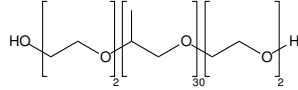
To this end, computer aided solvent selection (Bruce and Daugulis 1991; Vermuë and Tramper 1995; Abildskov et al. 2013) and integrated process and solvent design

(Wang and Achenie 2002; Cheng and Wang 2010; Moity et al. 2016) have been developed. Moreover, in recent years, increased attempts have been made to move away from a heuristic selection approach and instead to rationally select optimal solvents *a priori* for either substrate supply or product removal in biocatalytic systems (either enzymes or whole-cells). Zhou, Qi, and Sundmacher (2014) use theoretical quantum-chemical descriptors to quantify solvent effects in chemical reactions, rather than experimental parameters. Similarly, work has increasingly focused on investigating the influence of non-aqueous solvent properties on bio-catalysts and -reactions (Lousa, Baptista, and Soares 2013) to improve understanding of underlying mechanics. For example, the selection of polymers for two-phase partitioning bioreactors using thermodynamic models has been successfully shown (Bacon, Parent, and Daugulis 2014; Bacon et al. 2015). However, due to the high complexity of biochemical reactions, the application of universal models to predict outcomes *a priori* remains difficult.

Thus, this chapter aims at empirically investigating a range of co-solvents for the alkane bio-oxidation to determine their impact on product yields and specificity, as well as their biocompatibility. To this end, six co-solvents were chosen from literature and based on commercial availability. These span a wide range of polarities and structures, from very apolar small molecules such as bis(2-ethylhexyl) phthalate (BEHP) to more polar, polymeric molecules such as the nonionic triblock copolymer L-61 (Table 5.1).

It is hypothesised that the co-solvents cause a variety of effects. The more polar compounds (Tergitol, L-61 and Triton) would improve product extraction away from the biocatalyst and thereby alleviate product toxicity for improved overall yields. At the same time, the surfactants are likely to improve substrate access by promoting emulsion formation. This could result in increased yields, due to higher alkane substrate availability. In addition, reducing substrate limitations may favour the production of alcohol to over-oxidation. However, increased substrate availability may

Table 5.1: Overview of tested co-solvents, *FAME – fatty acid methyl ester.

Co-solvent	Structure	Details	References
Bis(2-ethyl-hexyl) phthalate		Non-toxic organic carrier phase for whole-cell FAME* oxidation; promotes over-oxidation	Cruz et al. (2004) and Schrewe et al. (2014)
Silicone oil		Non-toxic organic carrier phase for whole-cell phytosterol cleavage	Carvalho et al. (2009)
Ethyl oleate		Non-toxic organic carrier phase for whole-cell FAME oxidation; promotes over-oxidation	Kuhn et al. (2012) and Schrewe et al. (2014)
Triton X–Series		Biocompatible carrier phase for whole-cell bioconversion of sterols	Wang et al. (2004) and Wang et al. (2008a)
Tergitol 15-S-7		Biocompatible fatty acid extraction from algal cultures; recycling of surfactant	Glembin, Kerner, and Smirnova (2013)
Poloxamer L-61		Selective butanol extraction from ABE fermentation with L-62 (2×EO of L-61); recycling of surfactant	Dhamole et al. (2012)

also result in higher toxicity. In addition, the surfactants have been shown to form cloud-point systems, which can facilitate product separation and phase recycling, potentially alleviating the additional cost compared to an alkane-only organic phase (Wang 2007).

On the other hand, by use of the more apolar co-solvents (BEHP, silicone oil and ethyl oleate), it is expected that a dilution of the organic phase may reduce toxic hydrophobic compound concentrations and thereby mitigate their toxicity. Although BEHP has been widely used in the literature, ethyl oleate is included here as an en-

vironmentally friendly alternative (Kuhn et al. 2012). Silicone oil is included as an chemically inert alternative (El Aalam, Pauss, and Lebeault 1993).

The range of different molecules exemplifies the complexity of co-solvent selection. Further, in case of the alkane oxidation, the co-solvent approach attempts to potentially solve several problems: shielding the biocatalyst from excessive substrate or product toxicity whilst allowing substrate supply and extraction of products from the biocatalyst, preferentially the alcohol.

In order to efficiently investigate this breadth of aspects, the previously developed high-throughput microwell platform is leveraged. A multivariate data analysis (MVDA) approach is used to integrate physicochemical parameters of the co-solvents and reaction compounds into the analysis and maximise the utility of the experimental data.

5.2 Materials and methods

5.2.1 Solvent mixture preparation

All co-solvents were purchased from commercial sources (Sigma-Aldrich, UK) at the highest available purity; silicone oil was purchased from Acros Organics (Belgium).

In case of Triton surfactants, the surfactant was added to the aqueous buffer used for bioconversion reactions. All other co-solvent dilutions were prepared beforehand in the respective alkane substrate to either $50\,\mathrm{ml\,l^{-1}}$ or $300\,\mathrm{ml\,l^{-1}}$ concentration and stored in screw cap glass vials. Triton X-100 was prepared at $1\,\mathrm{ml\,l^{-1}}$ final concentration in the aqueous buffer, as before. Triton X-45/X-115 was prepared at $50\,\mathrm{ml\,l^{-1}}$ or $300\,\mathrm{ml\,l^{-1}}$ relative to the organic phase, despite being diluted in the aqueous phase. In all cases, except when using Triton X-100, the absolute aqueous and alkane phase volumes were kept constant and co-solvents were added in addition to the volumes used in the control reaction. For example, in case of an octane reaction with $30\,\%$ Tergitol, $100\,\mathrm{\mu l}$ of the prepared octane in Tergitol mixture ($300\,\mathrm{ml\,l^{-1}}$) were added

to 280 ul aqueous buffer. Reactions were performed at conditions determined in chapter 3, unless otherwise mentioned. Reactions with pentane as substrate were filled in a cold room at 4 °C to control excessive substrate evaporation before sealing the plate. Figure 5.1 provides a schematic description of the steps involved when running reactions with co-solvents in MPWs.
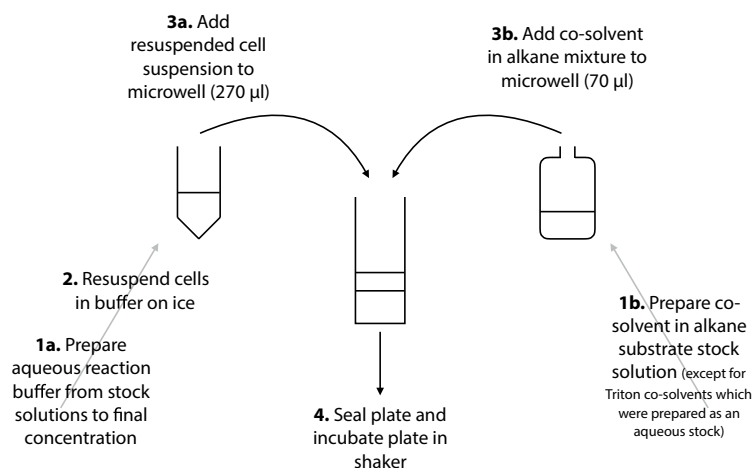
Figure 5.1: Scheme of microwell plate preparation for reactions with co-solvents.

5.2.2 Further hydrocarbon substrates

All further hydrocarbon substrates were purchased from commercial sources (Sigma-Aldrich, UK) at the highest available purity (>98 %).

5.2.3 Analytic procedures

Product recovery from solvent mixtures

Extraction efficiencies of reaction products in four co-solvents reaction mixtures (ethyl oleate, silicone oil, Tergitol, L-61) were tested at $300 \, \mathrm{ml \, l^{-1}}$ in the octane substrate. These were determined by spiking reaction mixtures without cells with known amounts of oxidation products. This was carried out in screw cap glass vials. Vials were mixed on a rotator for at least 2 h at room temperature before extraction with cyclohexane for GC analysis. After extraction for GC analysis and concentration determination, the amount of recovered product against the spiked amount can be calculated. Generally over 90 % of product was recovered from the reaction mixtures

(section D.1). However, in case of Tergitol, extraction drops to 70 % for the major products. This is partially due to the difficulty of separating the phases after mixing, a problem that did not occur when extracting reactions with cells in the aqueous phase. This illustrates a further problem, the presence of cells influences the phase composition for example by excretion of biosurfactants or due to surface active cell debris (Rojo 2010b).

Membrane extraction

In order to identify changes in the membrane lipid composition due to organic phase and co-solvent exposure, membrane extraction was performed similar to Royce et al. (2013) after the method by Bligh and Dyer (1959):

Cells exposed to a co-solvent reaction mixture were harvested and washed twice in 25 ml cold phosphate buffered saline (PBS) (pH 7) (Sigma-Aldrich) (centrifuge 5000 rpm, 4 °C for 15 min). The last resuspension was in 3 ml PBS followed by transfer in a 4 ml screw cap glass vial. The supernatant was removed after centrifugation (5000 rpm for 10 min). 50 µl of an internal standard were added followed by 1.4 ml methanol (Sigma-Aldrich, UK). The cell pellet was resuspended in the liquid and sonicated on ice for 3×20 s. After centrifugation at 5000 rpm for 10 min the supernatant was collected in a separate glass vial. The pellet was further incubated with 750 µl chloroform at 37 °C 150 rpm on a thermomixer for 5 min. A ternary mixture was used to separate the free fatty acids by combining the chloroform phase with the collected methanol phase and adding 1.4 ml of RO water. After phase separation 400 µl of the chloroform phase were collected in a new vial and the chloroform removed in an evaporator (Genevac). The remaining fatty acids were then methylated by adding 1 ml of 1.25 mol l^{-1} HCl in methanol (Sigma-Aldrich) and incubation at 80 °C for 30 min. After cooling, 0.5 ml of a 9 g l^{-1} NaCl solution were added and the sample was extracted with 2 ml cyclohexane for subsequent GC-MS analysis. The following compounds were found in the samples: myristic acid (C14:0), palmitic acid (C16:0), hexadecenoic

acid (C16:1), cyclopropane-C17:0 (C17cyc) and octadecenoic acid (C18:1). The peak areas of identified derivatised membrane fatty acids were used to calculate the length ratio (L) (Equation 5.3) and saturated versus unsaturated ratio (S : U) (Equation 5.4) (Royce et al. 2013).

$$L = \frac{14 \times C14{:}0 + 16 \times (C16{:}0 + C16{:}1 + C17cyc) + 18 \times C18{:}1}{C14{:}0 + C16{:}0 + C16{:}1 + C17cyc + C18{:}1} \tag{5.3}$$

$$S : U = \frac{C14{:}0 + C16{:}0}{C16{:}1 + C17cyc + C18{:}1} \tag{5.4}$$

Gas chromatography mass spectrometry

GC-MS was used to identify unknown bioconversion products from further substrates and membrane extractions. Samples from these reactions were prepared according to subsection 2.4.1.

Organic phase samples (1 µl) were separated by a Thermo Scientific Trace 1300 gas chromatography equipped with a Restek Rxi-5Sil MS column (30 m × 0.25 mm × 0.5 µm; Restek, USA) controlled by a Chromeleon 7.2 data system (ThermoScientific, USA). Helium was used as a carrier gas at constant flow (1.5 ml min^{-1}) with split injections (split ratio of 100).

For mass spectrometry a Thermo Scientific ISQ QD single quadrupole system was used with electron ionisation. Ion source temperatures and MS transfer line temperatures were set at 275 °C.

Further, GC-MS was used to identify and provide a relative quantification of membrane fatty acids from cell membrane extracts. Organic phase samples were prepared as detailed in section 5.2.3. However, in this case a constant helium flow rate of 1.4 ml min^{-1} and a split ratio of 50 were used for GC separation.

The temperature programmes for the GC can be found in Table 5.2. The C8

MS method was used for identification of new products, whereas the the FAME MS method was used for membrane extracts.

For detection of compounds, the instrument was set in full scan mode with range of 10 u to 350 u and a scan time of 0.12 s. Details of spectra for identified products can be found in Appendix E.

Table 5.2: Gas chromatography–mass spectrometry temperature programs.

Method	Injector T °C	Initial oven T °C	Ramp rate °C min^{-1}	Final oven T °C
C8 MS	260	90 (for 0.5 min)	25	270 (for 1 min)
FAME MS	270	160 (for 0.5 min)	15	270 (for 5 min)

Flow cytometry

Flow cytometry was performed to determine cell vitality after organic phase and co-solvent exposure by determining membrane integrity and thus permeability to DNA stains. Two stains are used, thiazole orange (TO) is a permeant stain and enters all cells live and dead, propidium iodide (PI) does not permeate cell membranes and stains cells to their degree of membrane damage. Thus, TO allows discrimination of cells from background noise and PO allows assessing the degree of membrane damage and therefore cell viability.

A PBS staining buffer (Sigma-Aldrich) (pH 7) was prepared with 1 mmol l^{-1} EDTA and 100 µl l^{-1} Tween 20. All buffers, including the reaction buffer, were filtered (0.22 µm) before use to reduce the background noise from small particles. Cells exposed to a co-solvent reaction mixture were harvested and washed twice in 12 ml cold staining buffer (centrifuge 5000 rpm, 4 °C for 15 min). The last resuspension was in 10 ml staining buffer followed by transfer of 10 µl solution to an Eppendorf tube prefilled with 490 µl staining buffer. Before flow cytometry analysis (Accuri C6, BD), 5 µl of thiazole orange (TO) (42 µmol l^{-1} in DMSO) and propidium iodide (PI) (4.3 mmol l^{-1} in water) were added and each sample was incubated for 5 min. Before

analysis sample tubes were gently mixed by repeatedly inverting the tube.

The flow cytometer (BD Accuri C6) thresholds were set at 5000 for SSC-H (side scatter) and 10 000 for FSC-H (forward scatter). A total of 50 000 events were recorded at medium flow rate (Figure D.2), unless otherwise mentioned.

For data analysis TO positive cells were gated on fluorescence detector FL1 (Figure D.3). The degree of PI staining of the gated population can be detected on detector FL3. A plot of FL1 versus FL3 allows discrimination of live and dead cell populations (Figure D.4). Excitation was done with a laser at 488 nm, filters were used at 533/33 (FL1) and 670/LP (FL3). Refer to section D.2 for exemplary raw data.

Cell concentrations in flow cytometer samples were estimated by dividing the number of recorded TO positive cell ('total cells') by the sample volume aspirate during analysis as recorded by the instrument.

Partition coefficient

Partition coefficients of reaction products between organic and aqueous phases were determined for four co-solvents reaction mixtures (ethyl oleate, silicone oil, Tergitol, L-61) at 300 ml l^{-1} in the octane substrate. These were determined by spiking reaction mixtures without cells with known amounts of oxidation products. This was carried out in screw cap glass vials. Vials were mixed on a rotator overnight at room temperature before centrifugation (5000 rpm, 20 °C for 15 min) for phase separation. The organic phase was subsequently removed and diluted in cyclohexane for GC analysis and organic phase concentrations were determined. Aqueous phase product concentrations were calculated by mass balance. Partition coefficients were then determined for each system using the Equation 5.5.

$$P_{org/aq} = \left(\frac{[solute]_{organic}}{[solute]_{aqueous}} \right) \tag{5.5}$$

5.2.4 Computational analysis

Physicochemical property estimation

Due to the difficulty of finding literature data for all compounds, estimation of Hansen and log$P$ parameters for co-solvents and reaction substrate and products was carried out using COMSOquick (Demo version 1.4, COSMOlogic, Germany). The quantitative structure property relationships models of the software were used to predict both parameters (Loschen and Klamt 2012). The Hansen parameter for silicone oil was estimated from Adamska, Voelkel, and Héberger (2007) and Woiton (2014).

The distance between two compounds in the Hansen space (R_S) and hence their solubility was estimated using the Equation 5.6 according to Hansen (2012). Here, the inverse was used to allow easier interpretation in subsequent analyses, thus, higher values represent better solubility.

$$R_S = \frac{1}{4\left(\delta_{d1} - \delta_{d2}\right)^2 + \left(\delta_{p1} - \delta_{p2}\right)^2 + \left(\delta_{h1} - \delta_{h2}\right)^2} \tag{5.6}$$

Multivariate data analysis

Partial least squares projections to latent structures (PLS) regression analysis was performed (SIMCA 13.0.2, Umetrics, Umeå, Sweden) for analysing multiple variables in one model (Wold, Sjöström, and Eriksson 2001). PLS models were fitted with default settings using autofit for model cross-validation. Relationships between factors and responses were assessed in loading plots. For interpretation, a line from a selected response was drawn through the origin of the plot and the X- and Y-variables were projected on the line. Variables at the opposite end of the line from the response were determined as negatively correlated, whereas variables close to the response are positively correlated with it. Model quality was assessed by goodness of fit (R2) and goodness of prediction (Q2). Model validation was carried out using permutation tests over 40 iterations.

5.3   Results and discussion

5.3.1   Solvent mixtures for alkane bio-oxidations

Solvent mixture screening

Initially, the six chosen co-solvents were screened together with control reactions without additional co-solvent and with 0.1 % Triton X-100. The screening was carried out at 5 % and 30 % co-solvent in five different alkane substrates over 24 h giving a total of 70 reactions (Figures 5.2 and 5.3).
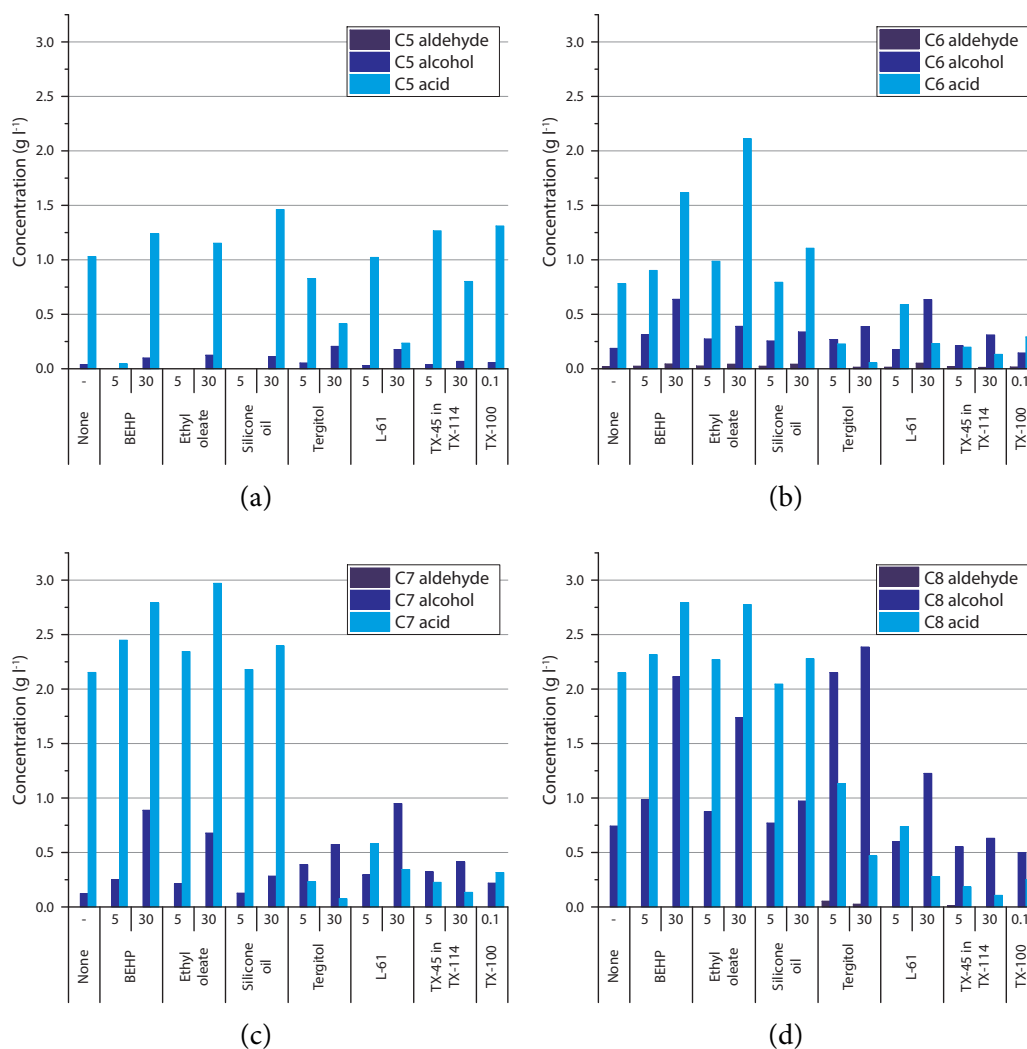
Figure 5.2: Co-solvent screening with pentane (a), hexane (b), heptane (c) and octane (d) after 24 h at 30 ℃ and 250 rpm, at varying co-solvent percentages in substrate indicated below x-axis, except TX-100 in aqueous buffer.

Interestingly, large, systematic variations in product concentrations were recor-

ded for the different reactions. A tendency towards over-oxidation to the acid product can be seen from the product concentrations, especially at the control conditions with no co-solvent. The aldehyde was found in trace amounts at its highest in all cases, suggesting that the alcohol oxidation is the rate-limiting step. In case of the dodecane substrate (Figure 5.3), high product concentrations are achieved only at low concentrations of Triton surfactants, as previously found (Grant et al. 2012).
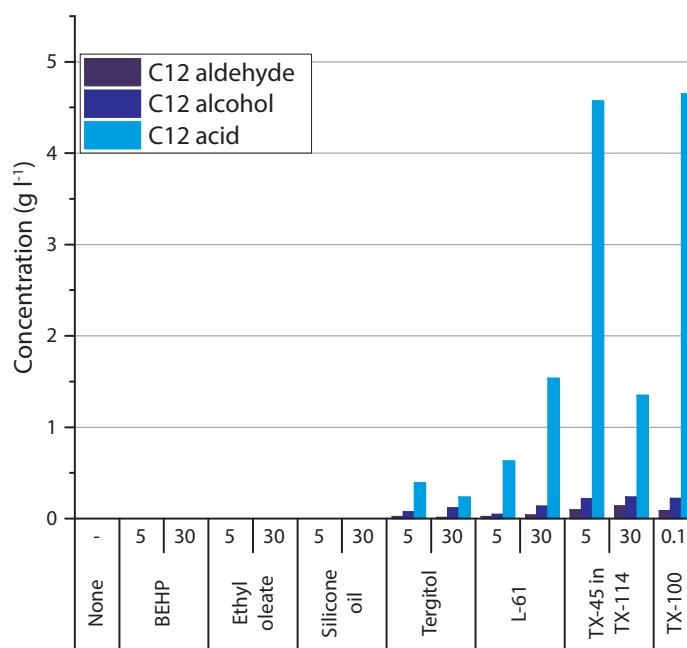
Figure 5.3: Co-solvent screening with dodecane after 24 h at 30 °C and 250 rpm, at varying co-solvent percentages in dodecane indicated below x-axis, except TX-100 in aqueous buffer.

With regard to the remaining data, the highest overall yields are achieved with the natural octane substrate (18.8 mmol l^{-1}), decreasing with substrate chain length (Figure 5.2d). Similarly, Beilen, Kingma, and Witholt (1994) found that shorter n-alkane substrates show reduced conversion rates, with longer chain substrates such as dodecane showing no conversion for a whole-cell system. This suggests that the biocatalyst is ideally suited for substrates of around eight carbon in chain length. However, Beilen, Kingma, and Witholt (1994) present *in vitro* results of a reconstituted AlkBGT system that shows conversion of longer chain substrates such as dodecane with similarly high rates to that of octane. This reiterates that with a whole-cell biocatalyst

not only do enzymatic limitations exist, but further constraints such as mass transfer influence product yields. In fact, the high product concentrations for the dodecane oxidation achieved with Triton X-100 show that the enzyme system is capable of very high conversion rates and that optimisation of substrate transport is vital. Similarly, the previously observed high hexanal production rate shows the potential of the enzyme system for high conversion rates (section 4.4).

Further, the average alcohol to acid product ratio is highest for the octane reactions (1.89), again, decreasing with substrate chain length. Therefore, similarly to the variation of total yields with chain length, the product spectrum is influenced by chain length. Again, whether this is a function of the biocatalyst, of the reaction conditions or a combination of both is unclear.

In terms of the product spectrum, it is interesting to note that reactions with the Tergitol, L-61 and Triton co-solvents achieve very high alcohol to acid ratios, on average 2.6, 1.2 and 1.7 respectively. For hexane and heptane over seven fold higher alcohol than acid product formation was seen after 24 h in the presence of 30 % Tergitol. Most interestingly, for the octane oxidation with 30 % Tergitol, an alcohol to acid ratio of 5.1 was seen with $2.4 \, \text{g} \, \text{l}^{-1}$ final 1-octanol concentration. This represents a 3.2 fold increase in alcohol yield relative to the control reaction without co-solvents for which the acid product dominates with a alcohol to acid ratio of 0.35 whilst maintaining similar overall product yields.

In case of hexane, heptane and octane, the overall highest product quantities were achieved with the more nonpolar solvents, namely BEHP, silicone oil and also ethyl oleate. Up to $35.6 \, \text{mmol} \, \text{l}^{-1}$ of products were formed in case of the octane oxidation with 30 % BEHP present. This represents a 1.7 times increase relative to the control reaction without co-solvent and 1.6 times higher than in the reaction with 30 % Tergitol. The increase in overall yield with higher concentrations of these co-solvents is contrary to previous findings were BEHP was seen to limit substrate access and promote

overoxidation (Cornelissen et al. 2013; Schrewe et al. 2014). However, in these studies, much lower substrate concentrations in BEHP were used compared to this study. Thus, it is likely that there is an optimum BEHP concentration that allows maximum overall product yields, before either limiting substrate access (at higher BEHP concentrations) or ineffectively mitigating substrate and product toxicity (at lower BEHP concentrations).

Solvent mixture time course

In order to verify the co-solvent effects seen in the initial screening and as a basis for further work, time course data was collected under selected of conditions. For that, four co-solvents were chosen, namely ethyl oleate, silicone oil, L-61 and Tergitol each at 30 % concentration in alkane substrate.

These were chosen to represent the whole spectrum of polarities and due to their effects on overall yield (ethyl oleate) or their effect on the alcohol to acid ratio (Tergitol and L-61). Silicone oil was included due to its inert properties despite its small effects on the reaction. Time course experiments were performed using the octane substrate and compared to a control reaction without co-solvent (Figures 5.4 and 5.5).

Overall, the trends of the screening were confirmed by the time course data. High overall yields were recorded in the presence of ethyl oleate and silicone oil with the octanoic acid product dominating (Figure 5.4).

In the presence of Tergitol and L-61, the trend of high 1-octanol yields and high alcohol to acid ratios was confirmed (Figure 5.4). Again, overall yields similar to the control reaction were achieved in case of Tergitol (Figure 5.5).

5.3.2 Solvent mixture effects on alkane bio-oxidations

On the basis of the time course experiments with octane, a more detailed investigation was initiated. The aim was to uncover physical and physiological causes for the effects of co-solvents on the alkane oxidation reaction, with a view to generalise these.
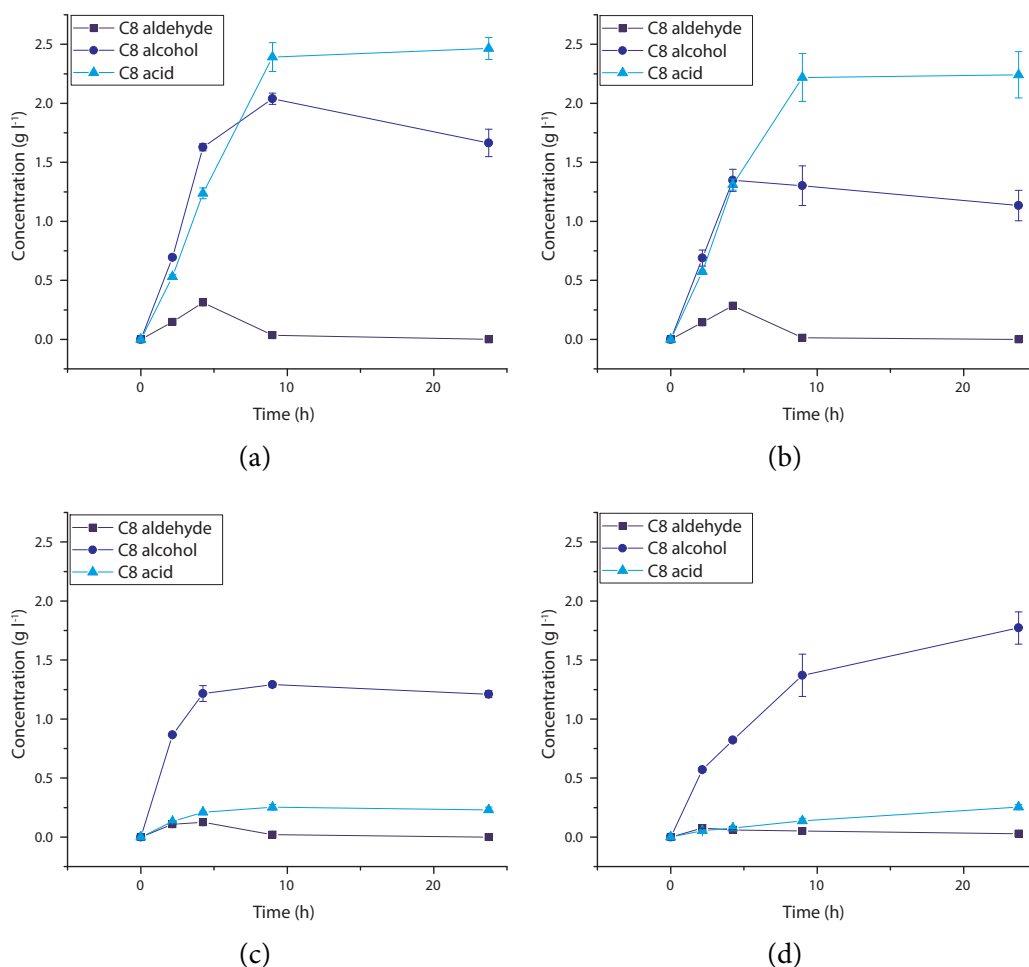
Figure 5.4: Bioconversion time course with co-solvents: 30 % ethyl oleate (a), silicone oil (b), L-61 (c) or Tergitol (d) in octane over 24 h at 30 °C and 250 rpm; n = 2, ±SD.

Product partition coefficients in solvent mixtures

The partition coefficient ($\log P$) of a compound reflects the ratio of its concentration in a mixture of two immiscible phases at equilibrium. Here, the partition coefficients for the three reaction products of an octane oxidation in reaction media with different co-solvents were determined under the reaction conditions (subsection 5.2.1) (Figure 5.6). This helps in understanding the efficiency of co-solvents to extract products from the aqueous phase.

Generally, the aldehyde and alcohol products mostly partition in the organic phase, whereas the acid product partitions in the aqueous phase (shown as $P_{aq/org}$). A large deviation (≈10 ×) relative to the control sample without co-solvent occurs when
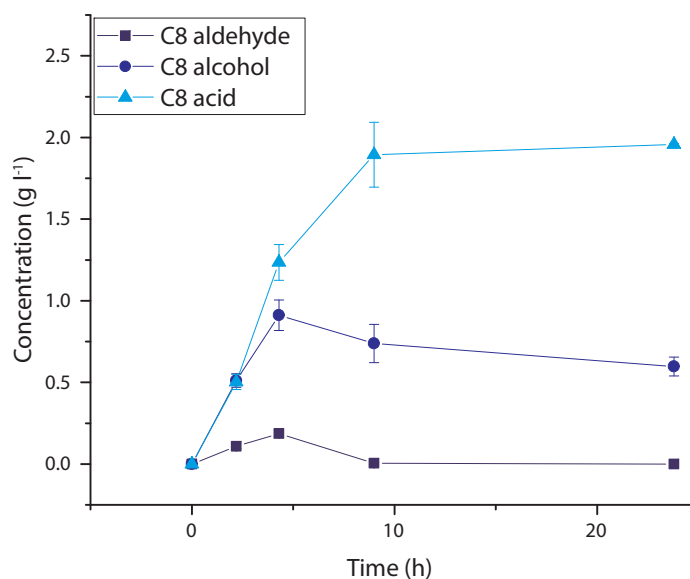
Figure 5.5: Bioconversion time course with octane only over 24 h at 30 °C and 250 rpm; $n = 2$, ±SD.
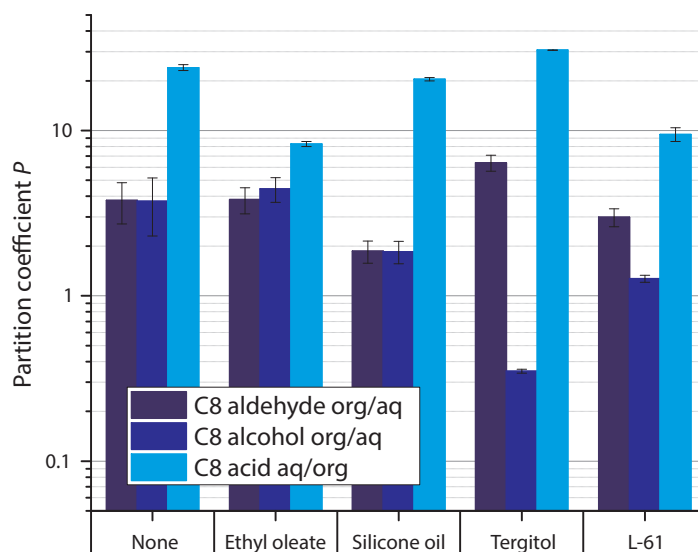
Figure 5.6: Partition coefficient for octane reaction products in different reaction media, co-solvents at 30 % in octane; $n = 3$, ±SD.

30 % Tergitol is added to the octane substrate. Here, the 1-octanol product partitions to the aqueous phase preferentially.

It is interesting to note that this seems to affect only the alcohol with the octanal and octanoic acid partitioning largely unchanged over the control without co-solvent. It would be expected that lower alcohol partition coefficient would lead to higher aqueous concentrations in reactions at identical overall concentrations. As a con-

sequence, higher toxic effects towards the biocatalyst would result. However, the overall octane oxidation yields with Tergitol as a co-solvent are not reduced when compared to the control reaction.

Potentially, at 30 %, the Tergitol forms a third, surfactant rich phase separate from the aqueous, which is not appropriately detected due to only measuring concentrations in the organic phase when determining the partition coefficient. In this case, the Tergitol may be extracting the alcohol from the catalyst into the surfactant phase resulting in the recorded high alcohol yields due to a reduction in over-oxidation and toxicity. With L-61, the partition coefficient of alcohol are slightly reduced compared to the control, this may lead to similar effects as seen with Tergitol albeit at lower overall yields.

Overall, the differences in partition coefficient between the co-solvents appear rather small. This indicates that the physical environment, measured by the partition coefficient of products, is not exclusively responsible for the recorded effects. Instead, the cellular impact of co-solvents may dominate.

Reaction media effect on cells

In order to assess the biocompatibility of the two-liquid phase culture a flow cytometry assay was used (Halan, Schmid, and Bühler 2011; González-Peñas et al. 2014). The aim was to detect cell membrane damage, a regular result of cellular contact with organic solvents. Dual staining was used, thiazole orange (TO) stains DNA in all cells irrespective of membrane damage whereas propidium iodide (PI) only stains DNA in damaged cells with permeable membranes.

Figure 5.7 shows cell survival under different co-solvents with control after 4.5 h incubation at 30 °C and 250 rpm. Four values are shown for each reaction, the 'total cell' value measures the percentage of identified cells (TO+) relative to all recorded particles. The 'dead', 'injured' and 'live cell' values then measure the degree of PI staining, where dead cells are PI+ and live cells are PI-; these values are relative to the
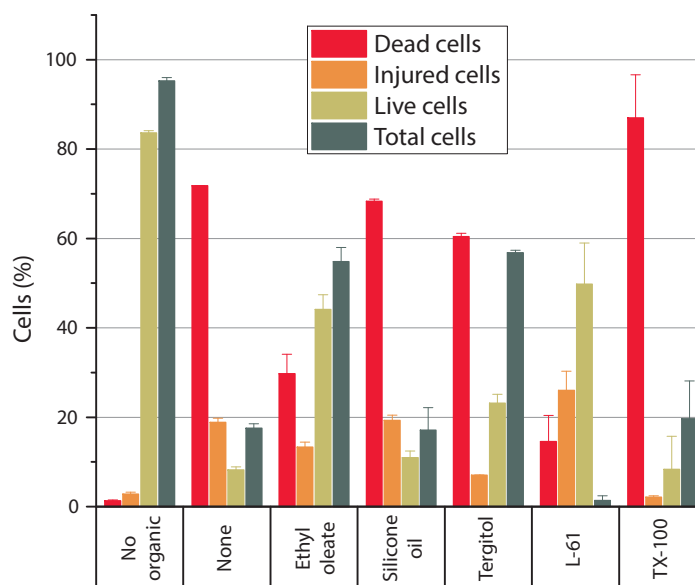
Figure 5.7: Cell survival after exposure to octane/co-solvent two-liquid phase systems measured by flow cytometry, after 4.5 h at 30 °C and 250 rpm; co-solvents at 30 % in octane, except for TX-100 at 0.1 % in aqueous buffer; 'no organic' – control containing no organic substrates or co-solvent, 'none' – control containing only octane; $n = 3$, ±SD.

number of TO+ cells. In addition, the flow cytometry data allows the approximation

of absolute cell concentrations shown in Table 5.3.

Table 5.3: Estimated cell concentrations after exposure to octane/co-solvent two-liquid phase systems, after 4.5 h at 30 °C and 250 rpm; co-solvents at 30 % in octane, except for TX-100 at 0.1 % in aqueous buffer; 'no organic' – control containing no organic substrates or co-solvent, 'none' – control containing only octane, $t = 0$ h sample was not exposed to organic solvents; *samples for which 25 000 events were recorded; $n = 2$, ±SD.

Reaction	Cell concentration cells/µl ±SD
At $t = 0$ h	3961 ± 468
No organic	2990 ± 288
None	393 ± 39
Ethyl oleate	1336 ± 33
Silicone oil	436 ± 114
Tergitol	403 ± 44
L-61	2 ± 1*
TX-100	27 ± 7*

Compared to the control without any organic phase, the concentration of cells

found in the reaction samples with co-solvents is drastically decreased and a large

proportion of the found cells is damaged. In case of the reaction with octane, the

percentage of total cells drops from 95 % to 18 %, at the same time the dead cells now represent 72 %. Marginally better results are achieved in the presence of silicone oil with 68 % dead cells. This is similar to reaction yields that show only small improvements in the presence of silicone oil. This information supports the hypothesis that silicone oil remains biochemically inert in the reactions and acts only by diluting the substrate phase and thereby marginally mitigating toxicity.

In contrast, the control reaction with Triton X-100 has a higher percentage of dead cells (87 %) than the control without co-solvents at a similar total cell recovery. In addition to acting as a surfactant, it is well know that Triton permeabilises cells (Miozzari, Niederberger, and Hütter 1978) allowing to overcome mass transfer limitations across cell membranes for water soluble (Van der Werf, Hartmans, and Tweel 1995; Cánovas, Torroglosa, and Iborra 2005) and hydrophobic compounds (Doig et al. 2003). Cánovas, Torroglosa, and Iborra (2005) show the outer membrane permeabilisation by Triton reducing the mass transfer limitations this membrane poses for hydrophobic compounds (Nikaido 2003). In this case, with excess amounts of octane present, the intended membrane permeabilisation and destabilisation may exacerbate the cellular toxicity of octane (or the reaction products) and thus reduce the biocatalyst performance due to leakage of ions and macromolecules, impeded co-factor regeneration and accelerated cell death. Ultimately, it is likely that this is the factor most contributing to the lowest overall product yields. Only in the case of dodecane significant yields are achieved when using a Triton surfactant, as reported previously (Grant 2012). Here, Triton is necessary to facility substrate mass transfer in the microwell system. Due to the much reduced toxicity of the longer chain dodecane substrate, the toxic effects of higher availability are less detrimental.

Interestingly, in the presence of ethyl oleate, a total cell value of 55 % was recorded with only 30 % dead cells. This correlates well with some of the highest overall product yields recorded in the presence of ethyl oleate during the initial screening (Figure 5.2).

The discrepancy between silicone oil and ethyl oleate suggests that in case of the latter, not only do physicochemical effects occur by diluting the substrate, but there are also biochemical effects that contribute to better biocompatibility and higher yields. In fact, Bird, Laposata, and Hamilton (1996) have shown that ethyl oleate integrates into small unilamellar phospholipid vesicles (SUV) at up to $0.25\,\text{mol}\,\text{mol}^{-1}$ of EO in SUV with the carbonyl group at the aqueous interface. Thus, it is possible that ethyl oleate has biological effects on the cells, for example stabilising the membrane by integrating into it.

Reactions with the surfactant Tergitol 15-S-7, exhibit an equally high total cell value (57 %). However, the proportion of those that were classified dead was higher at 60 %. Thus, compared to the control, Tergitol addition seems to mitigate substrate toxicity and cell death to some extent when using octane as a substrate.

In case of L-61 the least amount of cells was recovered from the reaction sample (2 %). Despite the product yields from reactions with L-61 being lower than the control, yields were still higher than the Triton control which shows better cell survival. It is unclear why this value is extremely low compared to the other samples, Poloxamers have been of interest in the biomedical field for their interactions with lipid membranes (Wang et al. 2013; Pitto-Barry and Barry 2014). It has been shown that poloxamers can cause temporary stabilisation of cell membranes, however, depending on their concentration and composition, interactions between polar head groups and hydrophilic blocks in the copolymer ultimately cause membrane instability leading to bending, increased permeability and eventually lysis (Nawaz et al. 2012; Hezaveh et al. 2012). Specifically, L-61 has been demonstrated to form pores in membranes (Krylova and Pohl 2004; Binder 2008) as well as accelerate transport specifically of large molecules with proton-donating groups (OH, COOH, NH) (Krylova et al. 2003; Bugrin and Melik-Nubarov 2007). Other poloxamers have been shown to seal damaged membranes (Adhikari et al. 2016).

This research suggests that the length of polypropylene oxide and polyethylene oxide chains is vitally important in determining the specific effects of poloxamers and that this needs to be a target for further optimisation. Budkina et al. (2012) show that in mammalian cells, L-61 has similar *in vitro* toxicity to TX-100. This suggests that similarly to TX-100, L-61 causes excessive membrane permeabilisation and cell lysis in the alkane oxidation reaction ultimately leading to the recorded low cell viability and recovery.

Process condition effects

In order to further investigate the 'mode of action' of the co-solvents, the impact of agitation and co-solvent concentration was tested. For the control reactions without co-solvent increasing agitation from 250 rpm to 350 rpm has no effect on yields (Figure 5.8). On the other hand, the reactions with co-solvents show large impacts, similar to those observed in the initial screening.

In case of ethyl oleate, an increase in co-solvent concentration in the substrate phase and increase in agitation results in increased yields after 24 h. Similarly, higher concentrations of silicone oil increase yields, however, increased agitation seems to have no positive impact. In fact, at 350 rpm there appears to be an optimum around 10 % co-solvent in substrate with no further increase in yield with high co-solvent concentration.

In both cases, it is assumed that co-solvent addition acts as a reservoir to reduce toxic effects of substrate and products. Addition of more co-solvent dilutes the toxic compounds, unspecifically reducing cellular toxicity. However, with ethyl oleate at 350 rpm yields are increased over the control and over samples at 250 rpm even at 1 % ethyl oleate. This suggests that adding ethyl oleate results in better phase mixing with increased agitation possible by acting as a mild detergent, ultimately resulting in better substrate access and 25 % higher yields at 350 rpm. The increased substrate access can also be responsible for increasing the average alcohol over acid product ratio by 20 %.
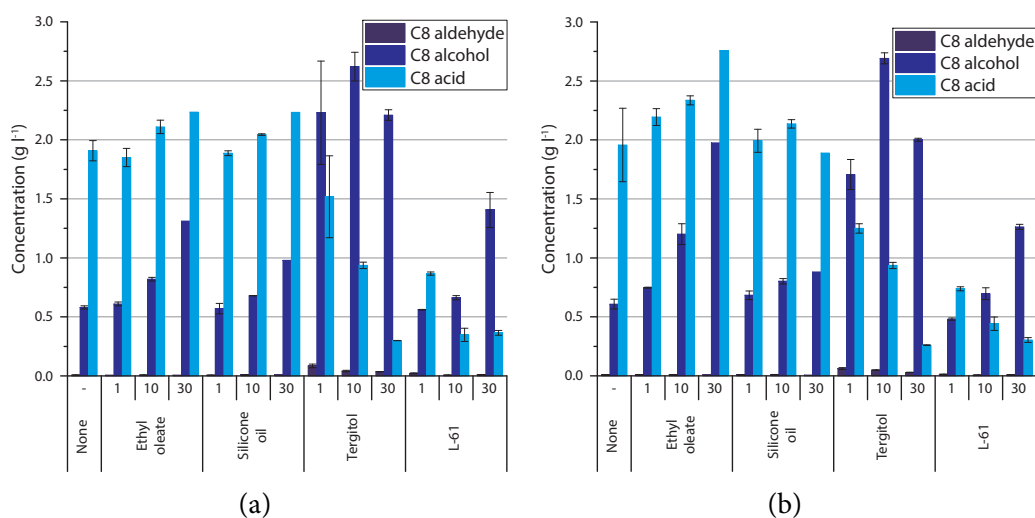
Figure 5.8: Co-solvent screening with octane at 250 rpm (a) and 350 rpm (b) after 24 h at 30 °C, at varying co-solvent percentages in octane indicated below x-axis; $n = 2$, ±SD.

Reactions with Tergitol show a clear influence of co-solvent concentration on the alcohol to acid ratio reaching a value of over seven at 30 % Tergitol in octane. The influence of agitation appears marginal over the range investigated here.

In case of L-61, the results follow similar trends, with dependence of the alcohol to acid ratio on the co-solvent concentration with the highest value of over 1.5 reached at 30 % L-61.

This supports the hypothesis that Tergitol and L-61 primarily act by improving substrate access, thereby favouring the oxidation of the n-alkane and 1-alcohol production rather than over-oxidation of the alcohol product. The generally lower yields with L-61 are likely to be a result of the lower biocompatibility of the copolymer as found previously (Figure 5.7).

Membrane composition effects

Membrane changes due to environmental influence has been well documented in bacteria (Zhang and Rock 2008). These include fatty acid composition, *cis* to *trans* fatty acid isomerisation, changes to saturated-to-unsaturated fatty acid ratio, changes in phospholipids and changes to lipopolysaccharide composition. Solubilisation of solvents in membranes generally results in an increase in the membranes' fluidity.

To reduce disruptive effects of organic solvents on membranes, bacterial cells reduce membrane fluidity through alterations in membrane composition (Mykytczuk et al. 2007). A short-term mechanism is the *cis* to *trans* isomerisation of unsaturated fatty acids in lipid bilayers and an increase in the saturated-to-unsaturated fatty acid ratio (S : U) as a longer-term response (Ramos et al. 2002). The average acyl acid chain length of phospholipids can also be increased as a response.

Here, the impact of the various non-conventional media on the cell membrane are investigated. It was expected that due to the exposure of cells to the organic alkane substrate a shift towards saturated fatty acids and longer acyl chains would be observed.
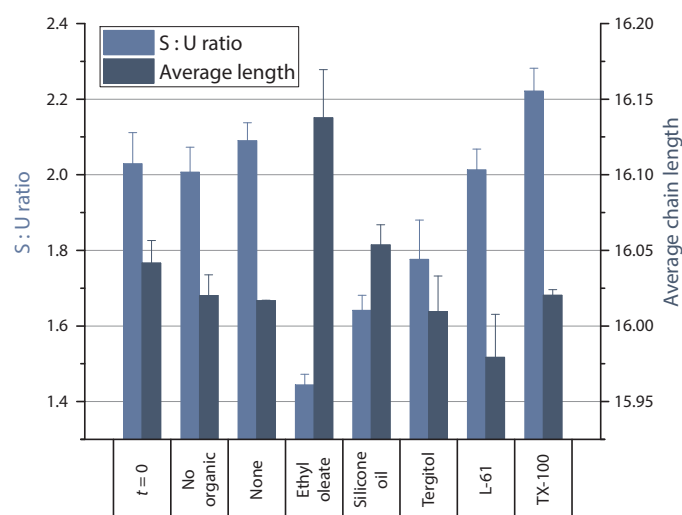
Figure 5.9: Changes to average fatty acid acyl chain length and saturated-to-unsaturated fatty acid ratio in cell membranes after 2 h exposure to octane/co-solvent two-liquid phase systems at 30 °C and 250 rpm; co-solvents at 30 % in octane, except TX-100 at 0.1 % in aqueous buffer; 'no organic' – control containing no organic substrates or co-solvent, 'none' – control containing only octane, $t = 0$ h sample was not exposed to organic solvents; $n = 3$, ±SD.

Figure 5.9 specifically shows changes in the average fatty acid chain length and the saturated-to-unsaturated chain length after 2 h exposure to various co-solvent mixtures in octane. Interestingly, only in case of the reaction containing Triton X-100 a shift towards more saturation fatty acids can be seen (10 % increase) compared to controls without organic compounds at $t = 0$ and after 2 h incubation.

In case of Tergitol, ethyl oleate and silicone oil, the ratio decreased by up to 28 %. This change, counter to the expectations, may be due to the short timeframe allowed for adaptation, however, a longer time would mean that in some cases a large amount of cells would have lysed already (compare section 5.3.2). However, Lennen et al. (2011) found a large increase in unsaturated fatty acid content after cytosolic exposure to free fatty acids (C8-C14). The authors point to the perturbation of membrane lipid homeostasis and the inability of cells to compensate an enrichment in unsaturated acyl-acyl-carrier-proteins, rather than a purposeful attempt at regulation. In fact, there appears to be a tendency in reactions with co-solvents for higher octanoic acid yields and a decrease in the S : U ratio (Figure 5.10). However, due to the multiple products in this reaction, it remains difficult to attribute this effect to the concentration of a single product or the substrate.

In case of the reaction with ethyl oleate the higher unsaturated fatty acid content as well as a longer fatty acid chains may be due to the integration of ethyl oleate into the membrane. However, the possibility that there was carry-over of ethyl oleate from the reaction into the sample was not controlled.
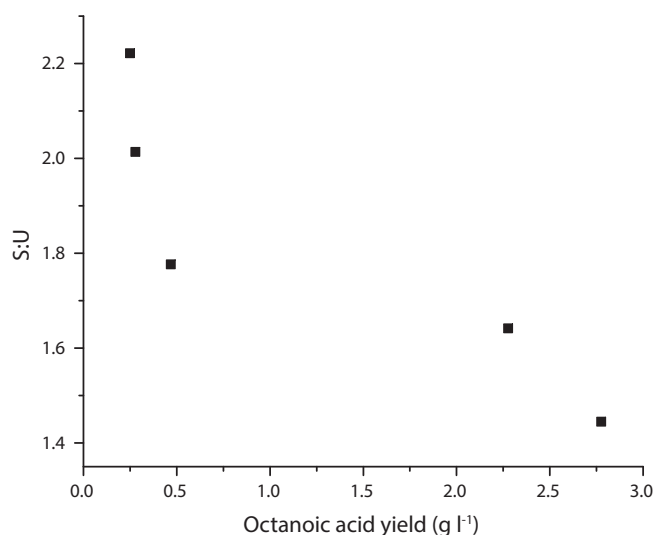
Figure 5.10: Scatter plot of octanoic acid yields from reactions with 30 % co-solvents (from Figure 5.2d) and corresponding S : U ratios (from Figure 5.9).

The average fatty acid length showed only small changes (maximum difference

of 0.16). Generally, longer fatty acid chains result in increased bilayer stability reduced fluidity. In samples from co-solvent reactions, the average length showed an inverse behaviour to the S : U ratio. This indicates an adaptation by the microorganism to the organic solvents in the reaction.

Overall, these results show the biological impact that the co-solvent reaction media have on the bio-oxidation of alkanes. Whether the changes in membrane composition are caused by direct interaction with the cells or indirectly by changing the toxic product or substrate concentrations remains unclear. In any case, the detrimental impact of membrane composition and homeostasis and the cells' inability to cope in the presence of free fatty acids presents a metabolic engineering opportunity to improve stability of whole-cell biocatalysts.

Phase behaviour visualisation

In order to visualise the phase behaviour and mixing of cell-free co-solvent reaction mixtures, samples were shaken with a 25 mm throw in a transparent microwell mimic and recorded using a high speed camera. Figure 5.11 shows the agitated conventional two-liquid phase medium for bio-oxidation of octane and with various co-solvents mixtures.

The figures show large qualitative differences between the various conditions. The attempt to quantify parameters such as droplet size to be used as a scale-up parameter (see Cull et al. (2002)) failed due to the high density emulsion formation and generally large differences between the mixtures. The lack of resolution and deep depth of field of the camera setup contributed to the problem. Nevertheless, some general, instructive trends can be seen. In case of no co-solvent addition (Figure 5.11a and 5.11b) and with silicone oil addition (Figure 5.11g and 5.11h), no phase mixing can be seen at either agitation speed. However, in case of the ethyl oleate (Figure 5.11f) and Triton X-100 Figure 5.11d, droplet formation can be seen at 350 rpm. Due to the droplet formation, ethyl oleate appears to act as a mild detergent.
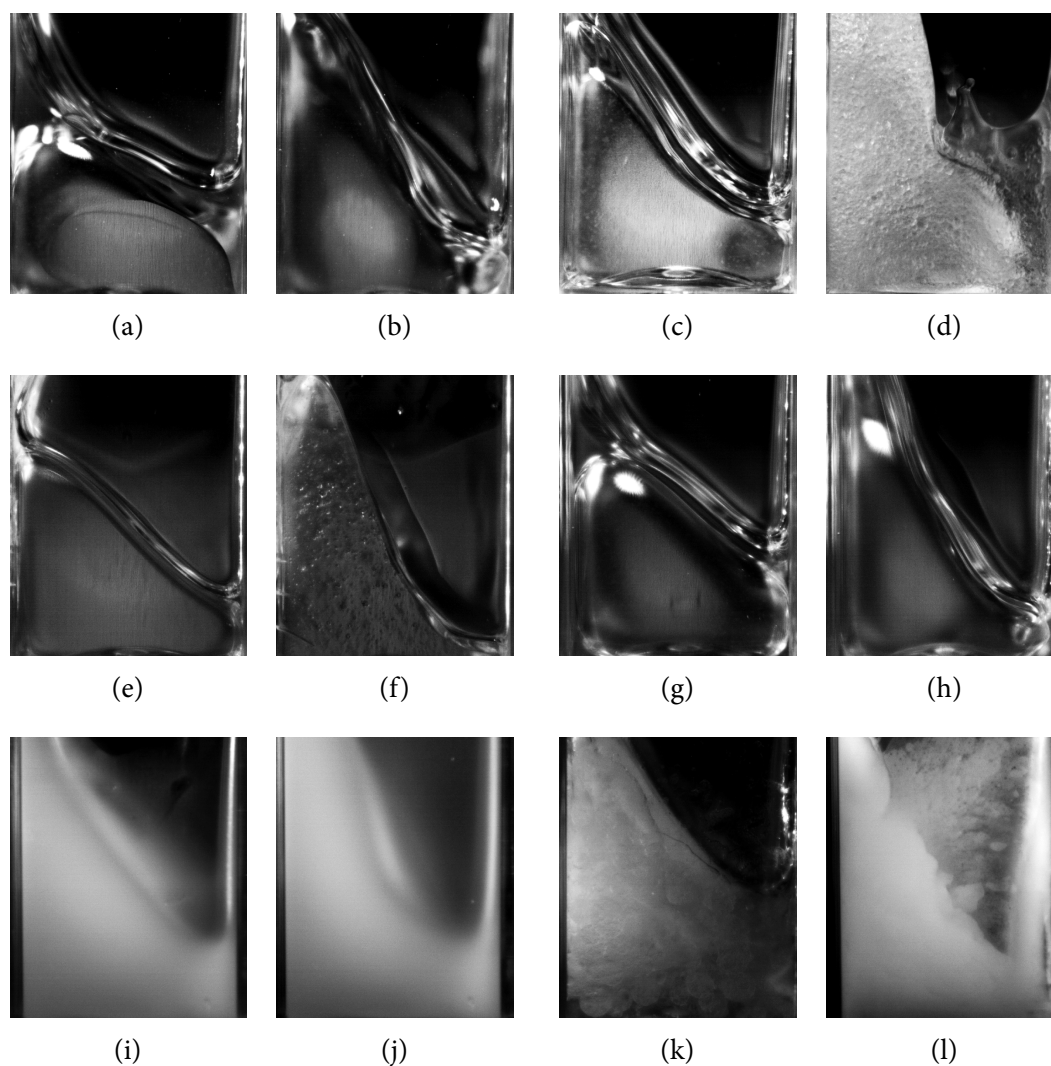
Figure 5.11: Mixing visualisation of two-phase bioconversion media in well mimic: with octane at (a) 250 rpm, (b) 350 rpm, octane with 0.1 % Triton X-100 at (c) 250 rpm, (d) 350 rpm, with 30 % ethyl oleate in octane at (e) 250 rpm, (f) 350 rpm, with 30 % silicone oil in octane at (g) 250 rpm, (h) 350 rpm, with 30 % Tergitol in octane at (i) 250 rpm, (j) 350 rpm, with 30 % L-61 in octane at (k) 250 rpm, (l) 350 rpm; all at 30 °C.

The droplet formation upon Triton X-100 addition agrees well with results from Grant et al. (2012) when using dodecane. In contrast to dodecane, octane conversion occurs even without phase mixing and no addition of co-solvents. This is likely to be a result of the over 150 times higher water solubility of octane (ChemSpider, RSC).

In case of Tergitol a very fine, stable emulsion is formed with no individual droplets visible (Figure 5.11i and 5.11j). It is not possible to differentiate between aqueous and organic phases. It is likely that the emulsion increases substrate access

of the biocatalyst by increasing the surface area available for mass transfer.

Addition of L-61 similarly results in an emulsion, however, the morphology is visibly heterogeneous (Figure 5.11k and 5.11l). Again, the organic and aqueous phases cannot be clearly differentiated or assigned as the continuous or dispersed phase.

The Tergitol and L-61 surfactants have cloud point temperatures at about 37 °C and 24 °C, respectively (Glembin, Kerner, and Smirnova 2013; Dhamole et al. 2012). Above these temperatures a separate, surfactant rich phase is formed. In case of Tergitol the cloud point temperature is higher than the reaction conditions, thus no phase separation is observed resulting in a homogeneous mixture. In the sample with L-61, with a reaction temperature above its cloud point temperature it appears that phase separation has occurred. This cloud point separation may cause compartmentalisation of the phases rather than increasing phase mixing and ultimately lower the overall product yields.
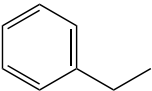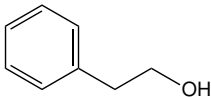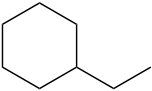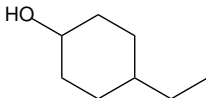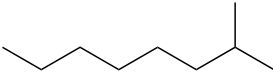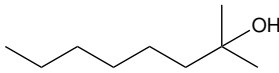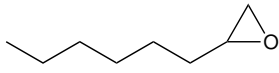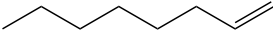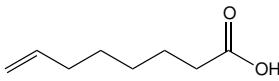
These results also have important implications for downstream processing, especially in case of the Tergitol and L-61 surfactants. The formed surfactant rich phase often solubilises apolar products well, and upon phase separation and removal, can allow efficient extraction of the product from the reaction.

5.3.3 Solvent mixtures with further alkane substrates

This investigation was focussed on assessing if hydrocarbon substrate other than n-alkanes show similar behaviour in reactions with co-solvents and if similar improvements can be achieved. Four hydrocarbon substrates with previously reported conversion by AlkBGT-based whole-cell biocatalysts were selected (Table 5.4, Smet et al. (1983) and Beilen, Kingma, and Witholt (1994)).

The further substrates were chosen based on their chemical diversity and commercial availability. Together with the four previously selected co-solvents, a screening was carried out with controls using Triton X-100 and no co-solvent in a total of 24

Table 5.4: Overview of further bio-oxidation substrates and respective products.

Substrate	Structure	Product	Structure
Ethylbenzene		2-Phenyl-ethanol	
Ethyl-cyclohexane		4-Ethylcyclo-hexanol	
2-Methyl-octane		2-Methyl-2-octanol	
		1,2-Epoxy-octane	
1-Octene		7-Octenoic acid	

experiments. New reaction products were first identified by GC-MS before quantification with external standards on a GC-FID system.

In case of ethylbenzene, ethylcyclohexane and 1-octene the identified products matched with the literature (Smet et al. 1983; Beilen, Kingma, and Witholt 1994). In case of 2-methyl-octane, this study identified 2-methyl-2-octanol as single reaction product, whereas Beilen, Kingma, and Witholt (1994) identified 7-methyl-1-octanol as the main reaction product with small amount of 2-methyl-1-octanol. Although the mass spectrum identification for the 2-methyl-2-octanol product in this study was good (see Appendix E), there is a possibility of misidentification of the products of this reaction.

In contrast to the n-alkane substrates were a considerable amount of acid product can be found routinely, the alcohol product dominates in case of the these substrates (Figure 5.12). Unfortunately, only in case of 1-octene are several products were formed in significant quantities, namely 1,2-epoxyoctane and 7-octenoic acid. Thus, the effect of co-solvents on the product spectrum could only be investigated for the 1-octene substrate, unlike the linear alkanes.
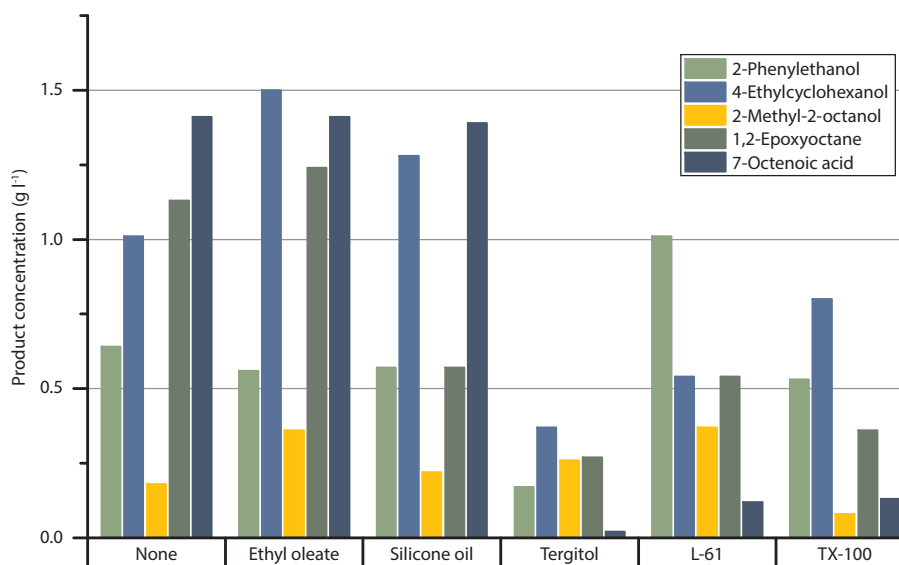
Figure 5.12: Product concentrations of co-solvent screening of further hydrocarbon substrates after 24 h at 30 °C and 250 rpm, at 30 % co-solvent in substrate, except for TX-100 at 0.1 % in aqueous buffer.

In case of ethylcyclohexane trace amounts of 4-ethylcyclohexanone and cyclohexaneethanol were found. However, the low concentrations were outside the calibration curve and below detection limit of the GC-FID ($<0.01\,\mathrm{g\,l^{-1}}$) and thus not quantified. It is interesting to note that only alcohol products were found and no substantial over-oxidation to the acid was recorded. This may be due to the bulkier nature of the substrates that does not allow further oxidation in the enzyme active site.

Interestingly, the epoxide to octenoic acid ratio changed similarly to the alcohol to acid ratios with n-alkanes with various co-solvents. 1-Octene reactions without co-solvent or ethyl oleate and silicone oil resulted in low ratios ($0.45\,\mathrm{mol\,mol^{-1}}$ to $0.98\,\mathrm{mol\,mol^{-1}}$), whereas conversions with Tergitol, L-61 and Triton resulted in high ratios ($2.96\,\mathrm{mol\,mol^{-1}}$ to $14.26\,\mathrm{mol\,mol^{-1}}$). An octane contamination in the 1-octene substrate was identified by GC-MS, this resulted in the production of 1-octanol and octanoic acid to an average of $0.12\,\mathrm{g\,l^{-1}}$ and $0.37\,\mathrm{g\,l^{-1}}$, respectively. These products were not considered here and thus their influence is not considered.

In general, the behaviour relative to the control samples without co-solvent was still similar to the behaviour of alkane substrates: Reactions with ethyl oleate resulted

in the overall highest product concentrations (7.7 mmol l^{-1}), followed by the control reaction without co-solvents (6.6 mmol l^{-1}) and silicone oil (6.1 mmol l^{-1}). Reactions with Tergitol resulted in the lowest average product concentrations (1.7 mmol l^{-1}) and similarly to alkanes, reactions with Triton X-100 always resulted in lower concentrations than the control experiments without co-solvents (average of 3.0 mmol l^{-1}).

The biggest improvement with co-solvents relative to the control reaction was seen for 2-methyl-octane with a 50 % improvement in product yields on average. Specifically, this is due to the percentage increase in yields (81 %) in reactions with polar co-solvents (Tergitol, L-61) when using the 2-methyl-octane substrate relative to the control reaction. Conversely, for the remaining substrates (including the similarly sized 1-octene substrate) the two polar co-solvents resulted in yields at 44 % of the control reaction, on average. Interestingly, this is similar to the reaction with alkanes, where the reactions with octane saw an increase in product yields with Tergitol and L-61. This indicates a strong dependency of product yields on chemo-physical properties of the substrate and their interaction with the co-solvents in addition to any enzyme specific limitations. Specifically, these properties may include solubility and membrane permeability and the resulting changes in toxicity.

Overall, the results broadly confirm the previously recorded behaviour of co-solvents during hydrocarbon oxidation. Further, the unpredictable nature of the behaviour and large difference in product yields between conditions reiterates the complexity of multiphase biocatalytic systems and the requirement for empirical data. Using the developed MWP platform allows efficient exploration of these conditions with the confidence that components of the reaction such as novel substrates or co-solvents do not interact with the plate material or substrate or product is lost by evaporation.

5.3.4 Multivariate data analysis of solvent mixture effect on alkane bio-oxidations

With modern high-throughput methodologies large amounts of quantitative data can be gathered, which require the use of appropriate analytical tools for reliably extracting a maximum of valuable information. Often these large datasets contain a battery of similar, correlated measurements that all describe a complex problem. In these cases, the analysis and modelling of one variable at a time is time consuming and does not capture the underlying behaviour of the system.

More advanced multivariate data analysis (MVDA) tools such as partial least squares projections to latent structures (PLS) allow modelling the fundamental association between matrices of X-variables (factors) and Y-variables (responses) by a linear multivariate model, as well as modelling the structure of X and Y matrices. Unlike multiple linear regression as used in Design of Experiment, PLS can analyse large amounts of noisy, collinear and even incomplete variables in both X and Y (Eriksson et al. 2013). To that end, PLS iteratively fits a few latent variables to a projection of the X dataset that describe the maximum variance in the Y space (Wold, Sjöström, and Eriksson 2001). These latent variables are often interpretable in terms of general properties of the system, its components or substituents and with only a small number of the latent variables there is little risk of 'over-fitting' the data. Ultimately, this results in a model with fewer dimensions than multiple linear regressions of individual responses making it easier to interpret especially when responses are correlated. The flexibility, together with its graphical orientation, make PLS a multipurpose tool for complex data analytical questions including data classification and cluster analysis or data summary, integration and mining for applications in process industries such as quantitative structure-property relationships, multivariate calibration and process understanding, modelling and control (Wold, Eriksson, and Kettaneh 2010).

Here, a PLS approach was adopted to gain further insight into the impact of

physicochemical parameters of the co-solvents on the reaction yields and whether an underlying relationship between these parameters and the reaction outcomes can be found. A particular focus was on investigating the ratio of alcohol to acid product. Therefore, only linear n-alkane substrates were investigated. Further, to not introduce large amounts of non-linearity in the model the pentane and dodecane substrates were not considered in this analysis due to their irregular results and low conversion (see Figure 5.3).

Table 5.5: PLS regression factors for model M1.

Factor name	Unit	Description
Substrate	Categoric	'Secondary ID' Identification of substrate
Cosolvent	Categoric	Identification of co-solvent
Concentration cosolvent	%	Co-solvent concentration effects
Substrate chain length		Characterisation of substrate
R_S Subs-Water	MPa^{-1}	Estimation of alkane substrate solubility in water
R_S CoSol-Subs	MPa^{-1}	Estimation of co-solvent solubility in substrate
R_S CoSol-Alc	MPa^{-1}	Estimation of alcohol product solubility in co-solvent
R_S CoSol-Acid	MPa^{-1}	Estimation of acid product solubility in co-solvent
log$P$ Substrate		log$P$ value of alkane substrate
log$P$ Alcohol		log$P$ value of alcohol product
log$P$ Acid		log$P$ value of acid product
log$P$ Cosolvent		log$P$ value of co-solvent

Two physicochemical parameters were chosen to describe all reaction components, the substrates and products as well as the co-solvent. The log$P$ and Hansen solubility parameters were determined using a computational approach as described in section 5.2.4. The log$P$ values were used to investigate the influence on the reaction according to Laane et al. (1987). The Hansen solubility parameters were used to derive solubility properties (R_S) of co-solvents, reaction substrates and products to be used as factors together with the substrate and co-solvent identity, co-solvent concentration and substrate chain length (Table 5.5). The reaction product concentrations as well as

the ratio of alcohol to acid were taken as responses (Table 5.6).

Table 5.6: PLS regression model responses.

Response name	Unit	Description
Total product	mmol l^{-1}	Sum of aldehyde, alcohol and acid product concentrations
Alcohol	mmol l^{-1}	Alcohol product concentration
Acid	mmol l^{-1}	Acid product concentration
Alcohol/Acid	Ratio	Ratio of alcohol to acid concentrations

The collection of responses and likelihood of correlation between them illustrates the requirement to use MVDA tools such as PLS. It is important to note that this analysis does not necessarily provide a good sense of absolute influence of one factor on a particular response or establishes a causal relationship, but it can help to understand the behaviour of the entire system and inform future work.

Model evaluation

An initial PLS model (model M1) was created from all data resulting in three components showing good correlation between the two matrices (Table F.1). The loading plot provides an overview of the interactions between factors and responses of the system displaying the first two components (Figure F.1). Interestingly, the log$P$ parameters for the substrate and products correlated strongly with the substrate carbon chain length and unsurprisingly with the R_S value for substrate solubility in water, however, only showing significance in the second component. The linear nature of the alkane substrate and hence products simplify the correlation of these parameters. Thus, log$P$ of the substrate can be used exemplary for all compounds in the dataset. The log$P$ of co-solvents shows even less influence on the model being close to the origin.

Based on this initial appraisal the log$P$ values for co-solvent and products, R_S Subs-Water parameter and the substrate chain length were removed from the initial model to simplify the model and instead focus on the more significant R_S values and log$P$ of the substrate for interpretation.

Table 5.7: PLS model M2 parameters, cumulative factor coefficients.

Component	R2X(cum)	R2Y(cum)	Q2Y(cum)
1	0.24	0.47	0.35
2	0.35	0.75	0.62

The new PLS model (model M2) found only two significant components, with overall good values for goodness of fit (R2Y) and prediction (Q2Y) (Table 5.7). The explained variation for the factors (R2X) in the model is low, which may be caused by large number of categoric variables. It is also indicative of influence from factors that are not represented in the dataset. Despite this, the low value is not thought to be cause for concern and the model remains useful to explain part of the variation seen.

No strong outliers were were detected either in the response space (Figure 5.13) or the factor space (Figure F.2). No critical moderate outliers in Distance to Model X (DModX) were found (data not shown). However, the control group with no co-solvent has consistently higher values, especially with the C8 substrate. This is likely to arise from the fact that these data points systematically lack values for R_S co-solvent in substrate values. Similarly, no moderate outliers were detected in the Distance to Model Y (DModY) (data not shown). The values for Tergitol in octane shows a high DModY value, but this was deemed acceptable since the experimental value was confirmed in further experiments including the time course (section 5.3.1).

Table 5.8: PLS model M2 parameters, cumulative response coefficients.

Response	R2VY(cum)	Q2VY(cum)
Alcohol/Acid	0.76	0.61
Total product	0.76	0.65
Alcohol	0.65	0.46
Acid	0.82	0.71

Table 5.8 shows the explained variation (R2VY) and the predicted variation (Q2VY) of the complete model for each response. Generally, the values show that the responses are well modelled. The alcohol yield scores worst, suggesting that vari-

ation in this variable is explained the least by the dataset. However, cross-validation ANOVA shows that PLS regression for all responses is significant ($p < 0.0005$).

Overall, with good fit and predictive power, the model shows a strong, quantitative relationship between the factors and responses.

Model summary

The model is interpreted using score and loading plots. These summarise the relation between the X and Y dataset. The X-scores (vector t) are predictors of Y and model X whilst maximising the covariance between X and Y. Thus, they represent the latent variables. The weights (vectors $w^\star$ and c, for the X and Y variables, respectively) describe how the X variables combine to form the scores (t), the basis of the quantitative relation between X and Y. By superimposing the X and Y weights in a loading plot, the relationship between the X variables, the Y variables and the relationship between all these variables can be visualised.

From the score plot of the PLS model (Figure 5.13) it can be seen that the response data is split by co-solvent type in two groups. The datapoints clearly group according to the used co-solvent; the apolar co-solvents (BEHP, silicone oil, ethyl oleate) on the left and the more polar co-solvents on the right (Tergitol, Triton, L-61). The control samples without co-solvent are associated with the left group.

When consulting the corresponding loading plot of the PLS model, it is evident that the first component along the x-axis includes the polarity properties of the co-solvent. Here specifically represented as the solubility R_S values of co-solvent with substrate or alcohol and acid products (Figure 5.14). With apolar solvents showing better solubility in the substrate and polar solvents better solubility of the alcohol and acid products. Interestingly, there is a clear association of high alcohol to acid ratio with good solubility of products in the co-solvent, especially Tergitol.

The second component along the y-axis is mostly described by the log$P$ of the substrate and the co-solvent concentration (Figure 5.14), bearing in mind that the
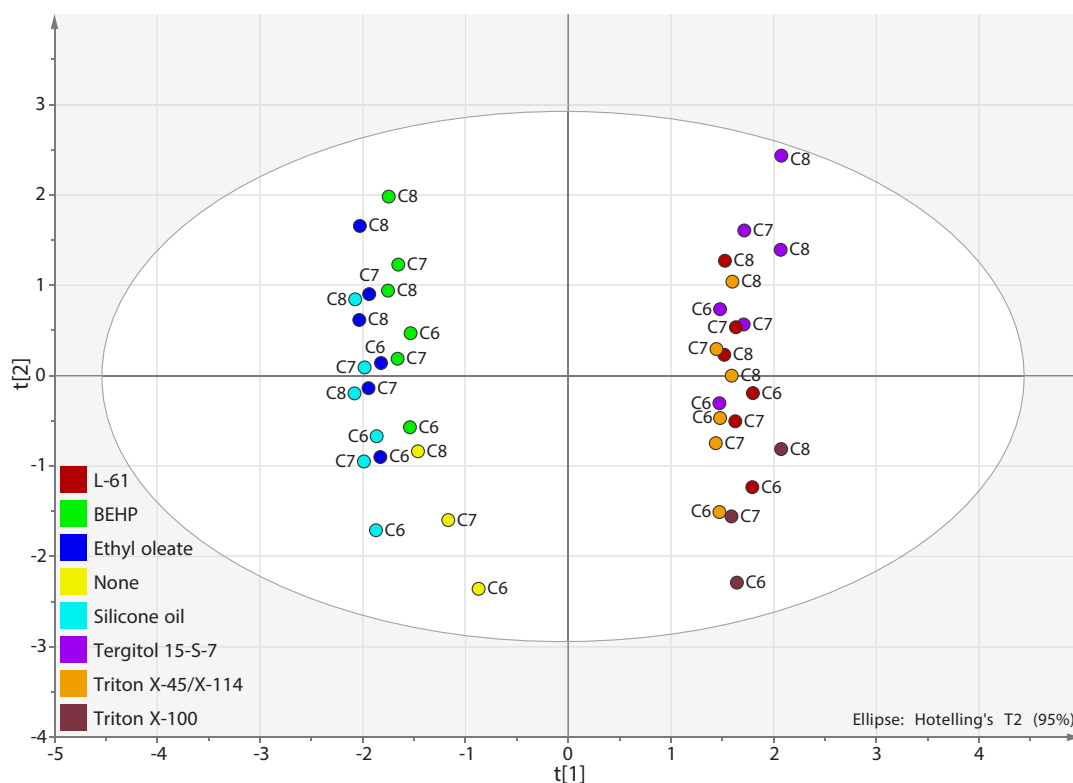
Figure 5.13: PLS model M2 score scatter plot of response data showing X-scores (*t*) of the first component along the x-axis and X-scores of the second along the y-axis, ellipse denotes Hotelling's T^2 95 % confidence interval.

log*P* for substrates is strongly correlated with the log*P* for alcohol and acid products (Figure F.1).

The interactions between both components summarises the effects over the entire dataset. Co-solvents such as BEHP or ethyl oleate result in high total product yields mainly due to high acid yields. On the other side, Tergitol results in high alcohol over acid ratio, but not in high total yields, there is a weak association with high alcohol yields similar to BEHP, though. In contrast, the Triton co-solvents have an overall negative effect on the reaction. Silicone oil has little effect on the reaction relative to the control reaction without co-solvent. The slight association of acid yield with total product yield shows that the former is the preferred product and high alcohol over acid ratios being opposed to this.

Further, higher log*P* values and higher co-solvent concentration specifically res-
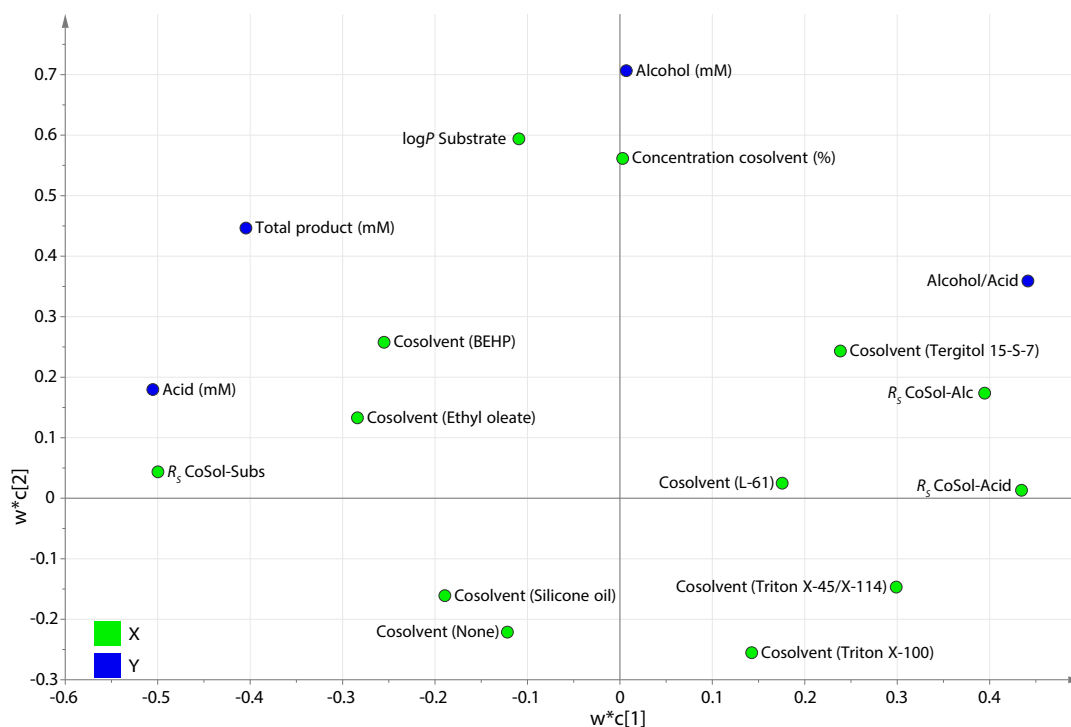
Figure 5.14: PLS model M2 loading scatter plot of the relation between factors and responses and the contribution of each variable to the PLS model; axes show weights for the factors and responses, denoted $w^\star$ and c, respectively, for each model component.

ult in higher alcohol yield. This is a good indication of organic compound toxicity as proposed by Laane et al. (1987), with toxicity decreasing with an increase in log$P$ (log$P > 4$). The clear association of this parameter with the alcohol yield suggests that toxicity is specifically associated with the alcohol product. The high toxicity of the alcohol product explains the difficulty of achieving high alcohol yields in these reactions. Further, it illustrates the need for *in situ* product removal to reduce toxic effects towards the biocatalyst and the resulting reduction in productivity. The positive correlation with the co-solvent concentration confirms their positive impact specifically on the alcohol yield. It can be speculated that this is in fact due to the extraction of the alcohol into the co-solvent due to preferential solubilisation in the co-solvent. This can also be seen by the association of the R_S value for co-solvent in alcohol with Tergitol. In addition, this effect can simply be due to the larger volume of co-solvent available for solubilisation.

On the other hand, high acid yields are achieved when maximising the solubility of substrates in co-solvents and essentially diluting the substrate. This reduces substrate access and promotes over-oxidation as previously argued (compare to section 5.1 and Schrewe et al. (2014)).
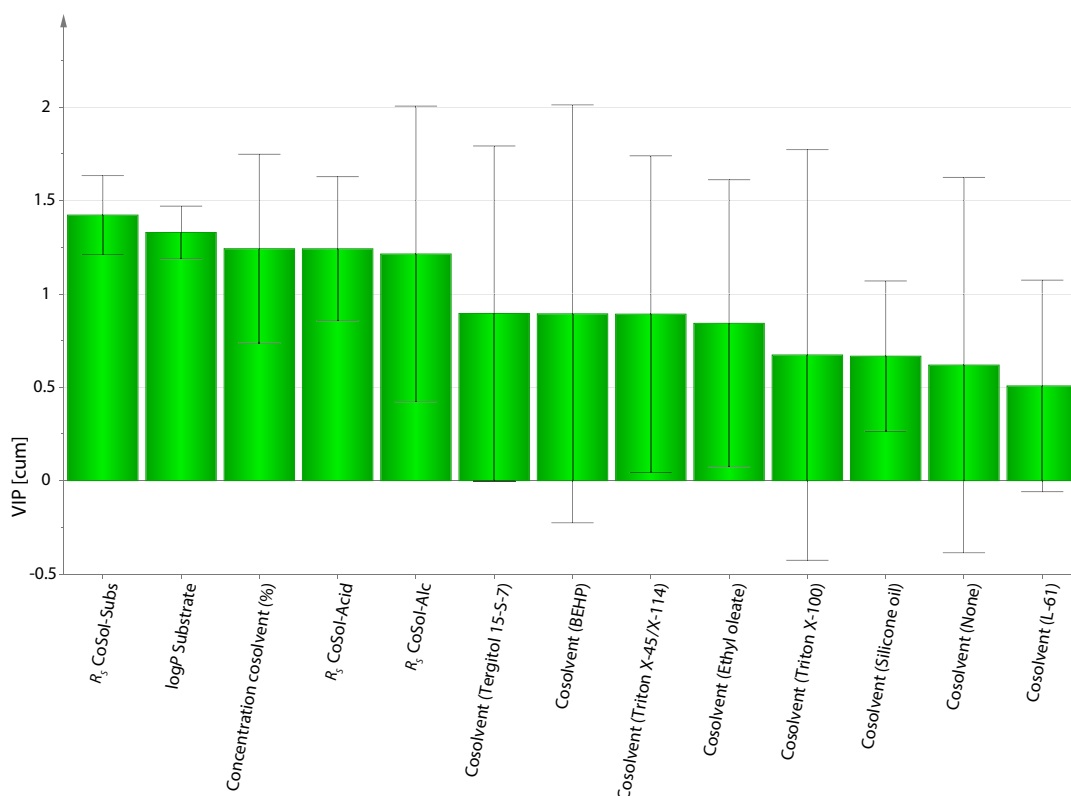
Figure 5.15: PLS model M2 cumulative Variable Influence on Projection (VIP) for each model factor; ±95 % confidence interval derived from jack-knifing.

The Variable Influence on Projection (VIP) plot of the PLS model (Figure 5.15) is a ranking of the influence of each factor on the response variables; values larger than 1 are considered highly important, and values large then 0.5 are considered relevant (MKS Umetrics 2012). Due to the large amount of categoric data and the associated variation, the co-solvent factors have a low score with large estimated confidence interval. Nevertheless, these variable remain central to the model. Overall, the most influential and reliable factor is the R_S co-solvent in substrate value followed by the substrate log$P$.

This reiterates the importance of the R_S values for co-solvent in substrate and

products and the substrate log*P*. Whilst this shows the general influence of substrate log*P* values on the bio-oxidation of alkanes, it provides a simplistic view and the impact of individual products cannot be captured with these highly correlated variables. It is interesting to see the strong correlation specifically with the alcohol product, suggesting that the alcohol product is primarily responsible for toxicity. Despite its own limitations, the application of R_S values has been shown to be much more insightful, especially for this complex multi-product reaction.

Finally, it is interesting to note that there is a clear separation of co-solvents by their ability to solubilise the reaction products. The solubility of substrate against products in the co-solvents indicates that preferential solubilisation of the product leads to an extraction away from the biocatalyst resulting in higher alcohol over acid ratios. For high absolute alcohol yields, the alcohol toxicity needs to be successfully mitigated, as well. On the other hand, with high substrate solubility in the co-solvent the substrate gets diluted and retained in the organic phase, resulting in worse mass transfer of substrate to the biocatalyst promoting the over-oxidation of 1-alcohol to acid (Schrewe et al. 2014).

Model validation

In order to assess the validity of the PLS regression model and its predictions, response permutations was used. This method leaves factor data unmodified but randomly shuffles the response data before fitting a new PLS model to the created dataset and calculating new R2Y and Q2Y values for the derived model. These permutations are repeated and can then be compared to the R2Y and Q2Y estimates of the original model. The case of random data producing a similarly good model as the original model, is an indication for an invalid or over-fitted model. Alternatively, the initial data for a particular response may have been very noisy, similar to random data. Usually, the permutation procedure is repeated between 25 - 100 times to produce a reference distribution for R2Y and Q2Y based on random data. By comparing this

reference distribution to the original PLS model, its significance can be confirmed.

Table 5.9 shows the correlation between the permutation results over 40 iterations and the original R2Y and Q2Y for the alkane bio-oxidation dataset. The generally low R2Y and Q2Y values indicate very good model validity of the PLS regression model for all responses.

Table 5.9: PLS model M2 validation permutations parameters.

Response	R2Y	Q2Y
Alcohol/Acid	0.081	-0.192
Total product	0.097	-0.204
Alcohol	0.104	-0.146
Acid	0.111	-0.211

Thus, the initial assessment of fitted components (Table 5.7) and response modelling (Table 5.8) and the response permutations show a highly significant model for the dataset. This emphasises the overall validity of a MVDA approach coupled to the developed high-throughput tool to investigate alkane bio-oxidations.

5.4   Conclusion

This chapter applies the developed high-throughput microscale platform to efficiently screen several co-solvents for the bio-oxidation of different hydrocarbons with a view on reducing organic phase toxicity and improving control over the product spectrum.

The presented data shows the large impact that co-solvents can have on the biooxidation of alkanes. Especially with 30 % Tergitol as co-solvent and the octane substrate, a 3.2 fold improvement in alcohol yield relative to the control reaction without co-solvents was achieved. At the same time the alcohol to acid ratio was increase from 0.35 to 5.1. The fact that this was achieved with the unoptimised screening conditions shows the potential of this approach for controlling the reaction product spectrum.

The highest overall yields were achieved using BEHP and ethyl oleate. In case of reactions with 30 % BEHP, up to 36 $mmol\,l^{-1}$ of products were formed with the octane

substrate, representing a 1.7 fold improvement relative to the control reaction without co-solvent and 1.6 times higher than the reaction with 30 % Tergitol.

Generally, the use of more polar co-solvent such as Tergitol markedly reduced the over-oxidation of octane reaction products and an accumulation of 1-octanol was recorded. In contrast, the apolar ethyl oleate showed improved overall yields with the acid product dominating.

PLS regression of the co-solvent screening dataset showed that the defining factor for product selectivity is the solubility properties of the co-solvent. The polar co-solvents are generally better solvents for the reaction products. This allows the conclusion that in this case, the products are in fact extracted away from the biocatalyst. This in turn results in reduced toxicity especially of the alcohol product.

The Hansen solubility framework that was used in the analysis can provide an universal and accessible overview of the impact of co-solvents on the reaction yields of whole-cell alkane oxidations. Especially the solubility parameters (R_S) for co-solvent in substrate and product have been shown to be influential.

Equally, there are large differences in membrane damage to cells when exposed to various reaction mixtures. The co-solvents with high product yields on octane were shown to cause less membrane damage. This can be partially explain by the extraction of products away from the cellular catalyst and the accompanying reduction in toxicity. Further, this is an indication that the effects of co-solvents are not only of physicochemical, but also of biological nature. In fact, the presented data suggests that there is a small influence of different reaction mixtures on cellular membrane composition.

Generally, large margins for optimisation based on the presented screening data remain; by choosing an appropriate co-solvent the reaction outcomes can be strongly influenced. The used co-solvents are generally commercially available with a large range of permutations, such as chain length of poloxamers. It is likely that local op-

timal designs exist that have not been captured or characterised in the present study.

Moreover, it remains difficult to attribute this to single factors, due to the large amounts of confounded variables that influence the system simultaneously. Nevertheless, this study shows the importance of two-liquid phase reaction engineering for optimising and directing biocatalytic reactions. The combination with computational and statistical tools was shown to be highly effective at pooling a wide range of experimental data, simplifying its interpretation and maximising its information output. The microwell platform allows integration of biocatalyst, process and reaction engineering early in development. The high fidelity data gained can help explore various options rapidly with high confidence.

In any case, the use of co-solvents and respective improvements in product specificity or yield need to be weighed against complications in downstream processing, for example strongly emulsifying surfactants or recyclability of co-solvents. Ease of phase and product separation have an important impact on the overall economics of a process; the use of cloud point surfactants may be beneficial. Moreover, combination and matching of co-solvents may allow further optimisation of the reaction conditions for alkane bio-oxidations.

Overall, the application of co-solvents is a promising strategy to influence whole-cell alkane oxidations. Further work needs to investigate efficient downstream processing options for the most promising candidates to fully leverage their advantages.

Chapter 6

General conclusion

Despite recent advances, numerous challenges remain to achieve industrially competitive space-time-yields and product titers for bio-oxidations. To improve on this, the ability to rapidly screen bioconversion reactions for characterisation and optimisation is of major importance in biocatalyst selection and process development. Aqueous-organic two-liquid phase systems are routinely employed to improve efficiency of biocatalytic processes. Further, the integration of bioprocess development with catalyst engineering using miniaturised systems is increasingly seen as a vital step to higher process efficiencies and ultimately industrial adoption.

However, standardised, high-throughput screening methods customised for biocatalysis in non-conventional media have rarely been demonstrated in the literature. Further, their adoption has been hindered by reliability issues, especially in industrial settings, where low reproducibility and robustness of applied methods can have significant negative economic impacts. To address these shortcomings, this study developed a multiwell platform that allows systematic screening of hydrocarbon bio-oxidations using an AlkBGT whole-cell catalyst. Specific concerns around material compatibility and evaporation of reaction components were controlled by using multiwell plates machined from polytetrafluoroethylene. Together with a sealing clamp, this system allows the reliable parallel screening of biocatalytic reactions with highly volatile compounds at microliter scale. One-way ANOVA analysis confirmed insigni-

ficant deviations ($\alpha = 0.01$) between replicate reactions with no significant edge effects found. Moreover, during method transfer no drop in reproducibility was seen, reiterating the robustness and reliability of the system. A design of experiment approach was adopted to determine an operating window in which over 70 % headspace oxygen is left after a 24 h bioconversion in sealed plates, by reducing fill volume and keeping cell density within a certain range.

To build on the integration with process conditions, a fed-batch approach was developed allowing glucose feeding in biocatalytic reactions whilst leveraging the reliability of the developed microwell plate. Using an enzymatic hydrolysis approach to release glucose, the proof-of-principle fed-batch implementation showed the large impact that different feeding strategies can have on the bio-oxidation of n-alkanes. Octanoic acid yields were increased by 50 % using a fed-batch strategy compared to optimised batch conditions. Similarly, for reactions with hexane a large and unpredicted effect on the aldehyde product concentration was noticed. In that case, up to $7\,\mathrm{g\,l^{-1}}$ of hexanal were produced intermittently in batch conditions, whereas under fed-batch conditions a 5.5 fold decrease was recorded.

Similarly, an investigation in the effects of co-solvents on hydrocarbon bio-oxidations has demonstrated the generic applicability of the platform. Here, six co-solvents were screened with different hydrocarbon substrates with a view on oxidation product spectrum and organic phase toxicity. It was shown that polar surfactants allowed the extraction of the alcohol product from the whole-cell catalyst, increasing the alcohol yield and reducing phase toxicity. Specifically in case of the octane substrate with 30 % Tergitol a 3.2 fold improvement in alcohol yield relative to the control reaction without co-solvents was achieved. At the same time the alcohol to acid product ratio increased from 0.35 to 5.1. The fact that this was achieved with the unoptimised screening conditions shows the potential of this approach for controlling the reaction product spectrum. In contrast, with apolar co-solvents such as bis(2-ethylhexyl)

phthalate and ethyl oleate the overall highest yields were achieved. In reactions with 30 % bis(2-ethylhexyl) phthalate a 1.7 fold improvement in yield relative to the control reaction without co-solvent was achieved, 1.6 times higher than in the reaction with 30 % Tergitol.

In addition, it was shown throughout that the consistent use of computational and statistical tools such as Design of Experiments and multivariate data analysis is a fundamental component of process development especially when dealing with the large amounts of data that can be generated with microscale tools. Specifically, the prediction of Hansen solubility parameters and use of multivariate data analysis revealed solubility of co-solvent in hydrocarbon substrate and product (R_S) as the defining factor for product selectivity.

In conclusion, this project demonstrated the high robustness and reliability of a microwell platform customised for the high-throughput investigation of alkane biooxidations in non-conventional media. This platform can be used to systematically study the biological and process optimisation strategies in a standardised way. Its high reliability and general applicability is hoped to foster adoption by academia and industry to ultimately accelerate process development in industrial biocatalysis.

6.1 Outlook

Scale-down systems for aqueous process development often have sophisticated sensors that allow online monitoring of a range of parameters such as pH and dissolved oxygen. The integration of sensors to enable online measurements of parameters for better characterisation is a key objective for the presented platform, however, incompatibilities with existing sensors has hindered adoption. Recent publications have successfully demonstrated the use of optical sensors in solvents (Ramesh et al. 2015). This presents a suitable opportunity to investigate the incorporation into the present system without compromising its robustness or material compatibility.

Similarly, improvements in the fed-batch implementation can leverage recent developments in microfluidics. In case better control of feed rate and feeding of compounds other than glucose is desired, microfluidic addition of compounds is required. Recently, microfluidic pump and valve designs using inert materials such as glass and fluorinated ethylene-propylene have been demonstrated at high densities and could enable inert flow-paths for use with two-liquid phase biocatalysis (Grover, Muhlen, and Manalis 2008; Yalikun and Tanaka 2016).

Both approaches would enhance the capabilities of the developed platform but require considerable engineering effort. In contrast, improvements in the fed-batch implementation can also be achieved by improving the solubility of the oligomeric carbon source. Use of dextrins that have higher water solubility than starch could improve this. This would enable a wider range of feed rates. However, the resistance of the substrate against degradability by a whole-cell biocatalyst needs to be verified.

In addition, the co-solvent investigation has revealed a range of effects. Specifically, the impact of co-solvents mixtures on the whole-cell biocatalyst, especially its membrane. Here, the membrane fluidity can be determined or the hydrophobicity of the cells and their direct interaction with hydrophobic substrates. Further, it is likely that there are optimum conditions for co-solvent concentration that have not been explored in this work. To this end, an optimisation experiment with the aim of either maximising total yield or the yield of a specific product could be performed. In combination with a search for novel co-solvents on the basis of the MVDA regression model and the R_S values for co-solvents and substrates, this could be used to validate the model and find more suitable co-solvents and show the full potential of this approach. To investigate the integration between biocatalyst and reaction engineering, the microwell platform could be used to investigate the interaction between co-solvents and transporter channels such as AlkL that have recently been demonstrated to have a large impact on biocatalytic performance (Cornelissen et al. 2013;

Call et al. 2016).

A crucial issue when using surfactant co-solvents is the downstream processing. Here, options for phase separation and extraction of products have to be investigated to fully leverage their benefits for productivity; the use of their cloud point properties is of particular interest, including reaction and separation temperatures (Wang et al. 2008b; Glembin, Kerner, and Smirnova 2013).

Finally, the development of methods to investigate complex co-solvent mixtures *in situ* to understand phase mixing and droplet size, as well as determine the composition of continuous and dispersed phases. These factors are important when considering scaling of reactions.

Ultimately, the use of the developed microwell system is thought to provide a superior platform for investigating a large range of issues concerning multi-phase bio-oxidations.

Appendix A

Bioprocess validation[i]

Research objectives

This research revolves around the development of a high-throughput microwell platform specifically for use with biocatalytic reactions in non-conventional media. As a model reaction, the direct ω-oxyfunctionalisation of highly volatile short chain aliphatic alkanes is used. Numerous challenges remain to achieve industrially competitive space-time-yields for bio-oxidations. The ability to rapidly screen biotransformation reactions for characterisation and optimisation is of major importance in bioprocess development and biocatalyst selection; studies at lab scale are time consuming and labour intensive with low experimental throughput. Yet, the adoption of microscale tools for highly volatile substrates has been hindered by excessive evaporation and material compatibility (Grant et al. 2012).

This study aimed at developing a suitable microwell platform for whole-cell two-liquid phase bio-oxidations. Using a response surface methodology, the platform was systematically characterised to identify non-limiting conditions. Further, the work aims at demonstrating robust scalability to pilot scale to enable translation of information gained at the small scale to industrial scale.

i. This chapter forms the additional material on bioprocess validation required for an Engineering Doctorate.

Research significance

The direct terminal oxidation of alkanes remains difficult to perform by industrial organic chemistry in a regio- and chemoselective manner. However, monooxygenases such as the AlkB enzyme complex from *Pseudomonas putida* efficiently catalyse these readily available substrates to fatty alcohols, aldehydes and acids under mild conditions. Using molecular oxygen as the oxidising agent, this biocatalytic route offers reduced energy demand, safety benefits and a reduction in synthesis steps compared to traditional chemical synthesis at elevated temperature and pressure. Coupled with a transaminase, a one pot synthesis of terminal amines is possible from non-activated carbon or renewable plant oils (Ladkau et al. 2016). This is of high value for the production of building blocks not only in the pharmaceutical industry.

Further, the ability to use small-scale tools to define operating conditions and windows that can be consistently translated to larger scales is of major importance in pharmaceutical process development. For approaches such as Quality by Design (QbD) small-scale studies can aid process design by growing the process knowledge. Particularly, definition of a design space and critical/key process parameters can be efficiently achieved using Design of Experiment (DoE) in combination with microscale tools.

Key validation issues

Evonik Industries AG (Evonik) is a speciality chemicals manufacturer with many leading market positions such as the production of non-animal amino acids. There are several products and markets in which Evonik operates that face regulatory and validation issues. In this text, three key areas will be highlighted to exemplify some of these issues:

- Manufacturing of cell culture ingredients of non-animal origin, for example, amino acids, keto-acids and peptides as well as services such as milling, blend-

ing and packaging all under (current) Good Manufacturing Practice ((c)GMP) conditions (Evonik Industries AG 2014).

- Manufacturing of polymers (PEEK, acrylates) for implants/medical devices that comply with class IV US Pharmacopoeia test for. These polymers can also be used in single use manufacturing equipment in the pharma industry.

- Lastly, Evonik provides materials and services around formulation development for parenteral or oral dosage forms. Delivery solutions range from antibody-drug conjugates to enteric coatings.

In terms of raw material manufacturing for upstream processes, validation efforts will be focused on providing a client with documented evidence that a certain product meets its pre-determined specification and quality attributes. The user would still need to verify the claims. Specifically, the stated cGMP compliance implies a validated process is in place for production of these compounds. This would include a design qualification that demonstrates that the proposed manufacturing process can meet the User Requirements Specification (URS) for a media ingredient this would include impurity levels such as endotoxins and overall bioburden as well as the homogeneity and ratio of any mixtures. Further the installation, operational and performance qualifications would assess that the process can consistently meet the previously determined targets, for example to document that a mixer is able to provide a homogenous mixture of two media components. Overall, a Validation Master Plan can tie all these individual components together to document how and when the parts of a validation program are implemented and completed.

A universally important part of the three mentioned examples is the analytical validation. This would demonstrate and document that a particular chemical, physical or biological analytical method is fit for purpose and that it satisfies the requirements.

These requirements include methodical parameters:

- Precision

- Accuracy

- Specificity/selectivity

- Robustness

- Limit of detection

- Limit of quantitation

- Repeatability

These need to be tested and fulfil pre-determined statistical parameters:

- Linearity

- Normality

- Equality of variance

- Standard deviation

- Correlation coefficient

In the case of polymers for medical devices or (single use) processing equipment there are prescribed requirements and tests laid out in the EU/US Pharmacopeia such as the USP Class VI. This sets out specific requirements for example in terms of biocompatibility, extractables/leachables and pyrogenicity. Whilst a customer would still be required to validate these for a particular process for chemical/physical compatibility, the generic requirements still need to be satisfied and tested beforehand.

Particularly for the formulation development further validation works is likely to be required concerning the cleaning validation as a Contract Manufacturer Organisation (CMO). The cleaning validation would have to show that residues of any active pharmaceutical ingredient, potential microbial contamination and cleaning aids have been removed from the equipment. The effectiveness of cleaning can be assessed by

the total organic carbon (TOC) method. Analysing last flush of equipment and swabs before introducing a new product, the level of trace contaminants can be determined. Further, the conductivity of the flush solution can be used as an indication of the removal of cleaning or storage solutions. Again, these analytical methods need to be validated to ensure they meet methodical and statistical requirements and can accurately assess the cleanliness. Care has to be taken when defining the level to which residuals have to be removed or are acceptable as the limit of detection of the assay. One approach is to set a maximum allowable carryover (MACO) as a fraction of some parameter of the API such as the median lethal dose (LD_{50}).

Regulatory validation issues concerning the project

The developed microwell tool is aimed at upstream process development and characterisation specifically for non-conventional media using two-liquid phase organic-aqueous systems. The current regulatory environment has implications for the use of scale-down systems.

Traditional validation strategies which can be summarised as the procedure by which a defined process or facility is demonstrated to consistently provide the desired outcome are being replaced by risk based approaches such as QbD that ensure quality of pharmaceuticals by employing statistical and risk-management methods in their design, development and manufacturing. The overarching goal is to ensure that sources of variability in a process are identified, understood and managed to consistently provide the desired predefined quality attributes. Thus, with QbD the development of an information pool early in process development is vital. The gained deeper process understanding helps to define critical process parameters and guide process development based on actionable data.

The aim of process development is to propose a system of a particular design controlled at specific setpoints for processing a particular volume, cleaned to certain standards and reused. During the subsequent process characterisation risk analysis

is used to indicate what parameters are most likely to matter and what parameters should be characterised by further experiments. Thus, the critical process parameters are identified and understood early and not at pilot scale when it becomes increasingly difficult to mitigate any complications arising. Ultimately, the goal is to reduce risks early in development.

The advantage of small scale tools is the ability to inform decision making through screening multiple conditions in parallel using only small quantities of material in a short amount of time. This potentially allows studying a larger number of parameters and including all parameters that have a probable impact on product quality. These variables can include:

- Ratio of organic phase to aqueous phase

- Addition of co-solvents (for improved DSP, to reduce toxicity or to improve mass transfer)

- Media components

- Agitation

- Aeration

Similarly, it allows studying wider ranges of each parameter without having to sacrifice resolution. This allows drawing up operating windows, studying of robustness and finding the edge of failure. The combination of microscale tools for upstream processes with DoE approaches allows the efficient exploration of the design space for a particular product.

Further, it is of great importance that the small scale gives a high fidelity representation of the larger scales to allow the successful translation of data from the small to the large scale. Thus, the scale-down model needs careful qualification and it is ideal to include a comparison to larger scales under the target conditions. However, it is possible to only focus on aspects of the model that are required most and justify

them based on scientific and engineering principles. Further challenges associated with small scale work relates to analytical methods. Some analytical methods used at the large scale require a large amount of sample that cannot be provided by the small scale. Especially in this case, the analytical methods used need to be validated for comparability to ensure transferability to larger scales.

Appendix B

Analytics reproducibility

B.1 Gas chromatography

Figure B.1 shows exemplary calibration curves for products of the octane and dodecane oxidation quantified by GC. Linear regression shows a high goodness of fit for all compounds ($R^2 > 0.9995$).
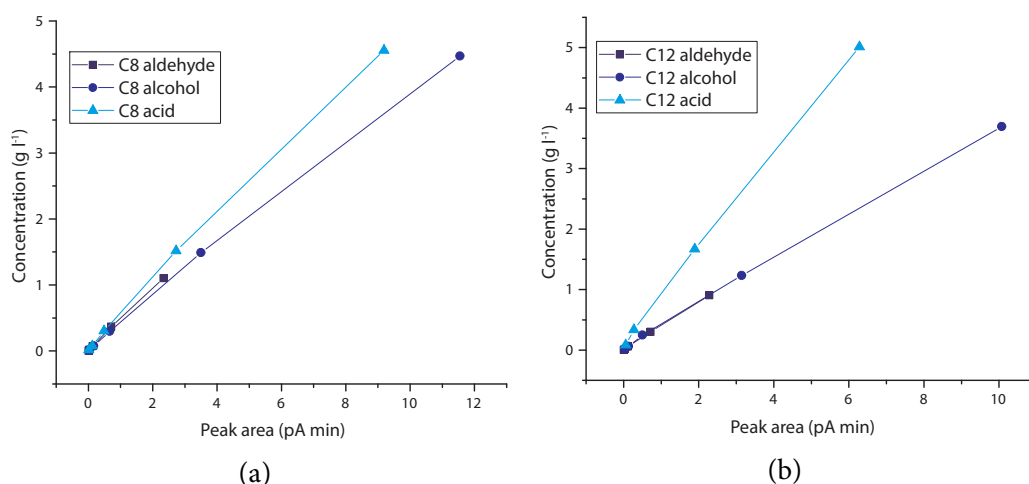
Figure B.1: C8 (a) and C12 (b) calibration curve, linear correlations show $R^2 > 0.9995$.

Table B.1 shows repeat injections for standards of octane and dodecane reaction products. Very good reproducibility was achieved for routine GC analysis.

Extraction efficiency of GC sample preparation was tested for reaction mixtures containing no cells spiked with dodecane products. Overall, good extraction was achieved with above 90 % product recovered during sample preparation (Table B.2).

Table B.1: GC analysis repeat injections for octane (a) and dodecane (b) reactions products; n=3, ±SD.

(a)

Product	Conc g l^{-1})	Peak area pA min
Aldehyde	0.018	0.0356 ±0.0008
Alcohol	0.074	0.1612 ±0.0063
Acid	0.076	0.1197 ±0.0026

(b)

Product	Conc g l^{-1})	Peak area pA min
Aldehyde	0.015	0.0334 ±0.0004
Alcohol	0.062	0.1303 ±0.0049
Acid	0.084	0.0646 ±0.0041

Table B.2: Extraction efficiency for GC samples spiked with dodecane reaction products; n=3, ±SD.

Product	Recovery (g g^{-1})
C12 aldehyde	0.93 ±0.03
C12 alcohol	0.92 ±0.02
C12 acid	0.90 ±0.03

B.2   High pressure liquid chromatography

Figure B.2 shows exemplary calibration curves for glucose and acetate quantified by HPLC. Linear regression shows a high goodness of fit for all compounds ($R^2 > 0.9995$). Further, the graph shows repeat injections for all standards of glucose and acetate products. Very good reproducibility was achieved for routine HPLC analysis.
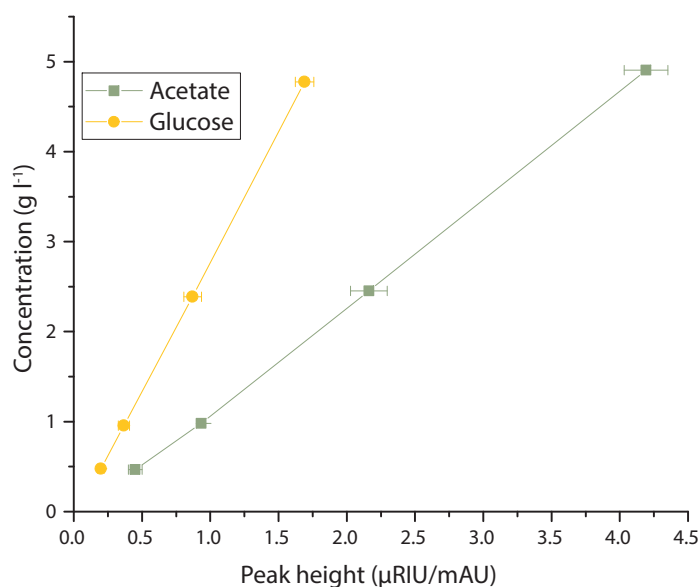
Figure B.2: Standard curve and reproducibility of HPLC injections, linear correlations show $R^2 > 0.9995$ n=3, ±SD.

Appendix C

Calculation of nutrient consumption for bio-oxidation

Calculation of oxygen and glucose consumption during bioconversion with resting cells in sealed plates.

C.1   Assumptions

Table C.1: Yield of alkane oxidation products on nutrients.

Product	Nutrient	Yield (mol mol^{-1})
Alcohol	Oxygen	1.0
	Glucose	10.0
Aldehyde	Oxygen	0.5
	Glucose	5.0
Acid	Oxygen	0.3
	Glucose	3.3

For these calculations, the reaction scheme according to Figure 1.5 is assumed. Further, it is assumed that a later product in the reaction was produced from the previous product(s). Thus, the production of an acid molecule carries three time the cost of an alcohol molecule. The yields for each product on oxygen (Y_{P/O_2}) and glucose ($Y_{P/glucose}$) are listed in Table C.1. This is based on the assumption that per glucose 10 NADH are generated from aerobic metabolism ($Y_{NADH/glucose}$). These calculations do not take the cellular maintenance requirements into account, specifically the oxygen and NADH requirements of the electron transport chain for ATP production.

C.2 Calculations

The amount of oxygen gas in a well can be calculated using Equation C.1. When filled with 350 µl reaction volume a well with typically 11 ml total volume contains about 93 µmol molecular oxygen (filled at 20 °C and 0.101 MPa).

$$n_{O_2} = V_{O_2} \times \rho_{O_2} \times M_{O_2} \tag{C.1}$$

The oxygen consumption of a reaction can be calculated by summing the consumption for each product of the reaction (Equation C.2).

$$\sum \left(n_P \div Y_{P/O_2} \right) \tag{C.2}$$

A well with 280 µl aqueous fill volume and $5.5 \, \mathrm{g \, l^{-1}}$ glucose, contains 8.6 µmol glucose. The total glucose consumption of a reaction can be calculated by summing the consumption for each product of the reaction (Equation C.3).

$$\sum \left(n_P \div Y_{P/glucose} \right) \tag{C.3}$$

Appendix D

Co-solvent data

D.1   Co-solvent product recovery
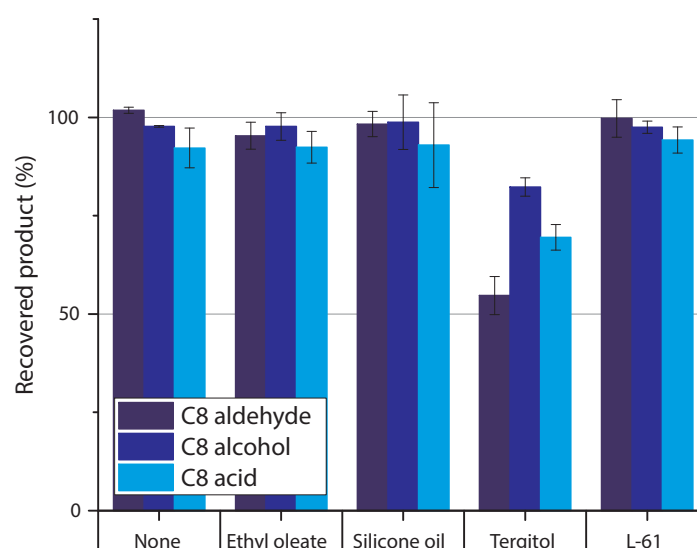
Figure D.1: Product recovery from spiked reaction samples with 30 % co-solvents in octane.

Figure D.1 shows recovery of products from different co-solvent mixtures using the octane substrate. Experiments were carried out with 30 % co-solvent in alkane substrate as described in section 5.2.3. 'None' describes the octane-only reaction without any added co-solvents.

D.2   Flow cytometer data

Exemplary flow cytometer data, flow cytometer settings according to section 5.2.3. Raw FC data (Figure D.2), TO^+ gate (representing the 'total cell' count) (Figure D.3)

and final TO^+ and PI^+ gated results (Figure D.4).
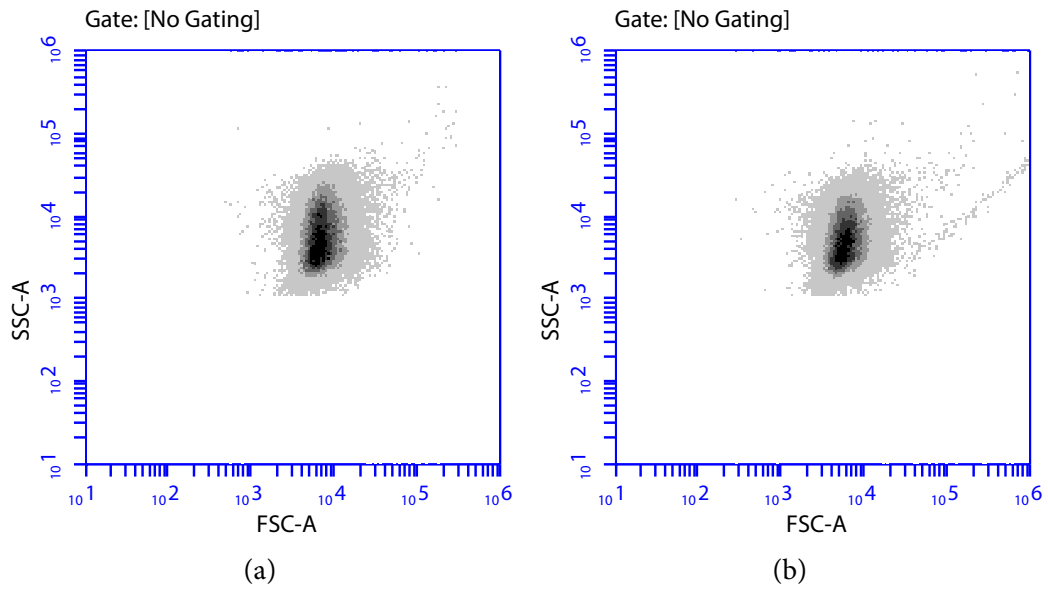
Figure D.2: Flow cytometer side-scatter (SSC) and front-scatter (FSC) data, without any organic (a) and octane organic phase (b) after 4.5 h at 30 °C and 250 rpm.
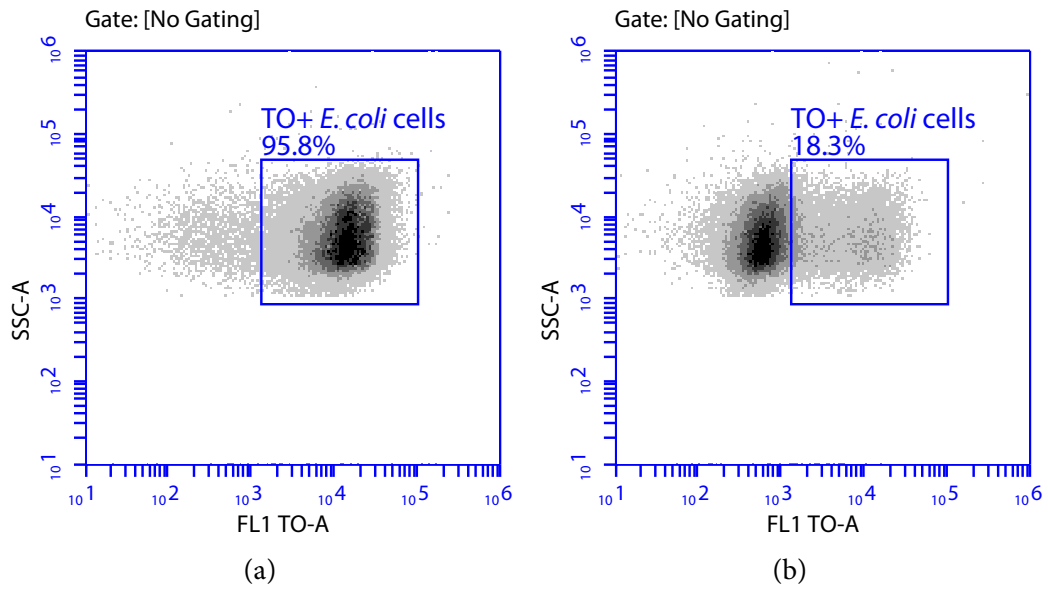
Figure D.3: Flow cytometer side-scatter (SSC) and fluorescnce (FL1) data with TO^+ gate displayed, without any organic (a) and octane organic phase (b) after 4.5 h at 30 °C and 250 rpm.
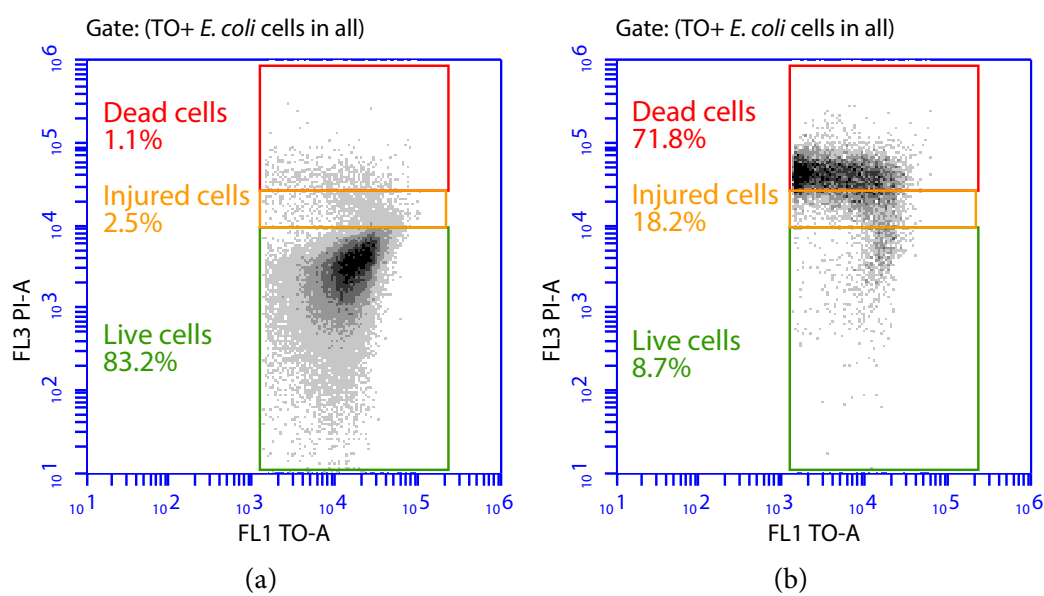
Figure D.4: Flow cytometer fluorescence (FL1 and FL3) data gated on TO^+ in (Figure D.3), without any organic (a) and octane organic phase (b) after 4.5 h at 30 °C and 250 rpm.

Appendix E

GC-MS identification

Mass spectrometer data previously recorded in Chromeleon 7 (Thermo Scientific) was matched to the NIST 14 mass spectral library using 'NIST Search 2.2' in order to identify unknown products of bioconversion reactions. Table E.1 shows the average match factor, probability and retention time of the identified products. The match factor represents the similarity between a library and a submitted spectrum, it scales from 0 to 999. Generally, a match factor above 800 is a good match between the library and the submitted spectra, above 900 is an excellent match. The probability value is derived assuming that the unknown compound is represented by a spectrum in the searched library; it gives the probability that a given library spectrum is the correct match for a submitted spectrum relative to the most similar library spectra. Figure E.1 shows exemplary mass spectra from experiments compared to the best library match.

Table E.1: MS data for product identification of further substrates.

Substrate	Product	Match factor %	Probability min	Retention time
Ethylbenzene	2-Phenylethanol	940	87.4	3.65
Ethylcyclohexane	4-Ethylcyclohexanol	933	82.6	3.33
2-Methyl-octane	2-Methyl-2-octanol	885	75.6	3.06
1-Octene	1,2-Epoxyoctane	895	73.5	2.95
	7-Octenoic acid	847	61.6	3.79
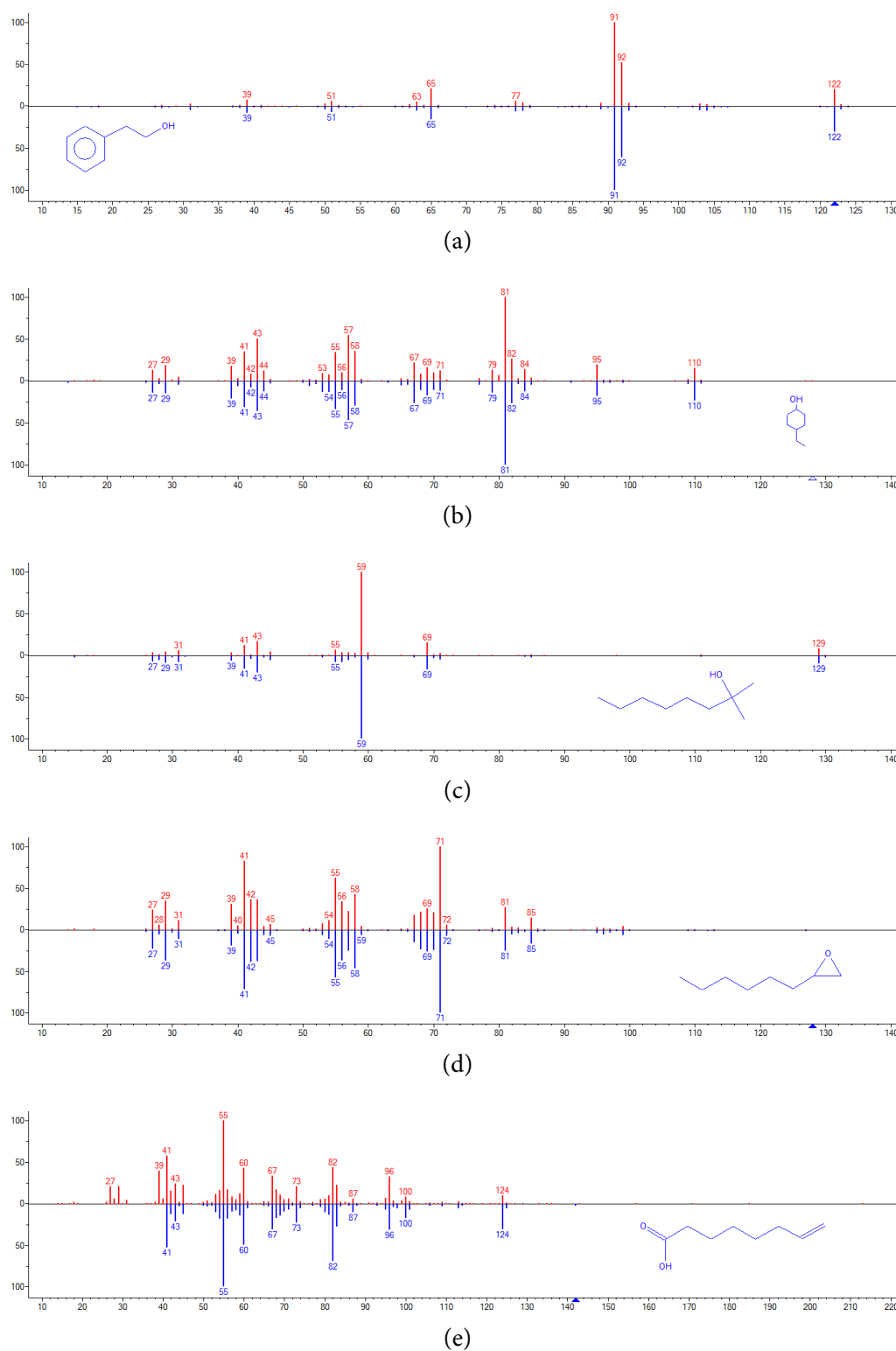
Figure E.1: MS spectra of identified reaction products: 2-Phenylethanol (a), 4-Ethylcyclo-hexanol (b), 2-Methyl-2-octanol (c), 1,2-Epoxyoctane (d), 7-octenoic acid (e).

Appendix F

Multivariate data analysis
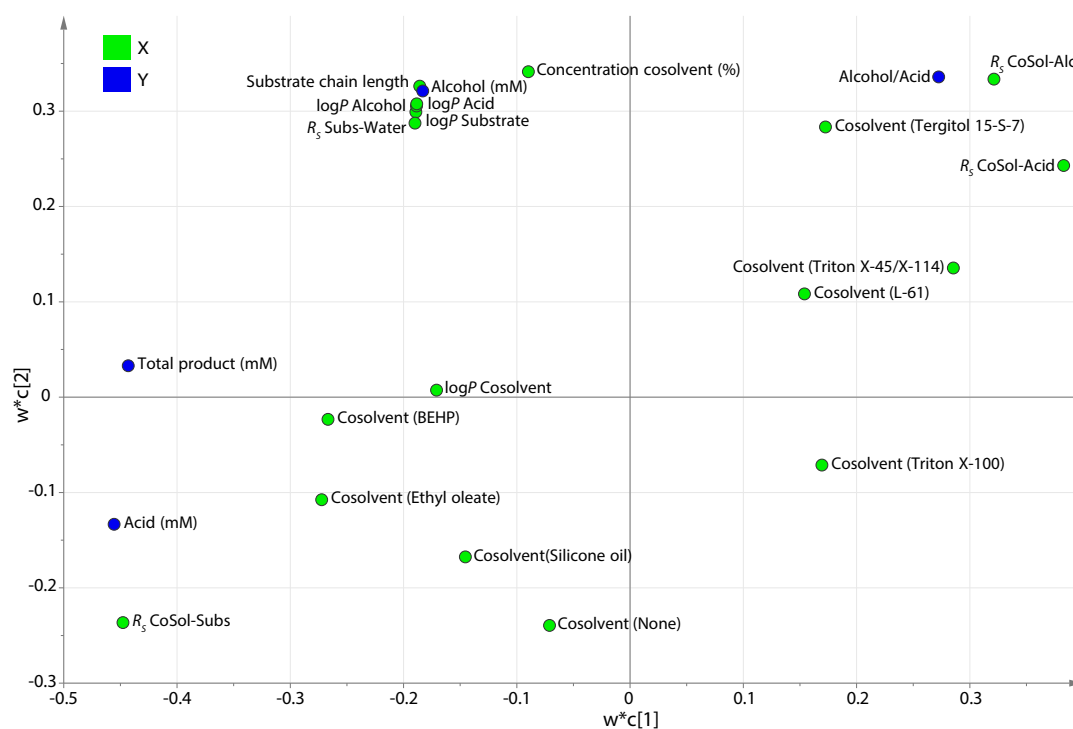
Figure F.1: PLS model M1 loading scatter plot of relation between factors and responses showing weights of the first model component along the x-axis and weights of the second along the y-axis.

Table F.1: PLS M1 model parameters, cumulative factor coefficients.

Component	R2X(cum)	R2Y(cum)	Q2Y(cum)
1	0.21	0.45	0.32
2	0.44	0.67	0.49
3	0.56	0.74	0.51

Figure F.1 and F.2 show the loading plot of PLS model M1 and the score plot of
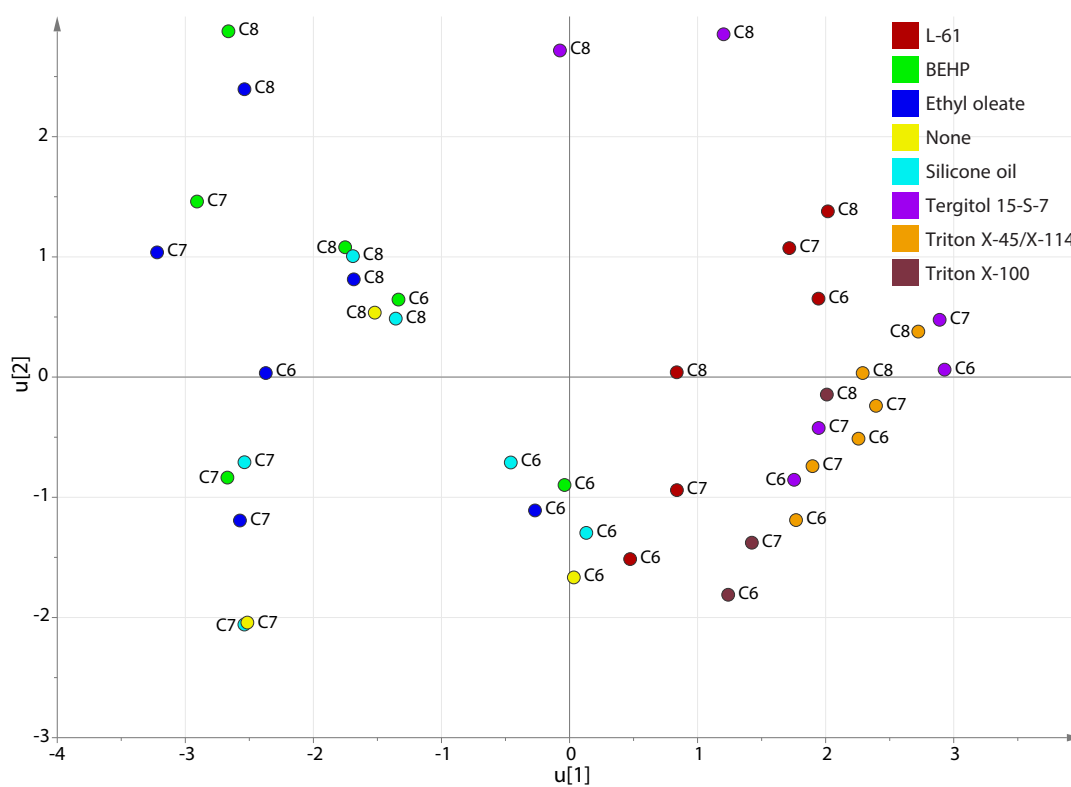
Figure F.2: PLS model M2 score scatter plot of factor data showing X-scores of first component along the x-axis and X-scores of the second along the y-axis.

PLS model M2 factor data respectively. Table F.1 shows the PLS model M1 cumulative component parameters.

Bibliography

Abdelaal, A. S., Ageez, A. M., Abd El-Hadi, A. E.-H. A., and Abdallah, N. A. 2014. 'Genetic improvement of n-butanol tolerance in *Escherichia coli* by heterologous overexpression of *groESL* operon from *Clostridium acetobutylicum*.' *3 Biotech*.

Abildskov, J., Leeuwen, M. B. van, Boeriu, C. G., and Broek, L. A. M. van den. 2013. 'Computer-aided solvent screening for biocatalysis.' *Journal of Molecular Catalysis B: Enzymatic* 85-86:200–213.

Adamska, K., Voelkel, A., and Héberger, K. 2007. 'Selection of solubility parameters for characterization of pharmaceutical excipients.' *Journal of Chromatography A* 1171 (1-2): 90–97.

Adhikari, U., Goliaei, A., Tsereteli, L., and Berkowitz, M. L. 2016. 'Properties of Poloxamer Molecules and Poloxamer Micelles Dissolved in Water and Next to Lipid Bilayers: Results from Computer Simulations.' *The Journal of Physical Chemistry B*.

Allwardt, A., Holzmüller-Laue, S., Wendler, C., and Stoll, N. 2008. 'A high parallel reaction system for efficient catalyst research.' *Catalysis Today* 137 (1): 11–16.

Alonso, H., Kleifeld, O., Yeheskel, A., Ong, P. C., Liu, Y. C., Stok, J. E., De Voss, J. J., and Roujeinikova, A. 2014. 'Structural and mechanistic insight into alkane hydroxylation by *Pseudomonas putida* AlkB.' *Biochemical Journal* 460 (2): 283–293.

Alonso, H. and Roujeinikova, A. 2012. 'Characterization and two-dimensional crystallization of membrane component AlkB of the medium-chain alkane hydroxylase system from *Pseudomonas putida* GPo1.' *Applied and Environmental Microbiology* 78 (22): 7946–7953.

Aono, R. and Kobayashi, H. 1997. 'Cell surface properties of organic solvent-tolerant mutants of *Escherichia coli* K-12.' *Applied and Environmental Microbiology* 63 (9): 3637–3642.

Arakawa, H., Aresta, M., Armor, J. N., Barteau, M. A., Beckman, E. J., Bell, A. T., Bercaw, J. E., et al. 2001. 'Catalysis Research of Relevance to Carbon Management: Progress, Challenges, and Opportunities.' *Chemical Reviews* 101 (4): 953–996.

Austin, R. N., Born, D., Lawton, T. J., and Hamilton, G. E. 2015. 'Protocols for Purifying and Characterizing Integral Membrane AlkB Enzymes.' In *Hydrocarbon and Lipid Microbiology Protocols,* edited by T. J. McGenity. Berlin Heidelberg: Springer Protocols Handbooks.

Austin, R. N. and Groves, J. T. 2011. 'Alkane-oxidizing metalloenzymes in the carbon cycle.' *Metallomics* 3 (8): 775.

Austin, R. N., Luddy, K., Erickson, K., Pender Cudlip, M., Bertrand, E. M., Deng, D., Buzdygon, R. S., Beilen, J. B. van, and Groves, J. T. 2008. 'Cage Escape Competes with Geminate Recombination during Alkane Hydroxylation by the Diiron Oxygenase AlkB.' *Angewandte Chemie International Edition* 47 (28): 5232–5234.

Ayala, M. and Torres, E. 2004. 'Enzymatic activation of alkanes: constraints and prospective.' *Applied Catalysis A, General* 272 (1-2): 1–13.

Baboo, J. Z., Galman, J. L., Lye, G. J., Ward, J. M., Hailes, H. C., and Micheletti, M. 2012. 'An automated microscale platform for evaluation and optimization of oxidative bioconversion processes.' *Biotechnology Progress* 28 (2): 392–405.

Bacon, S. L., Parent, J. S., and Daugulis, A. J. 2014. 'A framework to predict and experimentally evaluate polymer-solute thermodynamic affinity for two-phase partitioning bioreactor (TPPB) applications.' *Journal of Chemical Technology & Biotechnology* 89 (7): 948–956.

Bacon, S. L., Peterson, E. C., Daugulis, A. J., and Parent, J. S. 2015. 'Selecting polymers for two-phase partitioning bioreactors (TPPBs): Consideration of thermodynamic affinity, crystallinity, and glass transition temperature.' *Biotechnology Progress* 31 (6): 1500–1507.

Baik, M.-H., Newcomb, M., Friesner, R. A., and Lippard, S. J. 2003. 'Mechanistic Studies on the Hydroxylation of Methane by Methane Monooxygenase.' *Chemical Reviews* 103 (6): 2385–2420.

Balasubramanian, R., Smith, S. M., Rawat, S., Yatsunyk, L. A., Stemmler, T. L., and Rosenzweig, A. C. 2010. 'Oxidation of methane by a biological dicopper centre.' *Nature* 465 (7294): 115–119.

Baptist, J. N., Gholson, R. K., and Coon, M. J. 1963. 'Hydrocarbon oxidation by a bacterial enzyme system.' *Biochimica et Biophysica Acta* 69:40–47.

Battioni, P., Renaud, J. P., Bartoli, J. F., Reina-Artiles, M., Fort, M., and Mansuy, D. 1988. 'Monooxygenase-like oxidation of hydrocarbons by hydrogen peroxide catalyzed by manganese porphyrins and imidazole: selection of the best catalytic system and nature of the active oxygen species.' *Journal of the American Chemical Society* 110 (25): 8462–8470.

Beal, J., Adler, A., and Yaman, F. 2015. 'Managing bioengineering complexity with AI techniques.' *Biosystems.*

Beilen, J. B. van, Eggink, G., Enequist, H., Bos, R., and Witholt, B. 1992. 'DNA sequence determination and functional characterization of the OCT-plasmid-encoded *alkJKL* genes of *Pseudomonas oleovorans.*' *Molecular Microbiology* 6:3121–3136.

Beilen, J. B. van and Funhoff, E. G. 2007. 'Alkane hydroxylases involved in microbial alkane degradation.' *Applied Microbiology and Biotechnology* 74 (1): 13–21.

Beilen, J. B. van, Kingma, J., and Witholt, B. 1994. 'Substrate specificity of the alkane hydroxylase system of *Pseudomonas oleovorans* GPo1.' *Enzyme and Microbial Technology* 16 (10): 904–911.

Beilen, J. B. van, Li, Z., Duetz, W. A., Smits, T. H. M., and Witholt, B. 2003. 'Diversity of alkane hydroxylase systems in the environment.' *Oil & Gas Science and Technology* 58 (4): 427–440.

Beilen, J. B. van, Neuenschwander, M., Smits, T. H. M., Roth, C., Balada, S. B., and Witholt, B. 2002. 'Rubredoxins Involved in Alkane Oxidation.' *Journal of Bacteriology* 184 (6): 1722–1732.

Beilen, J. B. van, Panke, S., Lucchini, S., Franchini, A. G., Röthlisberger, M., and Witholt, B. 2001. 'Analysis of *Pseudomonas putida* alkane-degradation gene clusters and flanking insertion sequences: evolution and regulation of the *alk* genes.' *Microbiology* 147:1621–1630.

Beilen, J. B. van, Penninga, D., and Witholt, B. 1992. 'Topology of the membrane-bound alkane hydroxylase of *Pseudomonas oleovorans.*' *Journal of Biological Chemistry* 267 (13): 9194–9201.

Beilen, J. B. van, Smits, T. H. M., Roos, F. F., Brunner, T., Balada, S. B., Röthlisberger, M., and Witholt, B. 2005. 'Identification of an amino acid position that determines the substrate range of integral membrane alkane hydroxylases.' *Journal of Bacteriology* 187 (1): 85–91.

Beilen, J. B. van, Wubbolts, M. G., and Witholt, B. 1994. 'Genetics of alkane oxidation by *Pseudomonas oleovorans*.' *Biodegradation* 5 (3): 161–174.

Berg, B. van den. 2010. 'Going Forward Laterally: Transmembrane Passage of Hydrophobic Molecules through Protein Channel Walls.' *ChemBioChem* 11 (10): 1339–1343.

Bertrand, E. M., Keddis, R., Groves, J. T., Vetriani, C., and Austin, R. N. 2013. 'Identity and mechanisms of alkane-oxidizing metalloenzymes from deep-sea hydrothermal vents.' *Frontiers in Microbiology* 4.

Betts, J. I. and Baganz, F. 2006. 'Miniature bioreactors: current practices and future opportunities.' *Microbial Cell Factories* 5 (21).

Betts, J. I., Doig, S. D., and Baganz, F. 2006. 'Characterization and Application of a Miniature 10 mL Stirred-Tank Bioreactor, Showing Scale-Down Equivalence with a Conventional 7 L Reactor.' *Biotechnology Progress* 22 (3): 681–688.

Binder, W. H. 2008. 'Polymer-Induced Transient Pores in Lipid Membranes.' *Angewandte Chemie International Edition* 47 (17): 3092–3095.

Bird, D. A., Laposata, M., and Hamilton, J. A. 1996. 'Binding of ethyl oleate to low density lipoprotein, phospholipid vesicles, and albumin: a ^{13}C NMR study.' *Journal of Lipid Research* 37 (7): 1449–1458.

Blank, L. M., Ebert, B. E., Bühler, B., and Schmid, A. 2008a. 'Metabolic capacity estimation of *Escherichia coli* as a platform for redox biocatalysis: constraint-based modeling and experimental verification.' *Biotechnology and Bioengineering* 100 (6): 1050–1065.

Blank, L. M., Ebert, B. E., Bühler, K., and Bühler, B. 2010. 'Redox biocatalysis and metabolism: molecular mechanisms and metabolic network analysis.' *Antioxidants & Redox Signaling* 13 (3): 349–394.

Blank, L. M., Ionidis, G., Ebert, B. E., Bühler, B., and Schmid, A. 2008b. 'Metabolic response of *Pseudomonas putida* during redox biocatalysis in the presence of a second octanol phase.' *FEBS Journal* 275 (20): 5173–5190.

Bligh, E. G. and Dyer, W. J. 1959. 'A rapid method of total lipid extraction and purification.' *Canadian Journal of Biochemistry and Physiology* 37 (8): 911–917.

Boos, W. and Shuman, H. 1998. 'Maltose/maltodextrin system of *Escherichia coli*: transport, metabolism, and regulation.' *Microbiology and Molecular Biology Reviews* 62 (1): 204–229.

Bordeaux, M., Galarneau, A., and Drone, J. 2012. 'Catalytic, mild, and selective oxyfunctionalization of linear alkanes: current challenges.' *Angewandte Chemie International Edition* 51 (43): 10712–10723.

Bordeaux, M., Galarneau, A., and Drone, J. 2012. 'Katalytische, milde und selektive Oxyfunktionalisierung von linearen Alkanen: aktuelle Herausforderungen.' *Angewandte Chemie* 124 (43): 10870–10881.

Bordeaux, M., Galarneau, A., Fajula, F., and Drone, J. 2011. 'A regioselective biocatalyst for alkane activation under mild conditions.' *Angewandte Chemie International Edition* 50 (9): 2075–2079.

Bornscheuer, U. T., Huisman, G. W., Kazlauskas, R. J., Lutz, S., Moore, J. C., and Robins, K. 2012. 'Engineering the third wave of biocatalysis.' *Nature* 485 (7397): 185–194.

Brandenbusch, C., Bühler, B., Hoffmann, P., Sadowski, G., and Schmid, A. 2010. 'Efficient phase separation and product recovery in organic-aqueous bioprocessing using supercritical carbon dioxide.' *Biotechnology and Bioengineering* 107 (4): 642–651.

Brink, L. E. and Tramper, J. 1985. 'Optimization of organic solvent in multiphase biocatalysis.' *Biotechnology and Bioengineering* 27 (8): 1258–1269.

Bruce, L. J. and Daugulis, A. J. 1991. 'Solvent selection strategies for extractive biocatalysis.' *Biotechnology Progress* 7 (2): 116–124.

Büchs, J., Maier, U., Lotter, S., and Peter, C. P. 2007. 'Calculating liquid distribution in shake flasks on rotary shakers at waterlike viscosities.' *Biochemical Engineering Journal* 34 (3): 200–208.

Budkina, O. A., Demina, T. V., Dorodnykh, T. Y., Melik-Nubarov, N. S., and Grozdova, I. D. 2012. 'Cytotoxicity of nonionic amphiphilic copolymers.' *Polymer Science Series A* 54 (9): 707–717.

Bugrin, V. S. and Melik-Nubarov, N. S. 2007. 'Relationship between the structure of compounds and the effect of Pluronic L61 on their permeation through lipid membranes.' *Polymer Science Series A* 49 (9): 1034–1044.

Bühler, B., Bollhalder, I., Hauer, B., Witholt, B., and Schmid, A. 2003. 'Use of the two-liquid phase concept to exploit kinetically controlled multistep biocatalysis.' *Biotechnology and Bioengineering* 81 (6): 683–694.

Bühler, B., Park, J.-B., Blank, L. M., and Schmid, A. 2008. 'NADH availability limits asymmetric biocatalytic epoxidation in a growing recombinant *Escherichia coli* strain.' *Applied and Environmental Microbiology* 74 (5): 1436–1446.

Bühler, B. and Schmid, A. 2004. 'Process implementation aspects for biocatalytic hydrocarbon oxyfunctionalization.' *Journal of Biotechnology* 113 (1-3): 183–210.

Call, T. P., Akhtar, M. K., Baganz, F., and Grant, C. 2016. 'Modulating the import of medium-chain alkanes in *E. coli* through tuned expression of FadL.' *Journal of Biological Engineering* 10 (1): 1.

Canosa, I., Sánchez-Romero, J. M., Yuste, L., and Rojo, F. 2000. 'A positive feedback mechanism controls expression of AlkS, the transcriptional regulator of the *Pseudomonas oleovorans* alkane degradation pathway.' *Molecular Microbiology* 35 (4): 791–799.

Cánovas, M., Torroglosa, T., and Iborra, J. L. 2005. 'Permeabilization of *Escherichia coli* cells in the biotransformation of trimethylammonium compounds into L-carnitine.' *Enzyme and Microbial Technology* 37 (3): 300–308.

Carvalho, F., Marques, M. P. C., Carvalho, C. C. C. R. de, Cabral, J. M. S., and Fernandes, P. 2009. 'Sitosterol bioconversion with resting cells in liquid polymer based systems.' *Bioresource Technology* 100 (17): 4050–4053.

Chen, M. M. Y., Snow, C. D., Vizcarra, C. L., Mayo, S. L., and Arnold, F. H. 2012. 'Comparison of random mutagenesis and semi-rational designed libraries for improved cytochrome P450 BM3-catalyzed hydroxylation of small alkanes.' *Protein Engineering Design and Selection* 25 (4): 171–178.

Chen, R. R. 2007. 'Permeability issues in whole-cell bioprocesses and cellular membrane engineering.' *Applied Microbiology and Biotechnology* 74 (4): 730–738.

Cheng, H. C. and Wang, F. S. 2010. 'Computer-aided biocompatible solvent design for an integrated extractive fermentation–separation process.' *Chemical Engineering Journal* 162 (2): 809–820.

Collins, J., Grund, M., Brandenbusch, C., Sadowski, G., Schmid, A., and Bühler, B. 2015. 'The dynamic influence of cells on the formation of stable emulsions in organic–aqueous biotransformations.' *Journal of Industrial Microbiology & Biotechnology* 42 (7): 1011–1026.

Constable, D. J. C., Dunn, P. J., Hayler, J. D., Humphrey, G. R., Leazer Jr, J. L., Linderman, R. J., Lorenz, K., et al. 2007. 'Key green chemistry research areas - a perspective from pharmaceutical manufacturers.' *Green Chemistry* 9 (5): 411.

Contractor, R. M., Bergna, H. E., Horowitz, H. S., Blackstone, C. M., Malone, B., Torardi, C. C., Griffiths, B., Chowdhry, U., and Sleight, A. W. 1987. 'Butane oxidation to maleic anhydride over vanadium phosphate catalysts.' *Catalysis Today* 1 (1): 49–58.

Cooley, R. B., Dubbels, B. L., Sayavedra-Soto, L. A., Bottomley, P. J., and Arp, D. J. 2009. 'Kinetic characterization of the soluble butane monooxygenase from *Thauera butanivorans*, formerly '*Pseudomonas butanovora*'.' *Microbiology* 155 (6): 2086–2096.

Cooper, H. L. R., Mishra, G., Huang, X., Pender Cudlip, M., Austin, R. N., Shanklin, J., and Groves, J. T. 2012. 'Parallel and Competitive Pathways for Substrate Desaturation, Hydroxylation, and Radical Rearrangement by the Non-heme Diiron Hydroxylase AlkB.' *Journal of the American Chemical Society* 134 (50): 20365–20375.

Cornelissen, S., Julsing, M., Volmer, J., Riechert, O., Schmid, A., and Bühler, B. 2013. 'Whole-cell-based CYP153A6-catalyzed (S)-limonene hydroxylation efficiency depends on host background and profits from monoterpene uptake via AlkL.' *Biotechnology and Bioengineering* 110 (5): 1282–1292.

Cornelissen, S., Liu, S., Deshmukh, A. T., Schmid, A., and Bühler, B. 2011. 'Cell physiology rather than enzyme kinetics can determine the efficiency of cytochrome P450-catalyzed C–H-oxyfunctionalization.' *Journal of Industrial Microbiology & Biotechnology* 38 (9): 1359–1370.

Correa, N. M., Silber, J. J., Riter, R. E., and Levinger, N. E. 2012. 'Nonaqueous Polar Solvents in Reverse Micelle Systems.' *Chemical Reviews* 112 (8): 4569–4602.

Cruz, A., Fernandes, P., Cabral, J. M. S., and Pinheiro, H. M. 2004. 'Solvent partitioning and whole-cell sitosterol bioconversion activity in aqueous-organic two-phase systems.' *Enzyme and Microbial Technology* 34 (3-4): 342–353.

Cuellar, M. C., Heijnen, J. J., and Wielen, L. A. M. van der. 2013. 'Large-scale production of diesel-like biofuels - process design as an inherent part of microorganism development.' *Biotechnology Journal* 8 (6): 682–689.

Cull, S. G., Lovick, J. W., Lye, G. J., and Angeli, P. 2002. 'Scale-down studies on the hydrodynamics of two-liquid phase biocatalytic reactors.' *Bioprocess and Biosystems Engineering* 25 (3): 143–153.

Culpepper, M. A., Cutsail III, G. E., Gunderson, W. A., Hoffman, B. M., and Rosenzweig, A. C. 2014. 'Identification of the Valence and Coordination Environment of the Particulate Methane Monooxygenase Copper Centers by Advanced EPR Characterization.' *Journal of the American Chemical Society* 136 (33): 11767–11775.

Culpepper, M. A., Cutsail III, G. E., Hoffman, B. M., and Rosenzweig, A. C. 2012. 'Evidence for Oxygen Binding at the Active Site of Particulate Methane Monooxygenase.' *Journal of the American Chemical Society* 134 (18): 7640–7643.

Culpepper, M. A. and Rosenzweig, A. C. 2012. 'Architecture and active site of particulate methane monooxygenase.' *Critical Reviews in Biochemistry and Molecular Biology* 47 (6): 483–492.

Da Silva, J. C. S., Pennifold, R. C. R., Harvey, J. N., and Rocha, W. R. 2016. 'A radical rebound mechanism for the methane oxidation reaction promoted by the dicopper center of a pMMO enzyme: a computational perspective.' *Dalton Transactions* 45 (6): 2492–2504.

Dafoe, J. T. and Daugulis, A. J. 2013. 'In situ product removal in fermentation systems: improved process performance and rational extractant selection.' *Biotechnology Letters* 36 (3): 443–460.

Darracq, G., Couvert, A., Couriol, C., Amrane, A., and Le Cloirec, P. 2012. 'Removal of Hydrophobic Volatile Organic Compounds in an Integrated Process Coupling Absorption and Biodegradation—Selection of an Organic Liquid Phase.' *Water, Air, & Soil Pollution* 223 (8): 4969–4997.

Daugulis, A. J. 1988. 'Integrated Reaction and Product Recovery in Bioreactor Systems.' *Biotechnology Progress* 4 (3): 113–122.

Denisov, I. G., Grinkova, Y. V., and Sligar, S. G. 2012. 'Cryoradiolysis and Cryospectroscopy for Studies of Heme-Oxygen Intermediates in Cytochromes P450.' In *Spectroscopic Methods of Analysis,* 375–391. Totowa, NJ: Humana Press.

Déziel, E., Comeau, Y., and Villemur, R. 1999. 'Two-liquid-phase bioreactors for enhanced degradation of hydrophobic/toxic compounds.' *Biodegradation* 10 (3): 219–233.

Dhamole, P. B., Wang, Z., Liu, Y., Wang, B., and Feng, H. 2012. 'Extractive fermentation with non-ionic surfactants to enhance butanol production.' *Biomass and Bioenergy* 40:112–119.

Doig, S. D., Ortiz-Ochoa, K., Ward, J. M., and Baganz, F. 2008. 'Characterization of Oxygen Transfer in Miniature and Lab-Scale Bubble Column Bioreactors and Comparison of Microbial Growth Performance Based on Constant $k_L a$.' *Biotechnology Progress* 21 (4): 1175–1182.

Doig, S. D., Pickering, S. C. R., Lye, G. J., and Baganz, F. 2005. 'Modelling surface aeration rates in shaken microtitre plates using dimensionless groups.' *Chemical Engineering Science* 60 (10): 2741–2750.

Doig, S. D., Simpson, H., Alphand, V., and Furstoss, R. 2003. 'Characterization of a recombinant *Escherichia coli* TOP10 [pQR239] whole-cell biocatalyst for stereoselective Baeyer–Villiger oxidations.' *Enzyme and Microbial Technology* 32 (3-4): 347–355.

Duetz, W. A. 2007. 'Microtiter plates as mini-bioreactors: miniaturization of fermentation methods.' *Trends in Microbiology* 15 (10): 469–475.

Duetz, W. A., Rüedi, L., Hermann, R., O'Connor, K., Büchs, J., and Witholt, B. 2000. 'Methods for Intense Aeration, Growth, Storage, and Replication of Bacterial Strains in Microtiter Plates.' *Applied and Environmental Microbiology* 66 (6): 2641–2646.

Duetz, W. A. and Witholt, B. 2004. 'Oxygen transfer by orbital shaking of square vessels and deepwell microtiter plates of various dimensions.' *Biochemical Engineering Journal* 17 (3): 181–185.

Dunlop, M. J. 2011. 'Engineering microbes for tolerance to next-generation biofuels.' *Biotechnology for Biofuels* 4 (32).

Dunlop, M. J., Dossani, Z. Y., Szmidt, H. L., Chu, H. C., Lee, T. S., Keasling, J. D., Hadi, M. Z., and Mukhopadhyay, A. 2011. 'Engineering microbial biofuel tolerance and export using efflux pumps.' *Molecular Systems Biology* 7.

Ebert, B. E., Kurth, F., Grund, M., Blank, L. M., and Schmid, A. 2011. 'Response of *Pseudomonas putida* KT2440 to increased NADH and ATP demand.' *Applied and Environmental Microbiology* 77 (18): 6597–6605.

Eggink, G., Engel, H., Vriend, G., Terpstra, P., and Witholt, B. 1990. 'Rubredoxin reductase of *Pseudomonas oleovorans*: Structural relationship to other flavoprotein oxidoreductases based on one NAD and two FAD fingerprints.' *Journal of Molecular Biology* 212 (1): 135–142.

Eggink, G., Lageveen, R. G., Altenburg, B., and Witholt, B. 1987. 'Controlled and functional expression of the *Pseudomonas oleovorans* alkane utilizing system in *Pseudomonas putida* and *Escherichia coli*.' *Journal of Biological Chemistry* 262 (36): 17712–17718.

El Aalam, S., Pauss, A., and Lebeault, J. M. 1993. 'High efficiency styrene biodegradation in a biphasic organic/water continuous reactor.' *Applied Microbiology and Biotechnology* 39 (6): 696–699.

Eriksson, L., Byrne, T., Johansson, E., Trygg, J., and Vikström, C. 2013. *Multi- and Megavariate Data Analysis.* Basic Principles and Applications. Malmö, Sweden: MKS Umetrics AB.

Evonik Industries AG. 2013. 'Project BiOxAm.' *elements* 45 (4): 49.

Evonik Industries AG. 2014. *Cell culture reagents.*

Fasan, R., Meharenna, Y. T., Snow, C. D., Poulos, T. L., and Arnold, F. H. 2008. 'Evolutionary History of a Specialized P450 Propane Monooxygenase.' *Journal of Molecular Biology* 383 (5): 1–12.

Favre-Bulle, O., Weenink, E., Vos, T., Preusting, H., and Witholt, B. 1993. 'Continuous bioconversion of n-octane to octanoic acid by recombinant *Escherichia coli* (alk^+) growing in a two-liquid-phase chemostat.' *Biotechnology and Bioengineering* 41 (2): 263–272.

Fernandes, P. 2010. 'Miniaturization in Biocatalysis.' *International Journal of Molecular Sciences* 11 (3): 858–879.

Ferreira-Torres, C., Micheletti, M., and Lye, G. J. 2005. 'Microscale process evaluation of recombinant biocatalyst libraries: application to Baeyer–Villiger monooxygenase catalysed lactone synthesis.' *Bioprocess and Biosystems Engineering* 28 (2): 83–93.

Filho, M. V., Stillger, T., Müller, M., Liese, A., and Wandrey, C. 2003. 'Is log*P* a convenient criterion to guide the choice of solvents for biphasic enzymatic reactions?' *Angewandte Chemie International Edition* 42 (26): 2993–2996.

Freedman, L. P., Cockburn, I. M., and Simcoe, T. S. 2015. 'The Economics of Reproducibility in Preclinical Research.' *PLOS Biology* 13 (6): e1002165.

Friedman, A. M., Long, S. R., Brown, S. E., Buikema, W. J., and Ausubel, F. M. 1982. 'Construction of a broad host range cosmid cloning vector and its use in the genetic analysis of *Rhizobium* mutants.' *Gene* 18 (3): 289–296.

Funhoff, E. G. and Beilen, J. B. van. 2007. 'Alkane activation by P450 oxygenases.' *Biocatalysis and Biotransformation* 25 (2-4): 186–193.

Funke, M., Buchenauer, A., Mokwa, W., Kluge, S., Hein, L., Müller, C., Kensy, F., and Büchs, J. 2010a. 'Bioprocess Control in Microscale: Scalable Fermentations in Disposable and User-Friendly Microfluidic Systems.' *Microbial Cell Factories* 9 (1): 86.

Funke, M., Buchenauer, A., Schnakenberg, U., Mokwa, W., Diederichs, S., Mertens, A., Müller, C., Kensy, F., and Büchs, J. 2010b. 'Microfluidic biolector-microfluidic bioprocess control in microtiter plates.' *Biotechnology and Bioengineering* 107 (3): 497–505.

Funke, M., Diederichs, S., Kensy, F., Müller, C., and Büchs, J. 2009. 'The baffled microtiter plate: Increased oxygen transfer and improved online monitoring in small scale fermentations.' *Biotechnology and Bioengineering* 103 (6): 1118–1128.

Galdzicki, M., Clancy, K. P., Oberortner, E., Pocock, M., Quinn, J. Y., Rodriguez, C. A., Roehner, N., et al. 2014. 'The Synthetic Biology Open Language (SBOL) provides a community standard for communicating designs in synthetic biology.' *Nature Biotechnology* 32 (6): 545–550.

Ghisalba, O., Meyer, H. P., and Wohlgemuth, R. 2010. 'Industrial biotransformation.' In *Encyclopedia of Industrial Biotechnology,* edited by M. C. Flickinger. New York City.

Giese, H., Kruithof, P., Meier, K., Sieben, M., Antonov, E., Hommes, R. W. J., and Büchs, J. 2014. 'Improvement and scale-down of a *Trichoderma reesei* shake flask protocol to microtiter plates enables high-throughput screening.' *Journal of Bioscience and Bioengineering* 118 (6): 702–709.

Girvan, H. M. and Munro, A. W. 2016. 'Applications of microbial cytochrome P450 enzymes in biotechnology and synthetic biology.' *Current Opinion in Chemical Biology* 31:136–145.

Glazyrina, J., Krause, M., Junne, S., Glauche, F., Strom, D., and Neubauer, P. 2012. 'Glucose-limited high cell density cultivations from small to pilot plant scale using an enzyme-controlled glucose delivery system.' *New BIOTECHNOLOGY* 29 (2): 235–242.

Glembin, P., Kerner, M., and Smirnova, I. 2013. 'Cloud point extraction of microalgae cultures.' *Separation and Purification Technology* 103:21–27.

Gómez-Hortigüela, L., Corà, F., Sankar, G., Zicovich-Wilson, C. M., and Catlow, C. R. A. 2010. 'Catalytic Reaction Mechanism of Mn-Doped Nanoporous Aluminophosphates for the Aerobic Oxidation of Hydrocarbons.' *Chemistry - A European Journal* 16 (46): 13638–13645.

González-Peñas, H., Lu-Chau, T. A., Moreira, M. T., and Lema, J. M. 2014. 'Assessment of morphological changes of *Clostridium acetobutylicum* by flow cytometry during acetone/butanol/ethanol extractive fermentation.' *Biotechnology Letters* 37 (3).

Goodman, S. N., Fanelli, D., and Ioannidis, J. P. A. 2016. 'What does research reproducibility mean?' *Science Translational Medicine* 8 (341).

Grant, C. 2012. 'Evaluation of the Bio-oxidation of Alkanes.' PhD diss., University College London.

Grant, C., Deszcz, D., Wei, Y.-C., Martínez-Torres, R. J., Morris, P., Folliard, T., Sreenivasan, R., et al. 2014. 'Identification and use of an alkane transporter plug-in for applications in biocatalysis and whole-cell biosensing of alkanes.' *Scientific Reports* 4.

Grant, C., Silva Damas Pinto, A. C. da, Lui, H.-P., Woodley, J. M., and Baganz, F. 2012. 'Tools for characterizing the whole-cell bio-oxidation of alkanes at microscale.' *Biotechnology and Bioengineering* 109 (9): 2179–2189.

Grant, C., Woodley, J. M., and Baganz, F. 2011. 'Whole-cell bio-oxidation of n-dodecane using the alkane hydroxylase system of *P. putida* GPo1 expressed in *E. coli*.' *Enzyme and Microbial Technology* 48 (6-7): 480–486.

Gricman, Ł., Vogel, C., and Pleiss, J. 2013. 'Conservation analysis of class-specific positions in cytochrome P450 monooxygenases: Functional and structural relevance.' *Proteins: Structure, Function, and Bioinformatics* 82 (3): 491–504.

Grogan, G. 2011. 'Cytochromes P450: exploiting diversity and enabling application as biocatalysts.' *Current Opinion in Chemical Biology* 15 (2): 241–248.

Grosch, J.-H., Sieben, M., Lattermann, C., Kauffmann, K., Büchs, J., and Spiess, A. C. 2016. 'Enzyme activity deviates due to spatial and temporal temperature profiles in commercial microtiter plate readers.' *Biotechnology Journal* 11 (4): 519–529.

Grover, W. H., Muhlen, M. G. von, and Manalis, S. R. 2008. 'Teflon films for chemically-inert microfluidic valves and pumps.' *Lab on a Chip* 8 (6): 913–918.

Grund, A., Shapiro, J., Fennewald, M., Bacha, P., Leahy, J., Markbreiter, K., Nieder, M., and Toepfer, M. 1975. 'Regulation of alkane oxidation in *Pseudomonas putida*.' *Journal of Bacteriology* 123 (2): 546–556.

Gudiminchi, R. K., Randall, C., Opperman, D. J., Olaofe, O. A., Harrison, S. T. L., Albertyn, J., and Smit, M. S. 2012. 'Whole-cell hydroxylation of n-octane by *Escherichia coli* strains expressing the CYP153A6 operon.' *Applied Microbiology and Biotechnology* 96 (6): 1507–1516.

Halan, B., Schmid, A., and Bühler, K. 2011. 'Real-Time Solvent Tolerance Analysis of *Pseudomonas* sp. Strain VLB120 C Catalytic Biofilms.' *Applied and Environmental Microbiology* 77 (5): 1563–1571.

Halling, P. J. 1994. 'Thermodynamic predictions for biocatalysis in nonconventional media: Theory, tests, and recommendations for experimental design and analysis.' *Enzyme and Microbial Technology* 16 (3): 178–206.

Hansen, C. M. 2012. 'Solubility Parameters.' In *Paint and Coating Testing Manual,* edited by J. V. Koleske, 470–494. West Conshohocken, PA: ASTM International.

Harms, H., Smith, K. E. C., and Wick, L. Y. 2010. 'Microorganism-Hydrophobic Compound Interactions.' In *Handbook of Hydrocarbon and Lipid Microbiology,* 1479–1490. Berlin, Heidelberg: Springer Berlin Heidelberg.

Hearn, E. M., Patel, D. R., Lepore, B. W., Indic, M., and Berg, B. van den. 2009. 'Transmembrane passage of hydrophobic compounds through a protein channel wall.' *Nature* 458 (7236): 367–370.

Heinig, U., Scholz, S. A., Dahm, P., Grabowy, U., and Jennewein, S. 2010. 'Development of carbon plasma-coated multiwell plates for high-throughput mass spectrometric analysis of highly lipophilic fermentation products.' *Analytical Biochemistry* 403 (1-2): 108–113.

Heipieper, H. J. and Martínez, P. M. 2010. 'Toxicity of Hydrocarbons to Microorganisms.' In *Handbook of Hydrocarbon and Lipid Microbiology,* 1563–1573. Berlin, Heidelberg: Springer Berlin Heidelberg.

Hemmerich, J. 2011. 'Fed-Batch Cultivation in Baffled Shake Flasks.' *Genetic Engineering & Biotechnology News* 31 (14): 52–54.

Hermann, R., Lehmann, M., and Büchs, J. 2002. 'Characterization of gas-liquid mass transfer phenomena in microtiter plates.' *Biotechnology and Bioengineering* 81 (2): 178–186.

Hermann, R., Walther, N., Maier, U., and Büchs, J. 2001. 'Optical method for the determination of the oxygen-transfer capacity of small bioreactors based on sulfite oxidation.' *Biotechnology and Bioengineering* 74 (5): 355–363.

Hezaveh, S., Samanta, S., De Nicola, A., Milano, G., and Roccatano, D. 2012. 'Understanding the Interaction of Block Copolymers with DMPC Lipid Bilayer Using Coarse-Grained Molecular Dynamics Simulations.' *The Journal of Physical Chemistry B* 116 (49): 14333–14345.

Hill, C. L. 1989. *Activation and Functionalization of Alkanes.* New York City: John Wiley & Sons.

Hollmann, F., Arends, I. W. C. E., Bühler, K., Schallmey, A., and Bühler, B. 2011. 'Enzyme-mediated oxidations for the chemist.' *Green Chemistry* 13 (2): 226.

Hollmann, F., Hofstetter, K., Habicher, T., Hauer, B., and Schmid, A. 2005. 'Direct Electrochemical Regeneration of Monooxygenase Subunits for Biocatalytic Asymmetric Epoxidation.' *Journal of the American Chemical Society* 127 (18): 6540–6541.

Holtmann, D., Fraaije, M. W., Arends, I. W. C. E., Opperman, D. J., and Hollmann, F. 2014. 'The taming of oxygen: biocatalytic oxyfunctionalisations.' *Chemical Communications* 50 (87): 13180–13200.

Hua, F. and Wang, H. Q. 2014. 'Uptake and trans-membrane transport of petroleum hydrocarbons by microorganisms.' *Biotechnology & Biotechnological Equipment* 28 (2): 165–175.

Huf, S., Krügener, S., Hirth, T., Rupp, S., and Zibek, S. 2011. 'Biotechnological synthesis of long-chain dicarboxylic acids as building blocks for polymers.' *European Journal of Lipid Science and Technology* 113 (5): 548–561.

Hutchenson, K. W., La Marca, C., Patience, G. S., Laviolette, J.-P., and Bockrath, R. E. 2010. 'Parametric study of n-butane oxidation in a circulating fluidized bed reactor.' *Applied Catalysis A, General* 376 (1-2): 91–103.

Islam, R. S., Tisi, D., Levy, M. S., and Lye, G. J. 2007. 'Framework for the rapid optimization of soluble protein expression in *Escherichia coli* combining microscale experiments and statistical experimental design.' *Biotechnology Progress* 23 (4): 785–793.

Islam, R. S., Tisi, D., Levy, M. S., and Lye, G. J. 2008. 'Scale-up of *Escherichia coli* growth and recombinant protein expression conditions from microwell to laboratory and pilot scale based on matched $k_L a$.' *Biotechnology and Bioengineering* 99 (5): 1128–1139.

Jegannathan, K. R. and Nielsen, P. H. 2012. 'Environmental assessment of enzyme use in industrial production – a literature review.' *Journal of Cleaner Production* 42:228–240.

Jeude, M., Dittrich, B., Niederschulte, H., Anderlei, T., Knocke, C., Büchs, J., Klee, D., and Anderlei, T. 2006. 'Fed-batch mode in shake flasks by slow-release technique.' *Biotechnology and Bioengineering* 95 (3): 433–445.

Jones, D. F. and Howe, R. 1968. 'Microbiological oxidation of long-chain aliphatic compounds. Part I. Alkanes and alk-1-enes.' *Journal of the Chemical Society C: Organic:* 2801.

Jong, K. P. de, Zečević, J., Friedrich, H., Jongh, P. E. de, Bulut, M., Donk, S. van, Kenmogne, R., Finiels, A., Hulea, V., and Fajula, F. 2010. 'Zeolite Y Crystals with Trimodal Porosity as Ideal Hydrocracking Catalysts.' *Angewandte Chemie International Edition* 49 (52): 10074–10078.

Julsing, M., Cornelissen, S., Bühler, B., and Schmid, A. 2008. 'Heme-iron oxygenases: powerful industrial biocatalysts?' *Current Opinion in Chemical Biology* 12 (2): 177–186.

Julsing, M., Kuhn, D., Schmid, A., and Bühler, B. 2011. 'Resting cells of recombinant *E. coli* show high epoxidation yields on energy source and high sensitivity to product inhibition.' *Biotechnology and Bioengineering* 109 (5): 1109–1119.

Julsing, M., Schrewe, M., Cornelissen, S., Hermann, I., Schmid, A., and Bühler, B. 2012. 'Outer Membrane Protein AlkL Boosts Biocatalytic Oxyfunctionalization of Hydrophobic Substrates in *Escherichia coli*.' *Applied and Environmental Microbiology* 78 (16): 5724–5733.

Jung, S. T., Lauchli, R., and Arnold, F. H. 2011. 'Cytochrome P450: taming a wild type enzyme.' *Current Opinion in Biotechnology* 22 (6): 809–817.

Jurelevicius, D., Alvarez, V. M., Peixoto, R., Rosado, A. S., and Seldin, L. 2013. 'The Use of a Combination of *alkB* Primers to Better Characterize the Distribution of Alkane-Degrading Bacteria.' *PLoS ONE* 8 (6).

Kamata, K., Yonehara, K., Nakagawa, Y., Uehara, K., and Mizuno, N. 2010. 'Efficient stereo- and regioselective hydroxylation of alkanes catalysed by a bulky polyoxometalate.' *Nature Chemistry* 2 (6): 478–483.

Kara, S., Schrittwieser, J. H., Hollmann, F., and Ansorge-Schumacher, M. B. 2013. 'Recent trends and novel concepts in cofactor-dependent biotransformations.' *Applied Microbiology and Biotechnology* 98 (4): 1517–1529.

Keane, A., Lau, P. C. K., and Ghoshal, S. 2007. 'Use of a whole-cell biosensor to assess the bioavailability enhancement of aromatic hydrocarbon compounds by nonionic surfactants.' *Biotechnology and Bioengineering* 99 (1): 86–98.

Kell, D. B., Swainston, N., Pir, P., and Oliver, S. G. 2015. 'Membrane transporter engineering in industrial biotechnology and whole cell biocatalysis.' *Trends in Biotechnology* 33 (4): 237–246.

Kim, P.-Y., Pollard, D. J., and Woodley, J. M. 2007. 'Substrate supply for effective biocatalysis.' *Biotechnology Progress* 23 (1): 74–82.

Kirmair, L. and Skerra, A. 2014. 'Biochemical analysis of recombinant AlkJ from *Pseudomonas putida* reveals a membrane-associated, flavin adenine dinucleotide-dependent dehydrogenase suitable for the biosynthetic production of aliphatic aldehydes.' *Applied and Environmental Microbiology* 80 (8): 2468–2477.

Klöckner, W. and Büchs, J. 2012. 'Advances in shaking technologies.' *Trends in Biotechnology* 30 (6): 307–314.

Koch, D. J., Chen, M. M. Y., Beilen, J. B. van, and Arnold, F. H. 2009. 'In Vivo Evolution of Butane Oxidation by Terminal Alkane Hydroxylases AlkB and CYP153A6.' *Applied and Environmental Microbiology* 75 (2): 337–344.

Kok, M., Oldenhuis, R., Linden, M. P. van der, Meulenberg, C. H., Kingma, J., and Witholt, B. 1989a. 'The *Pseudomonas oleovorans alkBAC* operon encodes two structurally related rubredoxins and an aldehyde dehydrogenase.' *Journal of Biological Chemistry* 264 (10): 5442–5451.

Kok, M., Oldenhuis, R., Linden, M. P. van der, Raatjes, P., Kingma, J., Lelyveld, P. H. van, and Witholt, B. 1989b. 'The *Pseudomonas oleovorans* alkane hydroxylase gene. Sequence and expression.' *Journal of Biological Chemistry* 264 (10): 5435–5441.

Kollmer, A. 1997. 'Verfahrenstechnische Aspekte bei zweiphasigen Bioprozessen.' PhD diss., Eidgenössische Technische Hochschule Zürich.

Kollmer, A. and Rohr, R. von. 1997. 'Sichere Prozessbedingungen bei leichtflüchtigen Kohlenwasserstoffen durch erhöhten Druck.' *Chemie Ingenieur Technik* 69 (5): 681–685.

Kollmer, A. and Rohr, R. von. 1998. 'Verfahrenstechnische Aspekte bei zweiphasigen Bioprozessen.' *Chemie Ingenieur Technik* 70 (9): 1125–1126.

Kollmer, A., Schmid, A., Rohr, P. R. von, and Sonnleitner, B. 1999. 'On liquid-liquid mass transfer in two-liquid-phase fermentations.' *Bioprocess Engineering* 20 (5): 441.

Krause, M., Ukkonen, K., Haataja, T., Ruottinen, M., Glumoff, T., Neubauer, A., Neubauer, P., and Vasala, A. 2010. 'A novel fed-batch based cultivation method provides high cell-density and improves yield of soluble recombinant proteins in shaken cultures.' *Microbial Cell Factories* 9 (1).

Krell, T., Lacal, J., Guazzaroni, M. E., Busch, A., Silva-Jiménez, H., Fillet, S., Reyes-Darias, J. A., et al. 2012. 'Responses of *Pseudomonas putida* to toxic aromatic carbon sources.' *Journal of Biotechnology* 160 (1-2): 25–32.

Krylova, O. O., Melik-Nubarov, N. S., Badun, G. A., Ksenofontov, A. L., Menger, F. M., and Yaroslavov, A. A. 2003. 'Pluronic L61 Accelerates Flip–Flop and Transbilayer Doxorubicin Permeation.' *Chemistry - A European Journal* 9 (16): 3930–3936.

Krylova, O. O. and Pohl, P. 2004. 'Ionophoric Activity of Pluronic Block Copolymers.' *Biochemistry* 43 (12): 3696–3703.

Kubota, M., Nodate, M., Yasumoto-Hirose, M., Uchiyama, T., Kagami, O., Shizuri, Y., and Misawa, N. 2005. 'Isolation and functional analysis of cytochrome P450 CYP153A genes from various environments.' *Bioscience, Biotechnology and Biochemistry* 69 (12): 2421–2430.

Kuhn, D., Blank, L. M., Schmid, A., and Bühler, B. 2010. 'Systems biotechnology – Rational whole-cell biocatalyst and bioprocess design.' *Engineering in Life Sciences* 10 (5): 384–397.

Kuhn, D., Fritzsch, F. S. O., Zhang, X., Wendisch, V. F., Blank, L. M., Bühler, B., and Schmid, A. 2013. 'Subtoxic product levels limit the epoxidation capacity of recombinant *E. coli* by increasing microbial energy demands.' *Journal of Biotechnology* 163 (2): 194–203.

Kuhn, D., Julsing, M., Heinzle, E., and Bühler, B. 2012. 'Systematic optimization of a biocatalytic two-liquid phase oxyfunctionalization process guided by ecological and economic assessment.' *Green Chemistry* 14 (3): 645.

Kühn, I. 1980. 'Alcoholic Fermentation in an Aqueous Two-Phase System.' *Biotechnology and Bioengineering* 22 (11): 2393–2398.

Laane, C., Boeren, S., Vos, K., and Veeger, C. 1987. 'Rules for optimization of biocatalysis in organic solvents.' *Biotechnology and Bioengineering* 30 (1): 81–87.

Labinger, J. A. 2004. 'Selective alkane oxidation: hot and cold approaches to a hot problem.' *Journal of Molecular Catalysis A: Chemical* 220 (1): 27–35.

Ladkau, N., Assmann, M., Schrewe, M., Julsing, M., Schmid, A., and Bühler, B. 2016. 'Efficient production of the Nylon 12 monomer ω-aminododecanoic acid methyl ester from renewable dodecanoic acid methyl ester with engineered *Escherichia coli*.' *Metabolic Engineering* 36:1–9.

Lamping, S. R., Zhang, H., Allen, B., and Ayazi-Shamlou, P. 2003. 'Design of a prototype miniature bioreactor for high throughput automated bioprocessing.' *Chemical Engineering Science* 58 (3-6): 747–758.

Landwehr, M., Carbone, M., Otey, C. R., Li, Y., and Arnold, F. H. 2007. 'Diversification of Catalytic Function in a Synthetic Family of Chimeric Cytochrome P450s.' *Chemistry & Biology* 14 (3): 269–278.

Lattermann, C. and Büchs, J. 2015. 'Microscale and miniscale fermentation and screening.' *Current Opinion in Biotechnology* 35:1–6.

Ławniczak, Ł., Marecik, R., and Chrzanowski, Ł. 2013. 'Contributions of biosurfactants to natural or induced bioremediation.' *Applied Microbiology and Biotechnology* 97 (6): 2327–2339.

Leadbetter, E. R. and Foster, J. W. 1960. 'Bacterial oxidation of gaseous alkanes.' *Archives of Microbiology* 35 (1): 92–104.

Lee, J. N., Park, C., and Whitesides, G. M. 2003. 'Solvent compatibility of poly(dimethylsiloxane)-based microfluidic devices.' *Analytical Chemistry* 75 (23): 6544–6554.

Lee, S. J., McCormick, M. S., Lippard, S. J., and Cho, U.-S. 2013. 'Control of substrate access to the active site in methane monooxygenase.' *Nature* 494 (7437): 380–384.

Lennen, R. M., Kruziki, M. A., Kumar, K., Zinkel, R. A., Burnum, K. E., Lipton, M. S., Hoover, S. W., et al. 2011. 'Membrane stresses induced by overproduction of free fatty acids in *Escherichia coli*.' *Applied and Environmental Microbiology* 77 (22): 8114–8128.

Lepore, B. W., Indic, M., Pham, H., Hearn, E. M., Patel, D. R., and Berg, B. van den. 2011. 'Ligand-gated diffusion across the bacterial outer membrane.' *Proceedings of the National Academy of Sciences* 108 (25): 10121–10126.

Lewis, J. C., Coelho, P. S., and Arnold, F. H. 2011. 'Enzymatic functionalization of carbon–hydrogen bonds.' *Chemical Society Reviews* 40 (4): 2003–2021.

Li, J. L. and Chen, B. H. 2009. 'Surfactant-mediated biodegradation of polycyclic aromatic hydrocarbons.' *Materials* 2 (1): 76–94.

Li, Z., Beilen, J. B. van, Duetz, W. A., Schmid, A., Raadt, A. de, Griengl, H., and Witholt, B. 2002. 'Oxidative biotransformations using oxygenases.' *Current Opinion in Chemical Biology* 6 (2): 136–144.

Lide, D. R., ed. 2005. *CRC Handbook of Chemistry and Physics.* 86th ed. Boca Raton: CRC Press.

Liese, A., Seelbach, K., and Wandrey, C. 2006. *Industrial Biotransformations.* 2nd. Weinheim: Wiley-VCH.

Lima-Ramos, J., Neto, W., and Woodley, J. M. 2013. 'Engineering of Biocatalysts and Biocatalytic Processes.' *Topics in Catalysis* 57 (5): 301–320.

Liu, H., Xu, J., Liang, R., and Liu, J. 2014. 'Characterization of the medium- and long-chain n-alkanes degrading *Pseudomonas aeruginosa* strain SJTD-1 and its alkane hydroxylase genes.' *PLoS ONE* 9 (8): e105506.

Lo, T.-M., Teo, W. S., Ling, H., Chen, B., Kang, A., and Chang, M. W. 2013. 'Microbial engineering strategies to improve cell viability for biochemical production.' *Biotechnology Advances* 31 (6): 903–914.

Long, Q., Liu, X., Yang, Y., Li, L., Harvey, L., McNeil, B., and Bai, Z. 2014. 'The development and application of high throughput cultivation technology in bioprocess development.' *Journal of Biotechnology* 192:323–338.

Loschen, C. and Klamt, A. 2012. 'COSMO*quick*: A Novel Interface for Fast σ-Profile Composition and Its Application to COSMO-RS Solvent Screening Using Multiple Reference Solvents.' *Industrial & Engineering Chemistry Research* 51 (43): 14303–14308.

Lousa, D., Baptista, A. M., and Soares, C. M. 2013. 'A molecular perspective on non-aqueous biocatalysis: contributions from simulation studies.' *Physical Chemistry Chemical Physics* 15 (33): 13723.

Lu, W., Ness, J. E., Xie, W., Zhang, X., Minshull, J., and Gross, R. A. 2010. 'Biosynthesis of Monomers for Plastics from Renewable Oils.' *Journal of the American Chemical Society* 132 (43): 15451–15455.

Lundemo, M. T. and Woodley, J. M. 2015. 'Guidelines for development and implementation of biocatalytic P450 processes.' *Applied Microbiology and Biotechnology* 99 (6): 2465–2483.

Lye, G. J. and Woodley, J. M. 2001. 'Advances in the selection and design of two-liquid phase biocatalytic reactors.' In *Multiphase Bioreactor Design,* edited by J. M. S. Cabral, M. Mota, and J. Tramper. London: Taylor & Francis.

Maeng, J. H., Sakai, Y., Tani, Y., and Kato, N. 1996. 'Isolation and characterization of a novel oxygenase that catalyzes the first step of n-alkane oxidation in *Acinetobacter* sp. strain M-1.' *Journal of Bacteriology* 178 (13): 3695–3700.

Marques, M. P. C., Carvalho, C. C. C. R. de, Cabral, J. M. S., and Fernandes, P. 2010. 'Scaling-up of complex whole-cell bioconversions in conventional and non-conventional media.' *Biotechnology and Bioengineering* 106 (4): 619–626.

Marques, M. P. C., Carvalho, F., Magalhães, S., Cabral, J. M. S., and Fernandes, P. 2009. 'Screening for suitable solvents as substrate carriers for the microbial side-chain cleavage of sitosterol using microtitre plates.' *Process Biochemistry* 44 (5): 556–561.

Marques, M. P. C., Claudino, M. J., Cabral, J. M. S., Fernandes, P., and Carvalho, C. C. C. R. de. 2007. 'On the feasibility of the microscale approach for a multistep biotransformation: sitosterol side chain cleavage.' *Journal of Chemical Technology & Biotechnology* 82 (9): 856–863.

Mathys, R. G., Kut, O. M., and Witholt, B. 1998. 'Alkanol removal from the apolar phase of a two-liquid phase bioconversion system. Part 1: Comparison of a less volatile and a more volatile in-situ extraction solvent for the separation of 1-octanol by distillation.' *Journal of Chemical Technology & Biotechnology* 71 (4): 315–325.

Mathys, R. G., Schmid, A., Kut, O. M., and Witholt, B. 1998. 'Alkanol removal from the apolar phase of a two-liquid phase bioconversion system. Part 2: Effect of fermentation medium on batch distillation.' *Journal of Chemical Technology & Biotechnology* 71 (4): 326–334.

McKenna, E. J. and Coon, M. J. 1970. 'Enzymatic ω-oxidation.' *Journal of Biological Chemistry* 245 (15): 3882–3889.

McKenna, E. J. and Kallio, R. E. 1965. 'The biology of hydrocarbons.' *Annual Review of Microbiology* 19 (1): 183–208.

McLean, K. J., Leys, D., and Munro, A. W. 2015. 'Microbial Cytochromes P450.' In *Cytochrome P450,* 261–407. Cham: Springer International Publishing.

Micheletti, M., Barrett, T., Doig, S. D., Baganz, F., Levy, M. S., Woodley, J. M., and Lye, G. J. 2006. 'Fluid mixing in shaken bioreactors: Implications for scale-up predictions from microlitre-scale microbial and mammalian cell cultures.' *Chemical Engineering Science* 61 (9): 2939–2949.

Miozzari, G. F., Niederberger, P., and Hütter, R. 1978. 'Permeabilization of microorganisms by Triton X-100.' *Analytical Biochemistry* 90:220–233.

MKS Umetrics. 2012. *User Guide to SIMCA 13.* Malmö, Sweden: MKS Umetrics AB.

Moity, L., Molinier, V., Benazzouz, A., Joossen, B., Gerbaud, V., and Aubry, J.-M. 2016. 'A "top-down" *in silico* approach for designing *ad hoc* bio-based solvents: application to glycerol-derived solvents of nitrocellulose.' *Green Chemistry.*

Mukhopadhyay, A. 2015. 'Tolerance engineering in bacteria for the production of advanced biofuels and chemicals.' *Trends in Microbiology* 23 (8): 498–508.

Müller, C. A., Akkapurathu, B., Winkler, T., Staudt, S., Hummel, W., Gröger, H., and Schwaneberg, U. 2013. '*In Vitro* Double Oxidation of n-Heptane with Direct Cofactor Regeneration.' *Advanced Synthesis & Catalysis* 355 (9): 1787–1798.

Muñoz, R., Gan, E. I. H. H., Hernández, M., and Quijano, G. 2013. 'Hexane biodegradation in two-liquid phase bioreactors: High-performance operation based on the use of hydrophobic biomass.' *Biochemical Engineering Journal* 70:9–16.

Munro, A. W., Girvan, H. M., Mason, A. E., Dunford, A. J., and McLean, K. J. 2013. 'What makes a P450 tick?' *Trends in Biochemical Sciences:* 1–11.

Munro, A. W., Girvan, H. M., and McLean, K. J. 2007. 'Cytochrome P450–redox partner fusion enzymes.' *Biochimica et Biophysica Acta* 1770 (3): 345–359.

Munz, D. and Strassner, T. 2015. 'Alkane C–H Functionalization and Oxidation with Molecular Oxygen.' *Inorganic Chemistry* 54 (11): 5043–5052.

Murray, P. M., Bellany, F., Benhamou, L., Bučar, D.-K., Tabor, A. B., and Sheppard, T. D. 2016. 'The application of design of experiments (DoE) reaction optimisation and solvent selection in the development of new synthetic chemistry.' *Organic & Biomolecular Chemistry* 14 (8): 2373–2384.

Musser, M. T. 2011. *Cyclohexanol and Cyclohexanone.* Weinheim, Germany: Wiley-VCH Verlag.

Myers, D. 1999. 'Association colloids: Micelles, vesicles, and membranes.' In *Surfaces, Interfaces, and Colloids Principles and Applications,* 358–396. Surfaces.

Mykytczuk, N. C. S., Trevors, J. T., Leduc, L. G., and Ferroni, G. D. 2007. 'Fluorescence polarization in studies of bacterial cytoplasmic membrane fluidity under environmental stress.' *Progress in Biophysics and Molecular Biology* 95 (1-3): 60–82.

Naing, S.-H., Parvez, S., Pender Cudlip, M., Groves, J. T., and Austin, R. N. 2013. 'Substrate specificity and reaction mechanism of purified alkane hydroxylase from the hydrocarbonoclastic bacterium *Alcanivorax borkumensis* (*Ab*AlkB).' *Journal of Inorganic Biochemistry* 121:46–52.

Nakahara, T., Erickson, L. E., and Gutierrez, J. R. 1977. 'Characteristics of hydrocarbon uptake in cultures with two liquid phases.' *Biotechnology and Bioengineering* 19 (1): 9–25.

Nawaz, S., Redhead, M., Mantovani, G., Alexander, C., Bosquillon, C., and Carbone, P. 2012. 'Interactions of PEO–PPO–PEO block copolymers with lipid membranes: a computational and experimental study linking membrane lysis with polymer structure.' *Soft Matter* 8 (25): 6744–6754.

Nelson, D. R., Kamataki, T., Waxman, D. J., Guengerich, F. P., Estabrook, R. W., Feyereisen, R., Gonzalez, F. J., Coon, M. J., Gunsalus, I. C., and Gotoh, O. 1993. 'The P450 superfamily: update on new sequences, gene mapping, accession numbers, early trivial names of enzymes, and nomenclature.' *DNA and Cell Biology* 12 (1): 1–51.

Neubauer, P., Cruz, N., Glauche, F., Junne, S., Knepper, A., and Raven, M. 2013. 'Consistent development of bioprocesses from microliter cultures to the industrial scale.' *Engineering in Life Sciences* 13 (3): 224–238.

Newhouse, T. and Baran, P. S. 2011. 'If C–H bonds could talk: selective C–H bond oxidation.' *Angewandte Chemie International Edition* 50 (15): 3362–3374.

Ni, Y. and Chen, R. R. 2004. 'Accelerating whole-cell biocatalysis by reducing outer membrane permeability barrier.' *Biotechnology and Bioengineering* 87 (6): 804–811.

Ni, Y. and Chen, R. R. 2005. 'Lipoprotein mutation accelerates substrate permeability-limited toluene dioxygenase-catalyzed reaction.' *Biotechnology Progress* 21 (3): 799–805.

Nicolaou, S. A., Gaida, S. M., and Papoutsakis, E. T. 2010. 'A comparative view of metabolite and substrate stress and tolerance in microbial bioprocessing: From biofuels and chemicals, to biocatalysis and bioremediation.' *Metabolic Engineering* 12 (4): 307–331.

Nie, Y., Chi, C.-Q., Fang, H., Liang, J.-L., Lu, S.-L., Lai, G.-L., Tang, Y.-Q., and Wu, X.-L. 2014. 'Diverse alkane hydroxylase genes in microorganisms and environments.' *Scientific Reports* 4.

Nikaido, H. 2003. 'Molecular Basis of Bacterial Outer Membrane Permeability Revisited.' *Microbiology and Molecular Biology Reviews* 67 (4): 593–656.

Nikaido, H. and Takatsuka, Y. 2009. 'Mechanisms of RND multidrug efflux pumps.' *Biochimica et Biophysica Acta* 1794 (5): 769–781.

Nodate, M., Kubota, M., and Misawa, N. 2006. 'Functional expression system for cytochrome P450 genes using the reductase domain of self-sufficient P450RhF from *Rhodococcus* sp. NCIMB 9784.' *Applied Microbiology and Biotechnology* 71 (4): 455–462.

Norouzian, D., Akbarzadeh, A., Scharer, J. M., and Moo Young, M. 2006. 'Fungal glucoamylases.' *Biotechnology Advances* 24 (1): 80–85.

Olaofe, O. A., Fenner, C. J., Gudiminchi, R. K., Smit, M. S., and Harrison, S. T. L. 2013. 'The influence of microbial physiology on biocatalyst activity and efficiency in the terminal hydroxylation of n-octane using *Escherichia coli* expressing the alkane hydroxylase, CYP153A6.' *Microbial Cell Factories* 12 (1).

Oppermann, S., Stein, F., and Kragl, U. 2010. 'Ionic liquids for two-phase systems and their application for purification, extraction and biocatalysis.' *Applied Microbiology and Biotechnology* 89 (3): 493–499.

Ortiz de Montellano, P. R. 2010. 'Hydrocarbon Hydroxylation by Cytochrome P450 Enzymes.' *Chemical Reviews* 110 (2): 932–948.

Paddon, C. J. and Keasling, J. D. 2014. 'Semi-synthetic artemisinin: a model for the use of synthetic biology in pharmaceutical development.' *Nature Reviews Microbiology* 12 (5): 355–367.

Panke, S., Held, M., Wubbolts, M. G., Witholt, B., and Schmid, A. 2002. 'Pilot-scale production of (S)-styrene oxide from styrene by recombinant *Escherichia coli* synthesizing Styrene Monooxygenase.' *Biotechnology and Bioengineering* 80 (1): 33–41.

Panula-Perälä, J., Šiurkus, J., Vasala, A., Wilmanowski, R., Casteleijn, M. G., and Neubauer, P. 2008. 'Enzyme controlled glucose auto-delivery for high cell density cultivations in microplates and shake flasks.' *Microbial Cell Factories* 7 (1): 31.

Parales, R. E. and Ditty, J. L. 2010. 'Substrate Transport.' In *Handbook of Hydrocarbon and Lipid Microbiology,* 1545–1553. Berlin, Heidelberg: Springer Berlin Heidelberg.

Pazmino, D. T., Winkler, M., Glieder, A., and Fraaije, M. W. 2010. 'Monooxygenases as biocatalysts: Classification, mechanistic aspects and biotechnological applications.' *Journal of Biotechnology* 146 (1-2): 9–24.

Peabody, G. L. and Kao, K. C. 2016. 'Recent progress in biobutanol tolerance in microbial systems with an emphasis on *Clostridium*.' *FEMS Microbiology Letters* 363 (5).

Perfumo, A., Smyth, T. J. P., Marchant, R., and Banat, I. M. 2010. 'Production and Roles of Biosurfactants and Bioemulsifiers in Accessing Hydrophobic Substrates.' In *Handbook of Hydrocarbon and Lipid Microbiology,* 1501–1512. Berlin, Heidelberg: Springer Berlin Heidelberg.

Peter, C. P., Suzuki, Y., and Büchs, J. 2006. 'Hydromechanical stress in shake flasks: Correlation for the maximum local energy dissipation rate.' *Biotechnology and Bioengineering* 93 (6): 1164–1176.

Peter, C. P., Suzuki, Y., Rachinskiy, K., Lotter, S., and Büchs, J. 2006. 'Volumetric power consumption in baffled shake flasks.' *Chemical Engineering Science* 61 (11): 3771–3779.

Pfruender, H., Jones, R., and Weuster-Botz, D. 2006. 'Water immiscible ionic liquids as solvents for whole cell biocatalysis.' *Journal of Biotechnology* 124 (1): 182–190.

Pitto-Barry, A. and Barry, N. P. E. 2014. 'Pluronic block-copolymers in medicine: from chemical and biological versatility to rationalisation and clinical advances.' *Polymer Chemistry* 5 (10): 3291–3297.

Poblete-Castro, I., Becker, J., Dohnt, K., Santos, V. M., and Wittmann, C. 2012. 'Industrial biotechnology of *Pseudomonas putida* and related species.' *Applied Microbiology and Biotechnology* 93 (6): 2279–2290.

Pollard, D. J. and Woodley, J. M. 2007. 'Biocatalysis for pharmaceutical intermediates: the future is now.' *Trends in Biotechnology* 25 (2): 66–73.

Pradham, S., Bartley, J. K., Bethell, D., Golunski, S. E., and Hutchings, G. J. 2012. 'An Attempt at Enhancing the Regioselective Oxidation of Decane Using Catalysis with Reverse Micelles.' *Catalysis Letters* 142 (3): 302–307.

Prince, R. C., Gramain, A., and McGenity, T. J. 2010. 'Prokaryotic Hydrocarbon Degraders.' In *Handbook of Hydrocarbon and Lipid Microbiology,* 1669–1692. Berlin, Heidelberg: Springer Berlin Heidelberg.

Ramesh, H., Mayr, T., Hobisch, M., Borisov, S., Klimant, I., Krühne, U., and Woodley, J. M. 2015. 'Measurement of oxygen transfer from air into organic solvents.' *Journal of Chemical Technology & Biotechnology* 91 (3): 832–836.

Ramos, J.-L. L., Duque, E., Gallegos, M.-T., Godoy, P., Ramos-González, M. I., Rojas, A., Terán, W., and Segura, A. 2002. 'Mechanisms of solvent tolerance in gram-negative bacteria.' *Annual Review of Microbiology* 56 (1): 743–768.

Ramos, J.-L. L., Krell, T., Daniels, C., Segura, A., and Duque, E. 2009. 'Responses of *Pseudomonas* to small toxic molecules by a mosaic of domains.' *Current Opinion in Microbiology* 12 (2): 215–220.

Rittle, J. and Green, M. T. 2010. 'Cytochrome P450 Compound I: Capture, Characterization, and C–H Bond Activation Kinetics.' *Science* 330 (6006): 933–937.

Roduner, E., Kaim, W., Sarkar, B., Urlacher, V. B., Pleiss, J., Gläser, R., Einicke, W.-D., et al. 2012. 'Selective Catalytic Oxidation of C–H Bonds with Molecular Oxygen.' *ChemCatChem* 5 (1): 82–112.

Rojo, F. 2005. 'Specificity at the end of the tunnel: understanding substrate length discrimination by the AlkB alkane hydroxylase.' *Journal of Bacteriology* 187 (1): 19–22.

Rojo, F. 2010a. 'Carbon catabolite repression in *Pseudomonas*: optimizing metabolic versatility and interactions with the environment.' *FEMS Microbiology Reviews* 34 (5): 658–684.

Rojo, F. 2010b. 'Enzymes for Aerobic Degradation of Alkanes.' In *Handbook of Hydrocarbon and Lipid Microbiology,* 781–797. Berlin, Heidelberg: Springer Berlin Heidelberg.

Royce, L. A., Liu, P., Stebbins, M. J., Hanson, B. C., and Jarboe, L. R. 2013. 'The damaging effects of short chain fatty acids on *Escherichia coli* membranes.' *Applied Microbiology and Biotechnology* 97 (18): 8317–8327.

Royce, L. A., Yoon, J. M., Chen, Y., Rickenbach, E., Shanks, J. V., and Jarboe, L. R. 2015. 'Evolution for exogenous octanoic acid tolerance improves carboxylic acid production and membrane integrity.' *Metabolic Engineering* 29:180–188.

Rühl, J., Hein, E.-M., Hayen, H., Schmid, A., and Blank, L. M. 2012. 'The glycerophospholipid inventory of *Pseudomonas putida* is conserved between strains and enables growth condition-related alterations.' *Microbial Biotechnology* 5 (1): 45–58.

Sadowski, M. I., Grant, C., and Fell, T. S. 2016. 'Harnessing QbD, Programming Languages, and Automation for Reproducible Biology.' *Trends in Biotechnology* 34 (3): 214–227.

Schaffer, S. and Haas, T. 2014. 'Biocatalytic and Fermentative Production of α,ω-Bifunctional Polymer Precursors.' *Organic Process Research & Development* 18 (6): 752–766.

Scheidle, M., Jeude, M., Dittrich, B., Denter, S., Kensy, F., Suckow, M., Klee, D., and Büchs, J. 2010. 'High-throughput screening of *Hansenula polymorphaclones* in the batch compared with the controlled-release fed-batch mode on a small scale.' *FEMS Yeast Research* 10 (1): 83–92.

Scheps, D., Malca, S. H., Hoffmann, H., Nestl, B. M., and Hauer, B. 2011. 'Regioselective ω-hydroxylation of medium-chain n-alkanes and primary alcohols by CYP153 enzymes from *Mycobacterium marinum* and *Polaromonas* sp. strain JS666.' *Organic & Biomolecular Chemistry* 9 (19): 6727–6733.

Schlepütz, T. and Büchs, J. 2014. 'Scale-down of vinegar production into microtiter plates using a custom-made lid.' *Journal of Bioscience and Bioengineering* 117 (4): 485–496.

Schmid, A. 1997. 'Two-liquid Phase Bioprocess Development.' PhD diss., Swiss Federal Institute of Technology Zurich.

Schmid, A., Kollmer, A., Sonnleitner, B., and Witholt, B. 1999. 'Development of equipment and procedures for the safe operation of aerobic bacterial bioprocesses in the presence of bulk amounts of flammable organic solvents.' *Bioprocess and Biosystems Engineering* 20 (2): 91–100.

Schmid, A., Kollmer, A., and Witholt, B. 1998. 'Effects of biosurfactant and emulsification on two-liquid phase *Pseudomonas oleovorans* cultures and cell-free emulsions containing n-decane.' *Enzyme and Microbial Technology* 22 (6): 487–493.

Schmid, A., Sonnleitner, B., and Witholt, B. 1998. 'Medium chain length alkane solvent-cell transfer rates in two-liquid phase, *Pseudomonas oleovorans* cultures.' *Biotechnology and Bioengineering* 60 (1): 10–23.

Schneider, L. V. 1991. 'A three-dimensional solubility parameter approach to non-aqueous enzymology.' *Biotechnology and Bioengineering* 37 (7): 627–638.

Schott, H. 1995. 'Hydrophilic-Lipophilic Balance, Solubility Parameter, and Oil-Water Partition Coefficient as Universal Parameters of Nonionic Surfactants.' *Journal of Pharmaceutical Sciences* 84 (10): 1215–1222.

Schrewe, M., Julsing, M., Bühler, B., and Schmid, A. 2013. 'Whole-cell biocatalysis for selective and productive C–O functional group introduction and modification.' *Chemical Society Reviews* 42 (15): 6346–6377.

Schrewe, M., Julsing, M., Lange, K., Czarnotta, E., Schmid, A., and Bühler, B. 2014. 'Reaction and catalyst engineering to exploit kinetically controlled whole-cell multistep biocatalysis for terminal FAME oxyfunctionalization.' *Biotechnology and Bioengineering* 111 (9): 1820–1830.

Schwartz, R. D. and McCoy, C. J. 1973. '*Pseudomonas oleovorans* hydroxylation-epoxidation system: additional strain improvements.' *Applied and Environmental Microbiology* 26 (2): 217–218.

Segura, A., Molina, L., Fillet, S., Krell, T., Bernal, P., Muñoz-Rojas, J., and Ramos, J.-L. L. 2012. 'Solvent tolerance in Gram-negative bacteria.' *Current Opinion in Biotechnology* 23 (3): 415–421.

Shanklin, J. and Whittle, E. 2003. 'Evidence linking the *Pseudomonas oleovorans* alkane ω-hydroxylase, an integral membrane diiron enzyme, and the fatty acid desaturase family.' *FEBS Letters* 545 (2-3): 188–192.

Sikkema, J., Bont, J. A. M. de, and Poolman, B. 1995. 'Mechanisms of membrane toxicity of hydrocarbons.' *Microbiology and Molecular Biology Reviews* 59 (2): 201–222.

Sintra, T. E., Ventura, S., and Coutinho, J. 2014. 'Superactivity induced by micellar systems as the key for boosting the yield of enzymatic reactions.' *Journal of Molecular Catalysis B: Enzymatic* 107:140–151.

Smet, M.-J. de, Kingma, J., Wynberg, H., and Witholt, B. 1983. '*Pseudomonas oleovorans* as a tool in bioconversions of hydrocarbons: growth, morphology and conversion characteristics in different two-phase systems.' *Enzyme and Microbial Technology* 5 (5): 352–360.

Smits, T. H. M., Röthlisberger, M., Witholt, B., and Beilen, J. B. van. 1999. 'Molecular screening for alkane hydroxylase genes in Gram-negative and Gram-positive strains.' *Environmental Microbiology* 1 (4): 307–317.

Song, J.-W., Jeon, E.-Y., Song, D.-H., Jang, H.-Y., Bornscheuer, U. T., Oh, D.-K., and Park, J.-B. 2013. 'Multistep Enzymatic Synthesis of Long-Chain α,ω-Dicarboxylic and ω-Hydroxycarboxylic Acids from Renewable Fatty Acids and Plant Oils.' *Angewandte Chemie International Edition* 52 (9): 2534–2537.

Sono, M., Roach, M. P., Coulter, E. D., and Dawson, J. H. 1996. 'Heme-Containing Oxygenases.' *Chemical Reviews* 96 (7): 2841–2888.

Staijen, I. E., Marcionelli, R., and Witholt, B. 1999. 'The P$_{alkBFGHJKL}$ promoter is under carbon catabolite repression control in *Pseudomonas oleovorans* but not in *Escherichia coli* alk$^+$ recombinants.' *Journal of Bacteriology.*

Staudt, S., Müller, C. A., Marienhagen, J., Böing, C., Buchholz, S., Schwaneberg, U., and Gröger, H. 2012. 'Biocatalytic hydroxylation of n-butane with in situ cofactor regeneration at low temperature and under normal pressure.' *Beilstein Journal of Organic Chemistry* 8:186–191.

Straathof, A. J. J., Panke, S., and Schmid, A. 2002. 'The production of fine chemicals by biotransformations.' *Current Opinion in Biotechnology* 13 (6): 548–556.

Suresh, S., Srivastava, V. C., and Mishra, I. M. 2009. 'Critical analysis of engineering aspects of shaken flask bioreactors.' *Critical Reviews in Biotechnology* 29 (4): 255–278.

Tan, R.-K., Eberhard, W., and Büchs, J. 2011. 'Measurement and characterization of mixing time in shake flasks.' *Chemical Engineering Science* 66 (3): 440–447.

Tan, Z., Yoon, J. M., Nielsen, D. R., Shanks, J. V., and Jarboe, L. R. 2016. 'Membrane engineering via trans unsaturated fatty acids production improves *Escherichia coli* robustness and production of biorenewables.' *Metabolic Engineering* 35:105–113.

Thomas, J. M. 2012. 'The societal significance of catalysis and the growing practical importance of single-site heterogeneous catalysts.' *Proceedings of the Royal Society A: Mathematical, Physical and Engineering Sciences* 468 (2143): 1884–1903.

Thomas, J. M. and Raja, R. 2006. 'Innovations in oxidation catalysis leading to a sustainable society.' *Catalysis Today* 117 (1-3): 22–31.

Thomas, J. M., Raja, R., Sankar, G., and Bell, R. G. 1999. 'Molecular-sieve catalysts for the selective oxidation of linear alkanes by molecular oxygen.' *Nature* 398 (6724): 227–230.

Tinberg, C. E. and Lippard, S. J. 2011. 'Dioxygen Activation in Soluble Methane Monooxygenase.' *Accounts of Chemical Research* 44 (4): 280–288.

Tonova, K. and Lazarova, Z. 2008. 'Reversed micelle solvents as tools of enzyme purification and enzyme-catalyzed conversion.' *Biotechnology Advances* 26 (6): 516–532.

Tufvesson, P., Lima-Ramos, J., Nordblad, M., and Woodley, J. M. 2011. 'Guidelines and Cost Analysis for Catalyst Production in Biocatalytic Processes.' *Organic Process Research & Development* 15 (1): 266–274.

Udaondo, Z., Duque, E., Fernández, M., Molina, L., Torre, J. de la, Bernal, P., Niqui, J.-L., et al. 2012. 'Analysis of solvent tolerance in *Pseudomonas putida* DOT-T1E based on its genome sequence and a collection of mutants.' *FEBS Letters* 586 (18): 2932–2938.

Urlacher, V. B., Lutz-Wahl, S., and Schmid, R. D. 2004. 'Microbial P450 enzymes in biotechnology.' *Applied Microbiology and Biotechnology* 64 (3): 317–325.

Urlacher, V. B. and Schulz, S. 2014. 'Multi-Enzyme Systems and Cascade Reactions Involving Cytochrome P450 Monooxygenases.' In *Cascade Biocatalysis,* 87–132. Weinheim, Germany: Wiley-VCH Verlag GmbH & Co. KGaA.

Valgepea, K., Adamberg, K., Nahku, R., Lahtvee, P.-J., Arike, L., and Vilu, R. 2010. 'Systems biology approach reveals that overflow metabolism of acetate in *Escherichia coli* is triggered by carbon catabolite repression of acetyl-CoA synthetase.' *BMC Systems Biology* 4:166.

Vallon, T., Glemser, M., Malca, S. H., Scheps, D., Schmid, J., Siemann-Herzberg, M., Hauer, B., and Takors, R. 2013. 'Production of 1-Octanol from n-Octane by *Pseudomonas putida* KT2440.' *Chemie Ingenieur Technik* 85 (6): 841–848.

Van der Werf, M. J., Hartmans, S., and Tweel, W. J. J. van den. 1995. 'Permeabilization and lysis of *Pseudomonas pseudoalcaligenes* cells by Triton X-100 for efficient production of D-malate.' *Applied Microbiology and Biotechnology* 43 (4): 590–594.

Vanbleu, E., Marchal, K., and Vanderleyden, J. 2004. 'Genetic and Physical Map of the pLAFR1 Vector.' *DNA Sequence - The Journal of Sequencing and Mapping* 15 (3): 225–227.

Vermuë, M. H., Sikkema, J., Verheul, A., Bakker, R., and Tramper, J. 1993. 'Toxicity of homologous series of organic solvents for the gram-positive bacteria *Arthrobacter* and *Nocardia* Sp. and the gram-negative bacteria *Acinetobacter* and *Pseudomonas* Sp.' *Biotechnology and Bioengineering* 42 (6): 747–758.

Vermuë, M. H. and Tramper, J. 1995. 'Biocatalysis in non-conventional media: medium engineering aspects.' *Pure and Applied Chemistry* 67 (2).

Volmer, J., Schmid, A., and Bühler, B. 2015. 'Guiding bioprocess design by microbial ecology.' *Current Opinion in Microbiology* 25:25–32.

Wang, L., Wang, W., Lai, Q., and Shao, Z. 2010. 'Gene diversity of CYP153A and AlkB alkane hydroxylases in oil-degrading bacteria isolated from the Atlantic Ocean.' *Environmental Microbiology* 12 (5): 1230–1242.

Wang, W. and Shao, Z. 2013. 'Enzymes and genes involved in aerobic alkane degradation.' *Frontiers in Microbiology* 4.

Wang, W. and Shao, Z. 2014. 'The long-chain alkane metabolism network of *Alcanivorax dieselolei*.' *Nature Communications* 5.

Wang, W., Iacob, R. E., Luoh, R. P., Engen, J. R., and Lippard, S. J. 2014. 'Electron Transfer Control in Soluble Methane Monooxygenase.' *Journal of the American Chemical Society* 136 (27): 9754–9762.

Wang, W. and Lippard, S. J. 2014. 'Diiron Oxidation State Control of Substrate Access to the Active Site of Soluble Methane Monooxygenase Mediated by the Regulatory Component.' *Journal of the American Chemical Society* 136 (6): 2244–2247.

Wang, Y., Liu, E., Sun, X., Huang, P., Long, H., Wang, H., Yu, X., Zheng, C., and Huang, Y. 2013. 'Pluronic L61 as a long-circulating modifier for enhanced liposomal delivery of cancer drugs.' *Polymer Chemistry* 4 (10): 2958–2962.

Wang, Y. and Achenie, L. E. K. 2002. 'Computer aided solvent design for extractive fermentation.' *Fluid Phase Equilibria* 201 (1): 1–18.

Wang, Z. 2007. 'The potential of cloud point system as a novel two-phase partitioning system for biotransformation.' *Applied Microbiology and Biotechnology* 75 (1): 1–10.

Wang, Z. and Dai, Z. 2010. 'Extractive microbial fermentation in cloud point system.' *Enzyme and Microbial Technology* 46 (6): 407–418.

Wang, Z., Xu, J. H., Zhang, W., Zhuang, B., and Qi, H. 2008a. 'Cloud point of nonionic surfactant Triton X-45 in aqueous solution.' *Colloids and Surfaces B: Biointerfaces* 61 (1): 118–122.

Wang, Z., Xu, J. H., Zhang, W., Zhuang, B., and Qi, H. 2008b. 'In situ extraction of polar product of whole cell microbial transformation with polyethylene glycol-induced cloud point system.' *Biotechnology Progress* 24 (5): 1090–1095.

Wang, Z., Zhao, F., Hao, X., Chen, D., and Li, D. 2004. 'Microbial transformation of hydrophobic compound in cloud point system.' *Journal of Molecular Catalysis B: Enzymatic* 27 (4-6): 147–153.

Wenda, S., Illner, S., Mell, A., and Kragl, U. 2011. 'Industrial biotechnology—the future of green chemistry?' *Green Chemistry* 13 (11): 3007.

Wentzel, A., Ellingsen, T. E., Kotlar, H.-K., Zotchev, S. B., and Throne-Holst, M. 2007. 'Bacterial metabolism of long-chain n-alkanes.' *Applied Microbiology and Biotechnology* 76 (6): 1209–1221.

Weuster-Botz, D., Puskeiler, R., Kusterer, A., Kaufmann, K., John, G. T., and Arnold, M. 2005. 'Methods and milliliter scale devices for high-throughput bioprocess design.' *Bioprocess and Biosystems Engineering* 28 (2): 109–119.

Wewetzer, S. J., Kunze, M., Ladner, T., Luchterhand, B., Roth, S., Rahmen, N., Kloß, R., Costa e Silva, A., Regestein, L., and Büchs, J. 2015. 'Parallel use of shake flask and microtiter plate online measuring devices (RAMOS and BioLector) reduces the number of experiments in laboratory-scale stirred tank bioreactors.' *Journal of Biological Engineering* 9 (1).

White, R. E. and Coon, M. J. 1980. 'Oxygen Activation by Cytochrome P-450.' *Annual Review of Biochemistry* 49 (1): 315–356.

Whitehouse, C. J. C., Bell, S. G., and Wong, L.-L. 2012. 'P450BM3 (CYP102A1): connecting the dots.' *Chemical Society Reviews* 41 (3): 1218–1260.

Wilming, A., Bähr, C., Kamerke, C., and Büchs, J. 2014. 'Fed-batch operation in special microtiter plates: a new method for screening under production conditions.' *Journal of Industrial Microbiology & Biotechnology* 41 (3): 513–525.

Witholt, B., Smet, M.-J. de, Kingma, J., Beilen, J. B. van, Kok, M., Lageveen, R. G., and Eggink, G. 1990. 'Bioconversions of aliphatic compounds by *Pseudomonas oleovorans* in multiphase bioreactors: background and economic potential.' *Trends in Biotechnology* 8:46–52.

Wohlgemuth, R. 2010. 'Biocatalysis — key to sustainable industrial chemistry.' *Current Opinion in Biotechnology* 21 (6): 713–724.

Woiton, M. 2014. 'Netzartig strukturierte Oberflächen aus präkeramischen Polymeren.' PhD diss., Universität Erlangen-Nürnberg.

Wold, S., Eriksson, L., and Kettaneh, N. 2010. 'PLS in Data Mining and Data Integration.' In *Handbook of Partial Least Squares,* edited by V. Esposito Vinzi, W. W. Chin, J. Henseler, and H. Wang. Berlin Heidelberg: Springer Berlin Heidelberg.

Wold, S., Sjöström, M., and Eriksson, L. 2001. 'PLS-regression: a basic tool of chemometrics.' *Chemometrics and Intelligent Laboratory Systems* 58 (2): 109–130.

Woodley, J. M., Bisschops, M., Straathof, A. J. J., and Ottens, M. 2008. 'Future directions for *in-situ* product removal (ISPR).' *Journal of Chemical Technology & Biotechnology* 83 (2): 121–123.

Woodley, J. M., Breuer, M., and Mink, D. 2013. 'A future perspective on the role of industrial biotechnology for chemicals production.' *Chemical Engineering Research and Design* 91 (10): 1–17.

Woodruff, L. B. A., Boyle, N. R., and Gill, R. T. 2013. 'Engineering improved ethanol production in *Escherichia coli* with a genome-wide approach.' *Metabolic Engineering* 17:1–11.

Wubbolts, M. G., Favre-Bulle, O., and Witholt, B. 1996. 'Biosynthesis of synthons in two-liquid-phase media.' *Biotechnology and Bioengineering* 52 (2): 301–308.

Wubbolts, M. G., Hoven, J., Melgert, B., and Witholt, B. 1994. 'Efficient production of optically active styrene epoxides in two-liquid phase cultures.' *Enzyme and Microbial Technology* 16 (10): 887–894.

Xu, F., Bell, S. G., Lednik, J., Insley, A., Rao, Z., and Wong, L.-L. 2005. 'The Heme Monooxygenase Cytochrome P450cam Can Be Engineered to Oxidize Ethane to Ethanol.' *Angewandte Chemie International Edition* 44 (26): 4029–4032.

Yalikun, Y. and Tanaka, Y. 2016. 'Large-Scale Integration of All-Glass Valves on a Microfluidic Device.' *Micromachines* 7 (5): 83.

Zhang, H., Lamping, S. R., Pickering, S. C. R., Lye, G. J., and Shamlou, P. A. 2008. 'Engineering characterisation of a single well from 24-well and 96-well microtitre plates.' *Biochemical Engineering Journal* 40 (1): 138–149.

Zhang, Y., Zhang, N., Tang, Z.-R., and Xu, Y.-J. 2012. 'Transforming CdS into an efficient visible light photocatalyst for selective oxidation of saturated primary C–H bonds under ambient conditions.' *Chemical Science* 3 (9): 2812.

Zhang, Y.-M. and Rock, C. O. 2008. 'Membrane lipid homeostasis in bacteria.' *Nature Reviews Microbiology* 6 (3): 222–233.

Zhou, T., Qi, Z., and Sundmacher, K. 2014. 'Model-based method for the screening of solvents for chemical reactions.' *Chemical Engineering Science* 115:177–185.